Multi-Scale Spatio-Temporal Framework for Characterising Design and Operational Parameters of the Electrical Power System

ANDREAS IYAMBO ELOMBO

Christ Church

University of Oxford

A thesis submitted for the degree of

Doctor of Philosophy

Trinity 2020

In loving memory of beloved ***Meme Loide*** *and* ***Tate Erasmus****, and my late big brothers:* ***Naftal****,* ***Josef****, and* ***Simon****...*
And to the enduring love of family and friends...

Acknowledgements

Herewith recording my acknowledgements and appreciation for the support rendered to me during my studies at Oxford:

- Above all, my heart is filled with thanksgiving to God Almighty for His divine guidance and provision throughout my studies. His promises have kept me grounded and I am deeply grateful for His love and graciousness. In Isaiah 41:10, God declares the following: *Fear thou not; for I am with thee: be not dismayed; for I am thy God: I will strengthen thee; yea, I will help thee; yea, I will uphold thee with the right hand of my righteousness.* This assurance has been my fortress. *Esilohenda lyaTate Kalunga enene shili!*

- Deepest gratitude goes to my supervisor, Professor Malcolm Duncan McCulloch, for his academic support and guidance throughout this project. His invaluable mentorship and enthusiasm have allowed me to stay on-course even during tempestuous challenges that characterise the journey of a DPhil project.

- To Dr Thomas Morstyn, Dr Dimitra Apostolopoulou, and Dr Avinash Vijay, I am grateful for their insightful discussions and for critical reviews of my work. To all members of the Energy and Power Group (EPG), I am thankful for the supportive family they have been.

- I also wish to offer special thanks to my college advisers, Professor David Nowell and Professor Jeroen Bergmann for their invaluable counsel.

- I would be remiss if I did not acknowledge the immense contribution by the examiners of this dissertation, Professor Nick Eyre (University of Oxford) and Professor Jatin Nathwani (University of Waterloo), through their engaging and insightful discussions during my viva, and it is through their critiques and suggestions that this work was markedly improved.

- To all brothers and sisters in Christ, both in Namibia and Oxford, I could not have asked for a better family. Their fellowship and prayers have offered me immense forbearance and courage. A particular mention goes to the Weston, Comont, and Leverton families for their constant support.

- Thanks to Ndjodi, Saima, Selma, Ndahafa, Moctar, Saviour, Barbara, Christi, Ben, Esther, Chloe, Nick, Lea, Wilhelmina, Tobias, and many other friends for constantly cheering me on throughout my studies. Special thanks also go to Ms Mafenyeho (NamPower's Bursary Officer), Mr Shatona, and Dr Amunkete for their mentorship and support.

- To my siblings and the entire family, I am profoundly grateful for their love and encouragement. Special thanks must go to Tatekulu and Kuku Hango for being such wonderful guardian parents. I dedicate this thesis to beloved mom and dad in memory of their noble lives and for imparting lasting life values that will carry me through my life journey. Tributes also go to beloved late brothers: Naftal, Josef, and Simon.

- Finally, I would like to acknowledge with gratefulness the sponsorship received from Namibia Power Corporation (NamPower), the University of Oxford through the Mason Scholarship, and the Namibian Government through the Namibia Government Scholarship and Training Program (NGSTP).

Abstract

This thesis explores the key research question as stated below:

- *KEY RESEARCH QUESTION:* Given the increasing adoption of distributed variable energy resources and smart appliances onto the electrical power system, what methods can be developed to help electrical power system planners and operators gain insight into the design and operational parameters of the electrical power system for purposes of enabling greater adoption of distributed variable energy resources and smart appliances in an efficient and sustainable way?

This key research question covers a number of important elements that are essential for enabling the adoption of efficient and sustainable design and operational techniques to be applied on the modern electrical power system. Therefore, in order to arrive at logical answers in respect of the key research question, three further sub-questions were explored, namely:

- *SUB-QUESTION 1:* In view of increasing presence of distributed variable energy resources and smart appliances on the electrical power system, how do the planning and design parameters of a modern electrical power system vary when such parameters are characterised at different customer aggregation levels?

- *SUB-QUESTION 2:* With the objective to accurately estimate the planning and design parameters of a modern electrical power system, what effect does the use of time-series customer load data with different time granularities have on the estimated parameters?

- *SUB-QUESTION 3:* When considering a real electrical power system with a high presence of distributed variable energy resources and smart appliances, how do the design and operational parameters of a modern electrical power system vary when such parameters are characterised at different customer aggregation levels when using time-series customer load data with different time granularities?

It is important to note that sub-questions 1 and 2 relate to characterising planning and design parameters of the power system, which are derived from characterisations based on customer load profiles. Sub-question 1 relates to performing such characterisations at different customer aggregation levels, whereas sub-question 2 relates to the characterisations considered when using customer load profiles with different time granularities. The difference in the focus of sub-question 3 in relation to sub-questions 1 and 2 is that sub-question 3 seeks to characterise design and operational parameters on a real network with a composition of customer load profiles added to and/or removed from the network at different customer aggregation levels when using customer load profiles with different time granularities. So, sub-question 3 pertains to characterisations based on a real network with the inclusion of distributed variable energy resources and smart appliances.

The research work covered in this thesis pertains to the characterisation of design and operational parameters of the electrical power system, with a particular focus on distribution networks with significant penetration of distributed variable renewable energy and smart appliances.

The characterisation technique contributed by this thesis bears two major focus areas, namely: 1) to characterise the planning and design parameters of the electrical power system, and also, 2) to characterise the operational parameters of the electrical power system. For both focus areas, i.e., planning & design and operation, a characterisation of specific parameters is considered at different customer aggregation levels, using time-series customer load data with different time granularities. It is because of the spatial/sizing consideration of customer load aggregation and the temporal aspect of the time granularity of time-series customer load data that the over-arching characterisation technique which forms the integral contribution of this thesis is termed *spatio-temporal characterisation framework*.

Characterisation based on load profiles

The spatio-temporal characterisation framework is thus applied to several load profiles datasets, namely: a synthetic dataset (generated using an Excel Workbook model developed by the Centre for Renewable Energy Systems Technology (CREST) of Loughborough University) and real datasets from four different jurisdiction areas (i.e., the United Kingdom (UK, Northern Grid), United States of America (USA, Texas), Belgium (Mons), and Australia (Ausgrid)). This study characterises planning and design parameters such as the after-diversity maximum demand (ADMD, a measure for diversity), load variance (a measure for load variability), and the load factor (which is useful for calculating the expected network power losses). All of these parameters are characterised in relation to changing aggregation levels and time-scales. All the time-series customer load profiles datasets used in

this thesis are representative of residential customers. Both the ADMD (i.e. per customer capacity requirement) and load variance were found to asymptotically decrease toward a settling value, when both the size of customer groupings and averaging time intervals approached large numbers. Conversely, the load factor asymptotically increases toward a settling value, when both the size of home groupings and averaging time intervals increase.

Characterisation based on a distribution network

In order to understand the impact of the size of customer load aggregation and the time granularities of load profiles datasets on the design and operational parameters of a distribution network, the spatio-temporal characterisation framework was further applied to a UK low voltage (LV) network with a high presence of distributed solar PV based renewable energy and plug-in electric vehicles (PEVs) based flexible demand. This study characterises the network diversified peak demand, load variability, power losses, and the load-dependency loss factor, when different sizes of home groupings are either added to or disconnected from the network at a time, using time-series profiles (for the load, solar PV, and PEV charging) with different time granularities. The load-dependency loss factor is a newly introduced theoretical parameter, defined as the differential change in losses at a given aggregation level divided by the total demand at full load, which quantifies how the change in losses implicitly compares to the differential change in network load when varying aggregation levels for a given time granularity. The results for the characterisations based on a real distribution network are very comprehensive and they shed light on the appropriate time granularity of customer load data that can be used for purposes of accurately planning and designing a power system with a high composition of distributed variable energy resources and smart appliances. The results also give insight into the requisite time scales of managing and operating the modern power system. A detailed summary of these results is presented in Chapter 6 under sub-section 6.2.2. What is most noteworthy is that, additional to the aspects of customer aggregation levels and the time granularity of customer load profiles, the inclusion of solar PV and electric vehicles had a great impact on the characterisations of network diversified peak demand, load variability, power losses, and the load-dependency loss factor, particularly when the composition of such resources is varied on the network at different aggregation levels.

The spatio-temporal characterisation framework developed in this thesis provides a useful tool for distribution network planners and operators to derive planning and design parameters of a distribution network with a particular load size on the basis of the per-customer capacity requirement, and devise network-specific active

management schemes with carefully tailored control time scales on the basis of load variability. The characterisation of network power losses allows the distribution network operators to assess the network performance and implement appropriate network interventions for optimal network operation.

Contents

List of Figures

List of Tables

Nomenclature

Acronymns & Abbreviations

ADMD	After-Diversity Maximum Demand
AU-ARPV	A 30-minute granularity Ausgrid residential rooftop-PV (ARPV) dataset, representative of residential customers in the Ausgrid's electricity network area in Australia (AU)
BE-LVSM	A 15-minute granularity low voltage (LV) feeder smart meter (SM) dataset of real load profiles collected by the University of Mons in Belgium (BE)
COM	Component Object Model
DER	Distributed Energy Resource
DNO	Distribution Network Operator
DR	Demand Response
ENWL	Electricity North West Limited
EV	Electric Vehicle
GIS	Geographic Information System
LF	Load Factor
LLF	Loss Load Factor
LV	Low Voltage
OpenDSS	Open-Source Distribution System Simulator
PEV	Plug-in Electric Vehicle
PHEV	Plug-in Hybrid Electric Vehicle
PV	Photovoltaic

UK-CLNR	A customer-led network revolution (CLNR) project 1-minute granularity dataset of real load profiles representative of residential homes connected to the Northern Powergrid in the United Kingdom (UK)
UK-CREST	UK's 1-minute granularity synthetic residential load profiles dataset by the Centre for Renewable Energy Systems Technology (CREST)
USA-PSID	A 1-minute granularity dataset of load profiles sourced from the Pecan Street Inc. Dataport (PSID) database, representative of residential homes in Austin, Texas, United States of America (USA)
VAR	Variance

Symbols & Notations

α	Size of home groupings	
δL	Load-dependency loss factor	(%)
$\sigma_{\widetilde{x}}$	Sample standard deviation of parameter x	
τ	Time granularity of the load profile	$(minutes)$
$\widetilde{x}$	Sample mean of parameter x	
$base$	Base case scenario	
D_α	Power demand at α temporal aggregation	(kW)
D_o	Initial power demand before temporal aggregation	(kW)
e	Maximum percentage error	(%)
ev	This is the EV case study scenario where new EVs are incrementally added to homes with no existing solar PV generation at different sizes of home groupings.	
$existing\_pv$	This is the solar PV case study scenario where customers with existing solar PV generation are incrementally disconnected from the network at different sizes of home groupings.	
k	Monte Carlo iteration	
L_α	Power losses at α temporal aggregation	(kW)
L_o	Initial power losses before temporal aggregation	(kW)

n_k	Number of required Monte Carlo iterations	
new_pv	This is the solar PV case study scenario where solar PV generation is incrementally added to the network at different sizes of home groupings.	
S_α	Power supply at α temporal aggregation	(kW)
S_o	Initial power supply before temporal aggregation	(kW)
t	Time instant	
z_c	Confidence coefficient	
pv_ev	This is the EV case study scenario where new EVs are incrementally added to homes with existing solar PV generation at different sizes of home groupings.	
${}_{peak}S$	Diversified peak of the total power that must be supplied to the customers connected on the network	(kW)

Whilst great gains of efficiency and sustainability can be leveraged from the inclusion of new energy resources and smart appliances, failure to adopt thoroughly researched approaches to designing and operating the future power system may result in adverse performance of the power system.

— AI ELOMBO

Chapter 1
Introduction

Contents

1.1 Overview

This thesis explores the key research question as stated below:

- **KEY RESEARCH QUESTION:** *Given the increasing adoption of distributed variable energy resources and smart appliances onto the electrical power system, what methods can be developed to help electrical power system planners and operators gain insight into the design and operational parameters of the electrical power system for purposes of enabling greater adoption of distributed variable energy resources and smart appliances in an efficient and sustainable way?*

This key research question covers a number of important elements that would enable the adoption of efficient and sustainable design and operational techniques to be applied on the modern electrical power system. It is therefore important to break down this question into further sub-questions in order to arrive at logical answers in respect of the key research question being explored in this thesis.

The important elements encompassed by the key research question are two-fold, namely: the one aspect pertains to the *planning and design of a modern electrical power system*, and another aspect relates to the *operation of a modern electrical power system*. For both of these elements, the emphasis is on the modern electrical power systems with a significant presence of distributed variable energy resources and smart appliances. For both aspects, i.e., planning & design and operation, *a characterisation of specific parameters is considered at different customer aggregation levels, using time-series customer load data with different time granularities.* On this basis, therefore, the sub-questions that are explored in this thesis are as follows:

- **SUB-QUESTION 1:** *In view of increasing presence of distributed variable energy resources and smart appliances on the electrical power system, how do the planning and design parameters of a modern electrical power system vary when such parameters are characterised at different customer aggregation levels?*

- **SUB-QUESTION 2:** *With the objective to accurately estimate the planning and design parameters of a modern electrical power system, what effect does the use of time-series customer load data with different time granularities have on the estimated parameters?*

- **SUB-QUESTION 3:** *When considering a real electrical power system with a high presence of distributed variable energy resources and smart appliances, how do the design and operational parameters of a modern electrical power system vary when such parameters are characterised at different customer aggregation levels when using time-series customer load data with different time granularities?*

It is important to note that sub-questions 1 and 2 relate to characterising planning and design parameters of the power system, which are derived from characterisations based on customer load profiles. Sub-question 1 relates to performing such characterisations at different customer aggregation levels, whereas sub-question 2 relates to the characterisations considered when using customer load profiles with different time granularities. The difference in the focus of sub-question 3 in relation to sub-questions 1 and 2 is that sub-question 3 seeks to characterise design and operational parameters on a real network with a composition of customer load profiles added to and/or removed from the network at different customer aggregation levels when using customer load profiles with different time granularities. So, sub-question 3 pertains to characterisations based on a real network with the inclusion of distributed variable energy resources and smart appliances.

The following sections (1.2 - 1.5) provide context and preface for the work covered in this thesis. The background and motivation for exploring the afore-stated key research question is presented in Section 1.2; discussing the need for the adoption of revised design and operational techniques with the view to enhance the hosting capacity of distributed energy resources, electric vehicles, and the use of other smart appliances on the modern electrical power system. The specific scope of this thesis is detailed out in Section 1.3. The approach to exploring the identified

research questions is explained in Section 1.4. The layout of the thesis is presented in Figure 1.3 (under Section 1.4) with specific chapter allocations to the respective research questions. Finally, in respect of the research questions being explored in this thesis, key research contributions are presented in Section 1.5.

1.2 Background and Literature Context

The modern electrical power system is characterised by a dynamic composition of non-conventional energy resources and practices, such as the intermittent renewable energy resources, and energy storage technologies, as well the democratised energy prosumers (customers who both consume energy from the grid and inject the surplus of their locally generated energy into the grid). With the constantly increasing presence of renewable energy resources (such as solar photovoltaic (PV) and wind) on the grid and the adoption of distributed energy resources (DERs), the power system will continue to undergo a dynamic process of the *energy transition* evolution. This evolutionary process of the energy transition necessitates a dynamic approach for accurately determining parameters for the design of the modern power system, and also for deciding on effective operational schemes of the modern power system.

The emergence of new architectural and operational changes on the power system introduces a new level of complexity in both design and operation. Some of the architectural changes include the use of distributed renewable generation and energy storage technologies, and the increasing use of plug-in electric vehicles. Additionally, the emergence of demand response (DR) also adds a dimension of complexity by converting the traditionally passive consumers into active prosumers [1–6]. This new grid structure and the interaction of players on the grid are depicted in Figure 1.1. It therefore becomes important to conduct detailed analytic studies on system load profiles to uncover their complex nature. Such analyses give useful insights to distribution network planners, as well as distribution network operators (DNOs), in helping them adopt relevant planning and design strategies that would be best suited to accommodate variable energy resources and smart applications on the evolving distribution network [7, 8].

Understanding the dynamic residential electricity consumption patterns for the modern power system

The residential sector constitutes a significant proportion of the total system load,

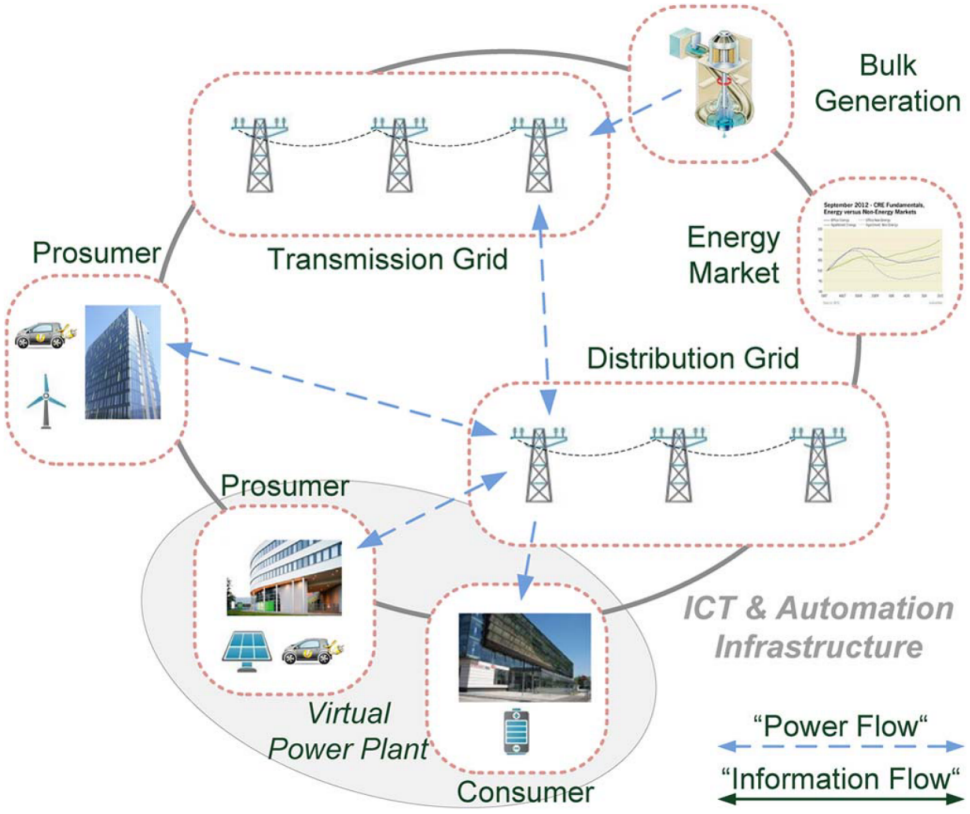

Figure 1.1: A visualisation of the future grid *[sourced from [9]]*

and it is commonly connected to the network twenty-four (24) hours a day, all through the year [7]. In particular, the UK's residential load demand represented about 35% of its total electricity demand in 2013 [10, 11]. Adding that to the fact that the use of DR strategies will increase significantly in residential homes, it will mean that such homes will have widely varying electricity consumption patterns, and it will be difficult to accurately forecast their upper-bound electricity consumption requirements. As a result, increased levels of uncertainty in the design and operation of the power system will abound, making the balancing of power demand and supply more challenging, especially at the distribution level. There is therefore a need to understand the underlying electricity consumption patterns that might exist at distribution level, both from the design and operational perspectives. The use of data loggers (and more recently, smart meters) has gained popularity in collecting electricity consumption data at residential homes in order to study the residential electricity consumption patterns [12–15]. Such data serve as valuable

input to load modelling and forecasting processes as demonstrated in [2, 16–18].

When designing a distribution network, it is a standard design method to estimate the expected peak demand of the feeder in order to determine the power ratings of the infrastructure to be installed [1]. This characteristic is known as the after-diversity maximum demand (ADMD) of the network, and it is defined as the maximum non-coincident demand per customer as the number of connected customers, each with an individual maximum demand, approaches infinity [2, 19, 20]. The significant increase in distributed variable energy resources and the application of smart appliances at distribution level therefore introduces the need to re-evaluate approaches to designing and managing distribution networks. This means that network planners and operators must understand how the system net load (with cognisance of distributed energy resources) varies by deriving such understanding from load data (whether using historical smart meter data or synthetic data from credible load modelling algorithms). Figure 1.2 shows a sectionalised grid architecture from local area level to national grid level.

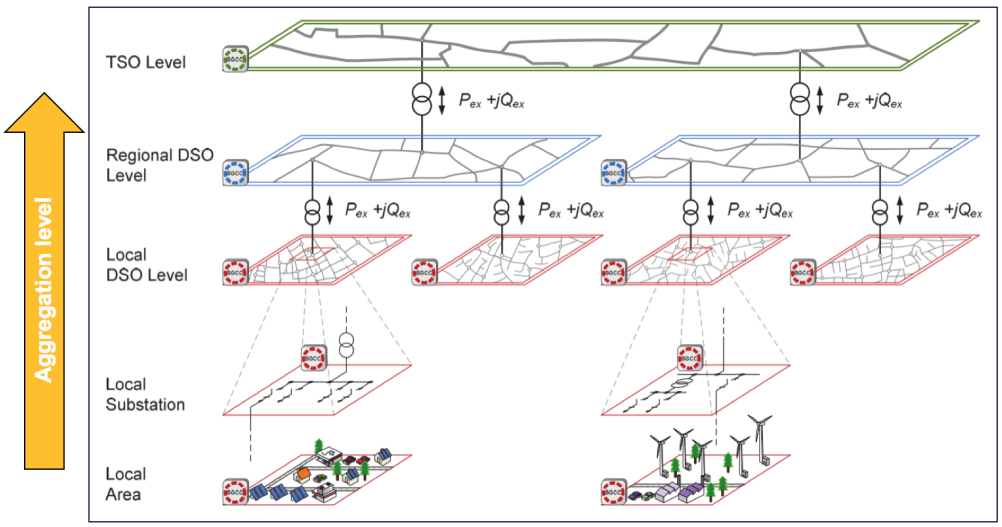

Figure 1.2: A multi-layer view of the power system *[adapted from [21]]*

Given the dynamic nature of the modern power system, it is important to understand how the design and operational requirements of the distribution network will vary when the customer composition of the network changes. In order to accurately do these assessments of the design and operational requirements of

the distribution networks with such dynamic customer composition, an accurate assessment approach must be put in place. In doing this, the question then becomes: what type of customer load data would be suitable for these assessments? The characterisation framework developed in this thesis therefore seeks to provide some insight into this question. In fact, the question around the type of customer load data to be used includes the aspect of the aggregation level of customers, as well as the time granularity of the customer load data, and how these two factors could affect the assessment of design and operational parameters of the distribution network.

Firstly, aggregating customer load profiles data gives insight into the dynamic characteristics of the load at different spatial scales of the distribution network, whilst the use of load profiles with different time granularities could provide information about the temporal implications on the network load characteristics. These insights can be derived by performing an assessment of load profiles with different time granularities aggregated at different grouping sizes to mimic different spatial load composition scales of the network. Whilst it is indisputable that these assessments are necessary, there is still very limited work in the literature that explicitly deals with the estimation of planning and operational parameters from load profiles using the approach of spatial and temporal assessments. The spatio-temporal framework of load data analysis, which is an integral contribution of this thesis, would therefore be a useful tool to assist DNOs with deriving a number of parameters useful for network design and operation.

Prior to the introduction of new energy resources and applications, which are mostly unpredictable in nature, it was fairly easy to predict the energy requirements of the power system. However, the modern power system now incorporates highly variable energy resources and applications such that the power system planners and operators need to be able to predict the variations in the power system demand in order to accurately ensure a healthy balance between power demand and supply [8, 12, 13]. The variation in power system demand almost requires real time monitoring. Therefore, there is a great need to analyse the impact of the time resolution of energy data and how this time resolution impacts on the planning and design of

the power system with different sizes of customers composition (i.e., the customer aggregation level). The current industry practice employs load data aggregation methods in the planning of the power system, but without the use of the time evolution of the energy data [22, 23].

The design and operation implications of the modern power system

The global shift from the traditional power system toward a de-carbonised and liberalised electricity market bears both positive and negative implications. The positive implications are that the power system becomes more robustly operable in an efficient and reliable manner, and also that the carbon emissions will be reduced due to a larger mix of de-carbonised energy resources. The negative implications are that there is limited established knowledge on how the system would behave under increased distributed energy resources, which operate in a liberalised manner. This means that, whilst great gains of efficiency and sustainability can be leveraged from the inclusion of these new energy resources, failure to adopt thoroughly researched approaches to designing and operating the future power system may result in adverse performance of the power system.

Distribution network operators (DNOs) must employ revised design and operational techniques to adapt to the inclusion of distributed energy resources, electric vehicles, and the use of other smart appliances. The goal is to mitigate potential challenges that could result from the integration of these new resources and appliances. Such potential challenges could include untenable voltage drop, voltage rise, frequency instability, thermal overloads of conductors and transformers, and power quality issues like harmonics [24]. Another important goal is to ensure that the electrical power is distributed across the network efficiently and cost-effectively, i.e., with minimal cost implications that may result from excessive power losses [25]. Generating this power deficit (losses) translates into monetary and environmental costs, and sending this additional power along with the required load demand creates extra currents, which could contribute to voltage and thermal capacity problems [26]. Whilst all the afore-mentioned network issues associated with increased

uptake of distributed energy resources and other smart appliances are of paramount importance in the design and operation of the modern power system, minimising network power losses particularly forms the integral focus of this thesis, as it would mean that most network performance indicators would be addressed implicitly.

Specific details on the literature gap analyses for the study aspects considered in Chapters 2 - 5 are given in the introductory segments of those chapters, and all this is presented in line with the thesis scope discussed in Section 1.3.

1.3 Thesis Scope

As explained in Section 1.1, the research work covered in this thesis pertains to the characterisation of design and operational parameters of the electrical power system, with a particular focus on distribution networks with significant penetration of distributed variable renewable energy and smart appliances.

The characterisation techniques contributed by this thesis bear two major focus areas, namely: 1) to characterise the planning and design parameters of the electrical power system, and also, 2) to characterise the operational parameters of the electrical power system. For both focus areas, i.e., planning & design and operation, a characterisation of specific parameters is considered at different customer aggregation levels, using time-series customer load data with different time granularities. It is because of the spatial/sizing consideration of customer load aggregation and the temporal aspect of the time granularity of time-series customer load data that the over-arching characterisation technique which forms the integral contribution of this thesis is termed the *spatio-temporal characterisation framework*. Within the premises of this scope, therefore, this thesis contributes a unique and deceptively simple, yet novel, technique that captures the essence of the problem of load variation when considering changing aggregation levels and time-scales.

Characterisation based on load profiles

This new technique (spatio-temporal characterisation framework) is thus applied to several load profiles datasets, namely: a synthetic dataset (generated using an Excel Workbook model developed by the Centre for Renewable Energy Systems Technology (CREST) of Loughborough University) and real datasets from four different jurisdiction areas (i.e., the United Kingdom (UK, Northern Grid), United States of America (USA, Texas), Belgium (Mons), and Australia (Ausgrid)). This study characterises planning and design parameters such the after-diversity maximum demand (ADMD, a measure for diversity), load variance (a measure for load variability), and the load factor (which is useful for calculating the expected

network power losses). All of these parameters were characterised in relation to changing aggregation levels and time-scales. Chapter 2 develops a spatio-temporal characterisation framework, which forms the basis for further characterisation studies presented in Chapters 3 - 5. The characterisation presented in Chapter 2 is based on a synthetic time-series customer load profiles dataset, using the ADMD and statistical load variance as characterisation metrics. A further characterisation metric, load factor, is considered in Chapter 3, where real datasets from four different jurisdiction areas (i.e., the United Kingdom (UK, Northern Grid), United States of America (USA, Texas), Belgium (Mons), and Australia (Ausgrid)) are used in the study. All the time-series customer load profiles datasets used in this thesis are representative of residential customers.

Characterisation based on a distribution network

In order to understand the impact of the size of customer load aggregation and the time granularities of load profiles datasets on the design and operational parameters of a distribution network, the spatio-temporal characterisation framework was further applied to a UK low voltage (LV) network with a high presence of distributed solar PV based renewable energy and plug-in electric vehicles (PEVs) based flexible demand.

This study characterises the network ADMD, statistical load variance, power losses, and the load-dependency loss factor, when different sizes of home groupings are either added to or disconnected from the network at a time, using time-series profiles (for the load, solar PV, and PEV charging) with different time granularities. The load-dependency loss factor is a new parameter, defined as the differential change in losses at a given aggregation level divided by the total demand at full load, which quantifies how the change in losses implicitly compares to the differential change in network load when varying aggregation levels for a given time granularity.

The characterisation of these parameters is considered under five scenarios, namely:

- **Base Case Study**
  - *scenario 1 - base case scenario:* where all homes connected on the network have no renewable energy resources or any new energy applications installed.
- **Solar PV Case Study**
  - *scenario 2 - existing solar PV:* where households with existing solar PV installations are incrementally disconnected from the network; and
  - *scenario 3 - new solar PV:* where solar PV installations are incrementally added to households connected on the network.
- **PEV Case Study**
  - *scenario 4 - new PEVs without solar PV:* where new electric vehicles are added to households with no solar PV installation; and
  - *scenario 5 - new PEVs with existing solar PV:* where new electric vehicles are added to households with existing solar PV installation.

Scenario 1 is covered in Chapter 4, which is representative of a scenario of a conventional distribution network. As we move to de-carbonise society, there will be new classes of high energy loads coming onto the electrical power system, including electric vehicles, heat pumps, and distributed generation. In particular, we consider roof-top solar PV based renewable energy and plug-in electric vehicles under scenarios 2 - 5. The characterisation studies considered under these scenarios (i.e., scenarios 2 - 5) are presented in Chapter 5 and these studies help shed new light on the impact of the energy transition on the distribution network peak power and losses over different aggregation levels of customers and time-scales.

Although a variety of design and operational parameters of the electrical power system are considered in this thesis as characterisation metrics, it is not within

the scope of this work to provide extensive discussions on the application of these parameters to both the design and operation of the electrical power system. The scope of this thesis is to provide a framework that can be used to understand how the design and operational parameters of the power system vary from the perspective of different sizes of customer load aggregation when using load profiles with different time granularities. These characterisation results provide new insight into future network design and operation rules for distribution networks, especially with cognisance of the variable nature of future network energy resources and applications. The spatio-temporal characterisation framework can be used to study any given characteristic of the electrical power system under the prescripts of the framework established in this thesis.

1.4 Thesis Philosophy and Layout: The Approach to Exploring the Key Research Question

As explained in Section 1.3, the scope of this thesis is to provide a framework that can be used to understand how the design and operational parameters of the power system vary from the perspective of different sizes of customer load aggregation when using load profiles with different time granularities. These characterisation results provide new insight into future network design and operation rules for distribution networks, especially with cognisance of the variable nature of future network energy resources and applications. The overview of the philosophy used in exploring the key research question of this thesis is illustrated in Figure 1.3, with specific chapter layout in relation to the respective research questions.

Sub-questions 1 & 2 seek to provide a methodology to characterise planning and design parameters of time-series customer load profiles with different time granularities when aggregated at different sizes. These sub-questions are first addressed in Chapter 2, where a new characterisation technique (spatio-temporal characterisation framework) is developed using a synthetic customer load profiles dataset (generated using an Excel Workbook model developed by the Centre for Renewable Energy Systems Technology (CREST) of Loughborough University). This characterisation technique forms the basis for further characterisation studies presented in subsequent chapters.

Chapter 2 considers planning and design parameters such as the after-diversity maximum demand (ADMD, a measure for diversity) and load variance (a measure for load variability). All of these parameters are characterised in relation to changing aggregation levels and time-scales of the considered load profiles dataset.

As a way of demonstrating the use of the spatio-temporal characterisation framework developed in Chapter 2, real customer load profiles datasets from four different jurisdiction areas (i.e., the United Kingdom (UK, Northern Grid), United States of America (USA, Texas), Belgium (Mons), and Australia (Ausgrid)) are

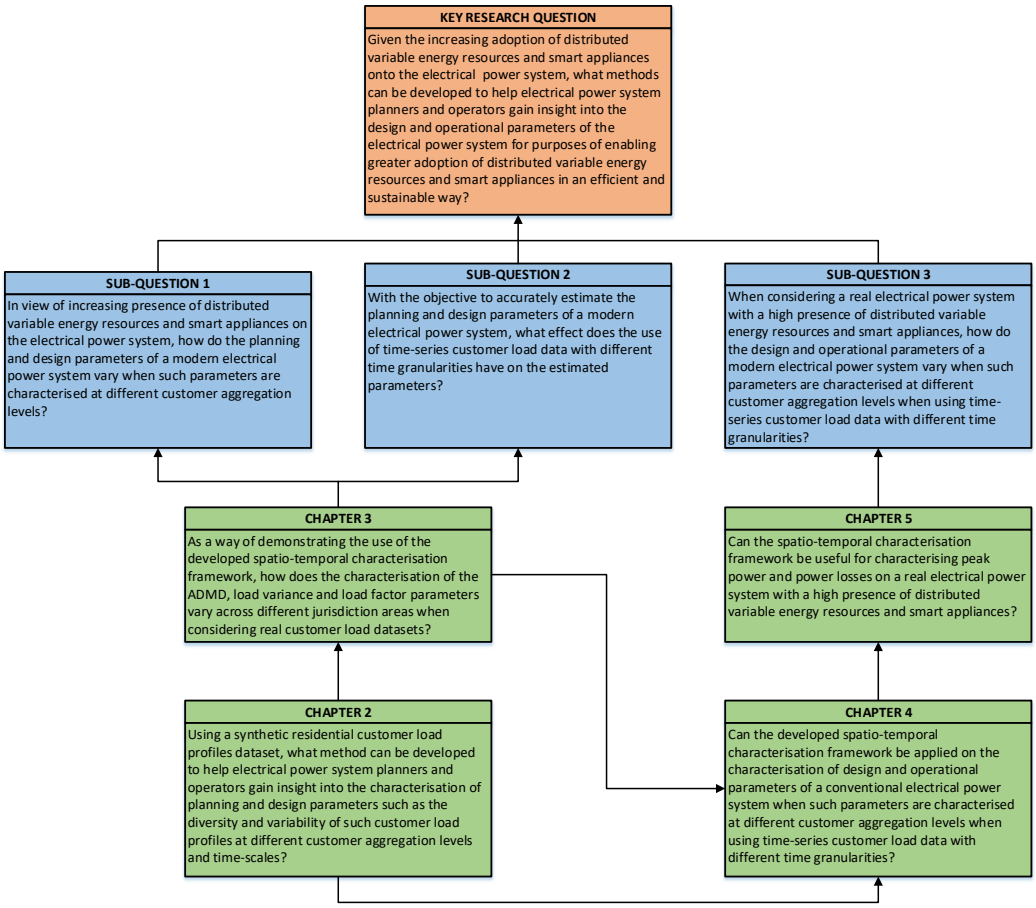

Figure 1.3: Thesis Map: depicting specific chapter allocations to the respective research questions explored in this thesis.

considered in Chapter 3 in order to demonstrate the application of the spatio-temporal characterisation framework on realistic customer load profiles. A further characterisation metric is considered in Chapter 3. This additional characterisation metric is the load factor, which is useful for calculating the expected network power losses, and this is introduced to create a link to the consideration of the aspect of network power losses covered in Chapters 4 & 5.

Sub-question 3 is addressed in Chapters 4 & 5, where the design and operational parameters of a real electrical power system with a high presence of distributed variable energy resources and smart appliances are characterised at different customer aggregation levels when using time-series customer load data with different time granularities. This characterisation is done on a low voltage distribution network.

Chapter 4 presents a base case scenario characterisation of the network ADMD, load variance, power losses, and the load-dependency loss factor, when different sizes of home groupings are either added to or disconnected from the network at a time, using time-series customer load profiles with different time granularities.

Chapter 5 considers two case studies, i.e., the case study that focuses on the integration of solar PV based renewable energy, and another case study that focuses on the inclusion of plug-in electric vehicles (PEVs). Two scenarios (as explained in Section 1.3) are considered under each of the case studies explored in Chapter 5. For each of these scenarios, the network ADMD, power losses, and the load-dependency loss factor are characterised using the spatio-temporal characterisation framework. The study presented in Chapter 5 provides useful insight on the impact of the inclusion of solar PV based renewable energy and PEVs on the distribution network peak power and losses over different aggregation levels of customers and time-scales.

The results obtained through the characterisation studies explored in Chapters 2 - 5 contribute to answering the key research question, which seeks to provide a useful tool for characterising design and operational parameters of the future electrical power system.

1.5 Key Thesis Contributions

On the basis of the over-arching research questions and the thesis philosophy established in Sections 1.1 & 1.4, respectively, this thesis makes the following key contributions:

1. *Methodology for characterising diversity and variability of electrical load profiles:*
   Methodology to characterise how the diversity and variability of electrical load profiles vary with different levels of customers aggregation and different sampling interval durations;

2. *New insight on the use of the spatio-temporal characterisation of electrical load profiles:*
   New insight is obtained by the application of the proposed new methodology in Contribution 1 on real customer load profiles datasets from four (4) different jurisdiction areas;

3. *Methodology for characterising design and operational parameters of a distribution network:*
   Methodology to characterise the peak power and power losses on a distribution network when the penetration level of distributed variable energy resources and smart appliances is varied across different customer aggregation levels when using time-series customer load data with different time granularities;

4. *New metric parameter for characterising the impact of solar PV and plug-in electric vehicles on a distribution network:*
   New theoretical parameter, termed: *load-dependency loss factor*, is introduced as a metric for characterising the impact of solar PV and plug-in electric vehicles on the power losses of a distribution network.

Essentially, all models are wrong, but some are more useful than others.

— GEORGE EDWARD PELHAM BOX, *British statistician*

Chapter 2

Spatio-Temporal Framework for Characterising Diversity and Variability of Electrical Load Profiles over Different Time and Aggregation Scales

Contents

2.1 Introduction

This chapter develops a spatio-temporal framework that seeks to characterise the diversity and variability of electrical load profiles over different aggregation levels and time-scales. This framework is the genesis of the key ideas on which the work presented in the subsequent chapters are based. On the outset, it is important to state that, although this thesis focuses on the use of customer load data profiles, the spatio-temporal characterisation framework is a versatile characterisation framework that can be applied on any power system parameter, including the generation output profiles of both conventional energy resources and the distributed variable energy resources.

The research question explored in this chapter is: *Using a synthetic residential customer load profiles dataset, what method can be developed to help electrical power system planners and operators gain insight into the characterisation of planning and design parameters such as the diversity and variability of such customer load profiles at different customer aggregation levels and time-scales?*

Several studies have established, through a statistical approach, that the maximum time-coincident demand per load entity and the uncertainty of such occurrences, both decrease at increasing aggregation scales [7, 19, 20, 22, 23]. A less explored aspect is the implication of using different time scales at different spatial scales of the network. Customer load data are sampled at different sampling intervals, with most available customer load data typically sampled at 30-minute intervals, and these data are commonly obtained by using advanced smart metering methods. The studies reported in [7, 22, 23] investigated the effect of aggregation and time scales on load variation patterns, i.e., the change in load from one sampling instant to another. Using statistical inference, these studies concluded that finer averaging time intervals are necessary to recognise the impact of individual customers on the aggregate demand. However, these studies did not explicitly consider the effect of averaging/sampling time intervals or aggregation scale on

demand diversity and variability, which are useful parameters for both the design and operation of the power grid.

The consideration of spatio-temporal implications of the ADMD (as a metric for demand diversity) will be important for the optimal placement of distributed energy resources and energy storage technologies, and the sizing of these resources [27]. The insight into load variance (as a metric for demand variability) is useful for active network monitoring and management strategies, such as stochastic optimal energy management [28] and network power losses minimisation [29–31]. In a study reported in [32], coordinated charging of plug-in hybrid electric vehicles (PHEVs) was used to explore ways of minimising network power losses, and it was found that load variance minimisation could be used in an optimisation problem to help achieve the minimisation of network power losses. This suggests that the consideration of the load variance would bear two-fold implications of uncovering information on the load variability and the expected network power losses. The insights gained from the framework proposed in this chapter will be particularly useful when designing distribution networks with a high presence of renewable energy resources (e.g., solar photovoltaic (PV)), flexible demand (e.g., plug-in electric vehicles - PEV), and energy storage (e.g., battery), and the characterisation of these metrics and those considered in subsequent chapters may be used to derive a rough estimate of the feeder-level penetration levels of new distributed energy resources and smart appliances that could potentially cause reliability and power quality issues in the feeder. Chapter 5 will explore the implications for solar PV and PEVs on a distribution network.

The contribution of this chapter is the *methodology to characterise how the diversity and variability of electrical load profiles vary with different levels of customers aggregation and different sampling interval durations.*

This chapter provides initial results of the proposed framework and it is based on a previous publication [33] by the author of this thesis. This framework will then be applied to real datasets from different jurisdiction areas, and the results of this detailed analysis are presented in Chapter 3.

Section 2.2 gives details of the dataset used in the study, and the methodology employed in developing the spatio-temporal characterisation framework, and a discussion of the initial results of the spatio-temporal characterisation of the ADMD and load variance obtained from the considered dataset is presented in Section 2.3. Lastly, Section 2.4 provides key observations from the study.

2.2 Details of the Proposed Framework

Here, we give a description of the proposed spatio-temporal characterisation framework. We first give details of the dataset used as input to the framework, and then give a step-by-step explanation of the methodology employed in the framework, including all mathematical formulations of the assessment metrics used in the characterisation.

2.2.1 Description of input dataset

A dataset of synthetic residential load profiles was used in order to demonstrate the use of the proposed framework.

- ***UK Centre for Renewable Energy Systems Technology (CREST) Dataset:***

  This dataset was generated using an Excel Workbook model developed by CREST of Loughborough University. The model generates 24-hour load profiles of UK homes at a 1-minute time granularity. Two hundred (200) load profiles were thus generated from the model to represent two hundred (200) homes. Detailed descriptions of the CREST load model are presented in [16].

  The load profiles generated from the CREST load model represent a set of daily activity profiles, which are a representation of the probability of the occurrence of different power consumption activities at different times of the day in a home. As shown in Figure 2.1, each home is assigned an active occupancy data series and a set of installed appliances [16]. Factors considered in this load model include the number of people at home (active occupancy), type of day (weekday vs weekend), the month (seasonal influence), and the uses of the appliances (level of power consumption).This dataset is henceforth referred to as UK-CREST.

It must be acknowledged that, whilst the CREST model is widely used to represent UK's household electricity consumption profiles, a study presented in [34] highlights

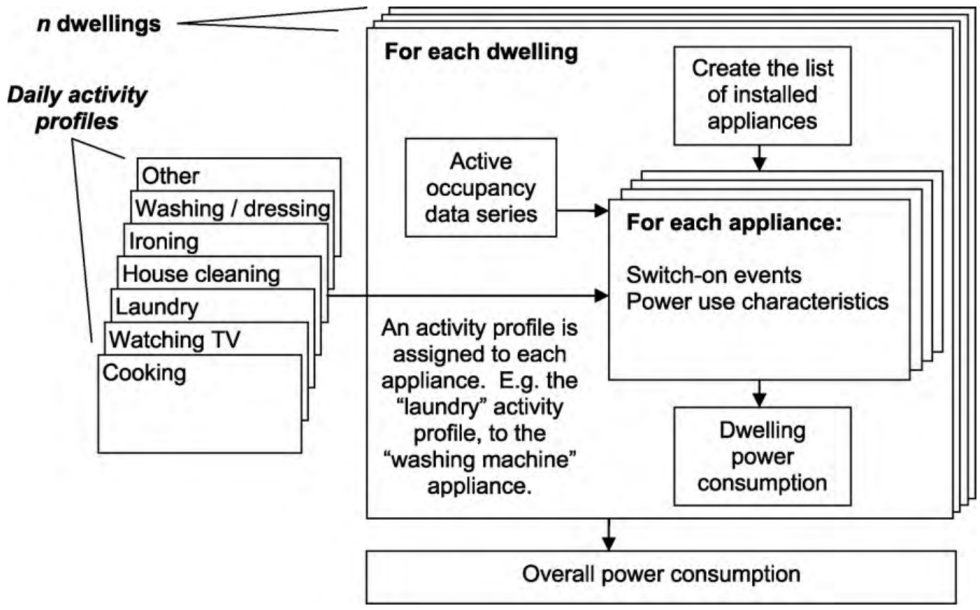

Figure 2.1: The CREST load model architecture *[sourced from [16]]*
When an appliance switch-on occurs, the appliance power use characteristics are used to determine its electricity demand (including the reactive power demand). Adding the power demands of all appliances within a dwelling gives the whole dwelling demand. The overall power demand for all dwellings is given by adding the whole-dwelling demands [16].

possible areas of improvement on the model. The shortcomings largely pertain to the assumptions related to the appliance-level consumption of the households when compared to the metered UK's Household Electricity Survey (HES) dataset. For purposes of this thesis, the CREST model was deemed relevant for use in demonstrating the characterisation framework proposed in this chapter. However, for studies related to detailed UK-specific residential loads, particular cognisance should be made on the shortcomings highlighted in [34] in order to ensure that a dataset that is accurately representative of UK's residential loads is used.

2.2.2 Methodology and metrics used

This section details out the proposed framework for characterising demand diversity and variability in relation to both time granularities and load aggregation scales. As a metric system for this work, diversity will be characterised in the form of the ADMD, whereas variability will be characterised in the form of variance. A summary of the algorithm employed in this framework is presented in the form of

a flowchart presented in Figure 2.2. The aim of this framework is to characterise the ADMD and variance of electricity demand profiles when considering a network with multi-sized groupings of customers monitored at different time intervals. It is therefore important to uncover trends in the ADMD and load variance that are representative of the considered dataset as accurately as possible. It would be ideal to use all of the data, but that would be computationally intractable (exponential number of consumer groupings). For this reason, we employ a Monte Carlo based approach. Using Monte Carlo experiments allows us to cover a large number of independent possible combinations of homes that could occur at each aggregation scale. As the number of Monte Carlo trials increase, the sample means of the observed parameters will converge toward the true mean of the population (i.e., the dataset described in Section 2.2.1), and these sample means will become normally distributed [35, 36]. These repeated experiments of randomly selected variables (which are the load profiles in this case) will make it possible to estimate the true values of the parameters of interest (which are the ADMD and load variance), exploiting the benefit of the law of large numbers and the central limit theorem. It is therefore important to determine the number of suitable Monte Carlo iterations to be performed in order to achieve the desired level of accuracy in estimating the values of the ADMD and load variance.

The random inputs to the framework are the individual customer load profiles at different time resolutions, and the output parameters of interest are the ADMD and load variance (denoted as VAR). For each time granularity, aggregation scales from 1 to 60 homes were considered. For the purpose of demonstrating the framework with the considered dataset, a total of 100 Monte Carlo trials were chosen to compute the framework outputs for each of the 60 aggregation scales. Chapter 3 will give a more comprehensive application of the framework, where the required number of Monte Carlo simulations will be calculated before the actual characterisation of the load datasets.

The original data obtained from the CREST load model were converted to different time granularities, ranging from the original time granularity to 60-minute

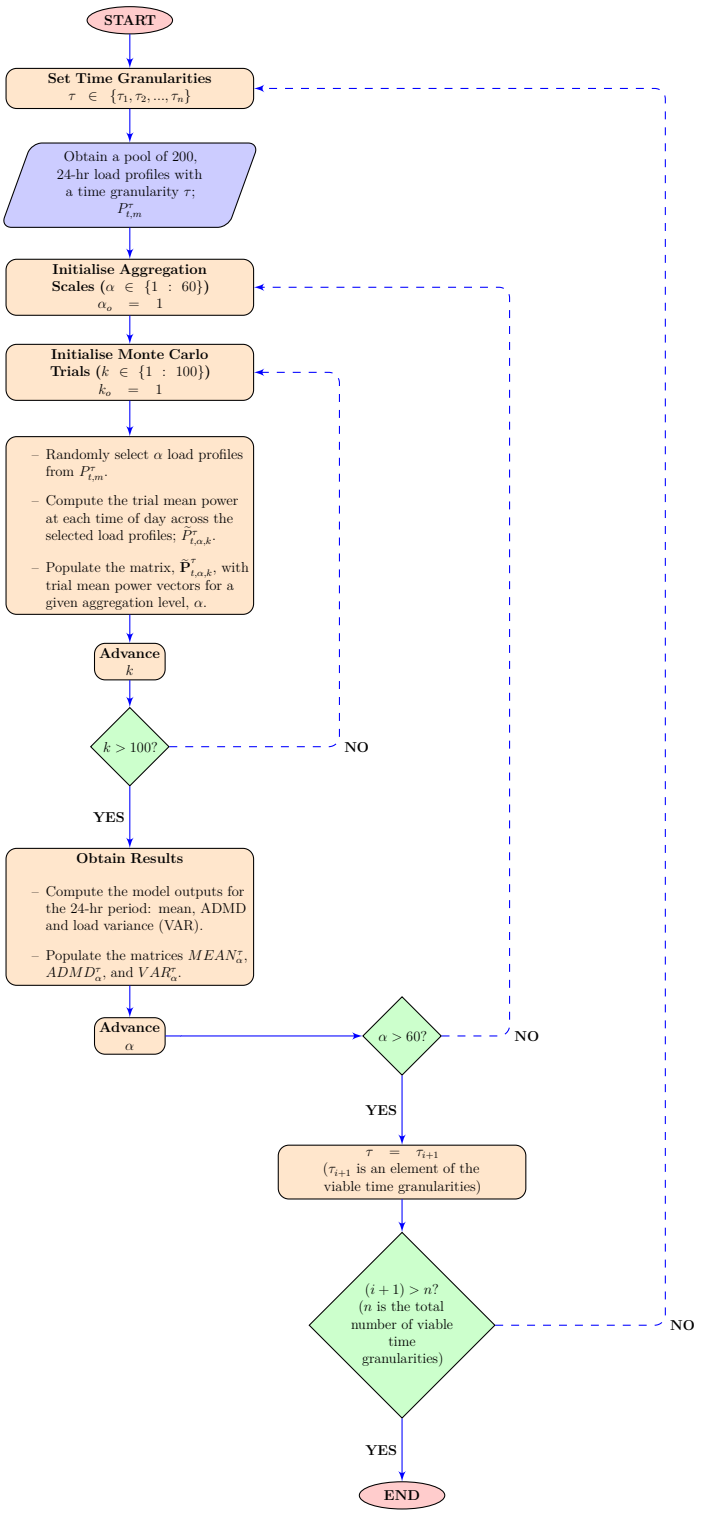

Figure 2.2: The flowchart of the Monte Carlo based framework for the spatio-temporal characterisation of the ADMD and load variance of aggregated residential load profiles using different time granularities.

sampling resolution. These time granularities were selected so that they are integer multiples of the original data time granularity, which would divide evenly into the total minutes of one hour (i.e., 60 minutes). This is necessary for assessing the temporal implications of load profiles on the ADMD and load variance (VAR). The considered dataset was thus converted to the viable time granularities (in minutes) shown in Equation (2.1).

$$\tau_{CREST} = \{1, 2, 3, 4, 5, 6, 10, 12, 15, 20, 30, 60\} \tag{2.1}$$

For a given time granularity in minutes, τ, a pool of 24-hour individual customer load profiles (from which inputs to the framework were randomly sampled) can be represented according to:

$$P^{\tau}_{t,m},\ t \in \{1, ..., T_\tau\},\ T_\tau = \frac{24 \times 60}{\tau}, \tag{2.2}$$

where $P^{\tau}_{t,m}$ is the load profile for customer $m \in \{1, ..., 200\}$ at the time instant t, for the time-series load profiles sampled at a given time granularity of τ minutes.

Aggregation levels from 1 to 60 customers were considered. For each aggregation level $\alpha \in \{1, ..., 60\}$, 100 Monte Carlo trials are completed. For the k^{th} Monte Carlo trial at aggregation level α, a set of α homes, H^{α}_{k}, is randomly obtained by sampling customers without replacement. Then, the column vector of the average powers at each time of day for the aggregated group of customers at the time granularity τ is given by:

$$\begin{aligned} \widetilde{\mathbf{P}}^{\tau}_{t,\alpha,k} &= \left[\frac{1}{\alpha} \sum_{m \in H^{\alpha}_{k}} \left(P^{\tau}_{1,m} \right), ..., \frac{1}{\alpha} \sum_{m \in H^{\alpha}_{k}} \left(P^{\tau}_{T_\tau,m} \right) \right]^T \\ &= \left[\widetilde{P}^{\tau}_{1,\alpha,k}, ..., \widetilde{P}^{\tau}_{T_\tau,\alpha,k} \right]^T \end{aligned} \tag{2.3}$$

The ADMD in kW and load variance (VAR) in kW^2 are thus computed according to:

$$ADMD^{\tau}_{\alpha} = max \Big|^{100}_{k=1} \left(max \Big|^{T_\tau}_{t=1} \left(\widetilde{\mathbf{P}}^{\tau}_{t,\alpha,k} \right) \right), \tag{2.4}$$

and

$$VAR^{\tau}_{\alpha} = \frac{1}{100} \sum_{k=1}^{100} \left(\frac{1}{T_\tau} \sum_{t=1}^{T_\tau} \left(\widetilde{\mathbf{P}}^{\tau}_{t,\alpha,k} - MEAN^{\tau}_{\alpha} \right)^2 \right), \tag{2.5}$$

where the $MEAN$ in kW is given as:

$$MEAN_{\alpha}^{\tau} = \frac{1}{100}\sum_{k=1}^{100}\left(\frac{1}{T_{\tau}}\sum_{t=1}^{T_{\tau}}\left(\widetilde{\mathbf{P}}_{t,\alpha,k}^{\tau}\right)\right). \tag{2.6}$$

According to the proposed framework, the results are given in the format represented in Table 2.1.

Table 2.1: Representation of the assessment metrics as characterised using the proposed spatio-temporal framework

Parameter		**Output Matrix**			
$MEAN_{\alpha}^{\tau}$		α_1	α_2	...	α_{60}
	τ_1	$MEAN_{\alpha_1}^{\tau_1}$	$MEAN_{\alpha_2}^{\tau_1}$	...	$MEAN_{\alpha_{60}}^{\tau_1}$
	τ_2	$MEAN_{\alpha_1}^{\tau_2}$	$MEAN_{\alpha_2}^{\tau_2}$	...	$MEAN_{\alpha_{60}}^{\tau_2}$
	$\vdots$	$\vdots$	$\vdots$	$\vdots$	$\vdots$
	τ_n	$MEAN_{\alpha_1}^{\tau_n}$	$MEAN_{\alpha_2}^{\tau_n}$	...	$MEAN_{\alpha_{60}}^{\tau_n}$
$ADMD_{\alpha}^{\tau}$		α_1	α_2	...	α_{60}
	τ_1	$ADMD_{\alpha_1}^{\tau_1}$	$ADMD_{\alpha_2}^{\tau_1}$	...	$ADMD_{\alpha_{60}}^{\tau_1}$
	τ_2	$ADMD_{\alpha_1}^{\tau_2}$	$ADMD_{\alpha_2}^{\tau_2}$	...	$ADMD_{\alpha_{60}}^{\tau_2}$
	$\vdots$	$\vdots$	$\vdots$	$\vdots$	$\vdots$
	τ_n	$ADMD_{\alpha_1}^{\tau_n}$	$ADMD_{\alpha_2}^{\tau_n}$	...	$ADMD_{\alpha_{60}}^{\tau_n}$
VAR_{α}^{τ}		α_1	α_2	...	α_{60}
	τ_1	$VAR_{\alpha_1}^{\tau_1}$	$VAR_{\alpha_2}^{\tau_1}$	...	$VAR_{\alpha_{60}}^{\tau_1}$
	τ_2	$VAR_{\alpha_1}^{\tau_2}$	$VAR_{\alpha_2}^{\tau_2}$	...	$VAR_{\alpha_{60}}^{\tau_2}$
	$\vdots$	$\vdots$	$\vdots$	$\vdots$	$\vdots$
	τ_n	$VAR_{\alpha_1}^{\tau_n}$	$VAR_{\alpha_2}^{\tau_n}$	...	$VAR_{\alpha_{60}}^{\tau_n}$

n denotes the total number of viable time granularities considered in the study

2.3 Results and Discussions

This section presents the results obtained from the framework described in Section 2.2.2. A synthetic dataset representative of UK residential homes was used for the demonstration of the framework, using two assessment metrics, viz. the ADMD and load variance. The proposed spatio-temporal characterisation framework was applied to this dataset in order to demonstrate its capabilities. It was observed that the average demand for the different sizes of customer groupings tends toward the population mean as the size of customer groupings increases, and this is in line with

what would be statistically expected. As expected, it was also observed that the average demand was the same for all time granularities across all aggregation levels and this is evident in Figure 2.3 , where it can be seen that the daily average demand plots for all time granularities are superimposed on one another. These expected results serve as useful indicators that the proposed methodology works correctly.

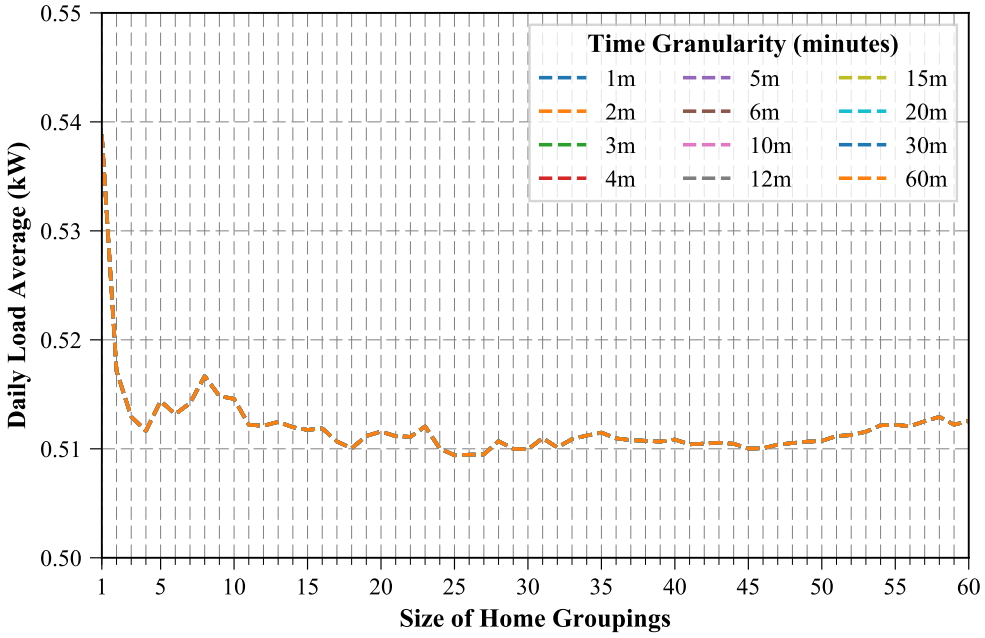

Figure 2.3: UK-CREST: The daily average demand variations versus aggregation levels across different time granularities, where it can be seen that the daily average demand plots for all time granularities are superimposed on one another.

The remainder of this section presents the characterisation of the ADMD and load variance for the UK-CREST dataset. This characterisation is given in a form of contour plots, where it shows the 2D view of the assessment metrics against both aggregation and time scales. The main objective of this chapter is to be able to obtain the first results from the proposed spatio-temporal framework in order that we would gain confidence in applying it to more advanced cases, especially using real datasets in Chapter 3, where more assessment metrics will be introduced.

2.3.1 After-diversity maximum demand

The per-customer capacity requirement (ADMD) was found to decrease as the size of customer groupings increases. As expected, the highest ADMD was recorded

for an aggregation level of one customer, as illustrated in Figure 2.4. As it can be seen from Figure 2.4, the ADMD tends toward a settling value as the aggregation level continues to increase. A settling value just under 2kW was recorded for all the time granularities.

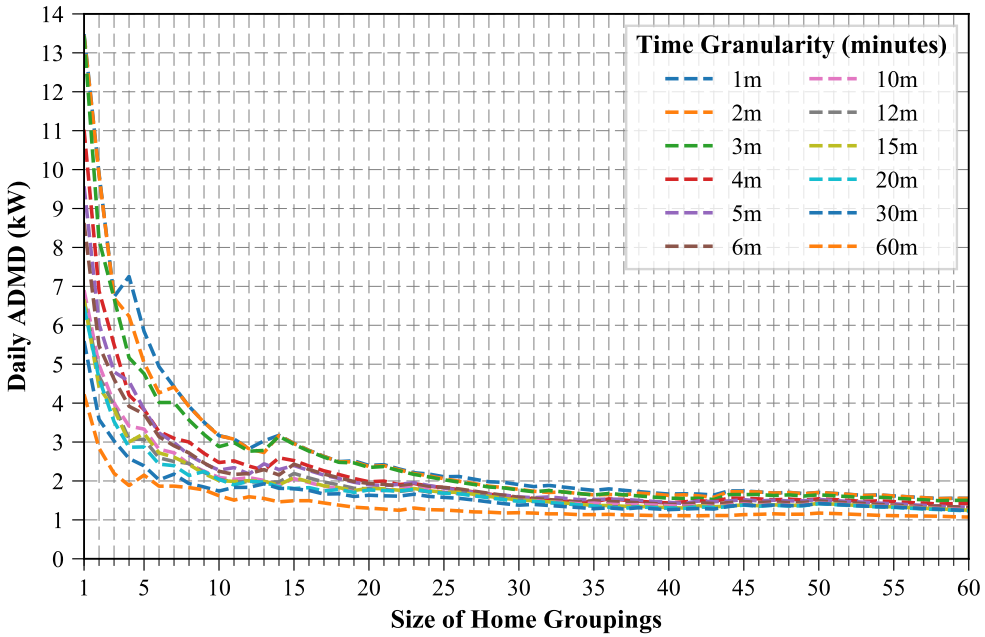

Figure 2.4: The ADMD variations versus aggregation levels across different time granularities

Figure 2.5 illustrates how the ADMD level changes versus both the time granularity and size of customer grouping, and it can be observed that higher ADMD values were obtained at both finer time granularities and smaller customer grouping sizes.

2.3.2 Load variance

The highest variance was obtained for an aggregation level of one customer grouping. As it can be seen in Figure 2.6, the variance decreases as both the level of aggregation and time granularity increase.

The combined effect of the time granularities and sizes of customer grouping on the variance is summarised in Figure 2.7. The variance decreases as the data time granularity increases. Large time granularities introduce a temporal averaging

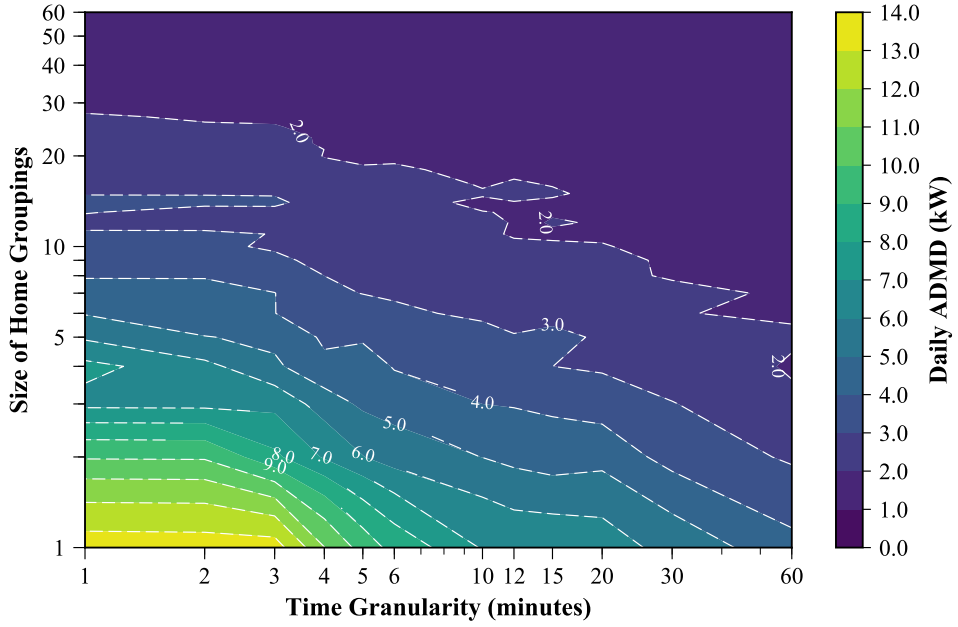

Figure 2.5: A characterisation of the ADMD variations when loads of different customer grouping sizes are aggregated across different time granularities

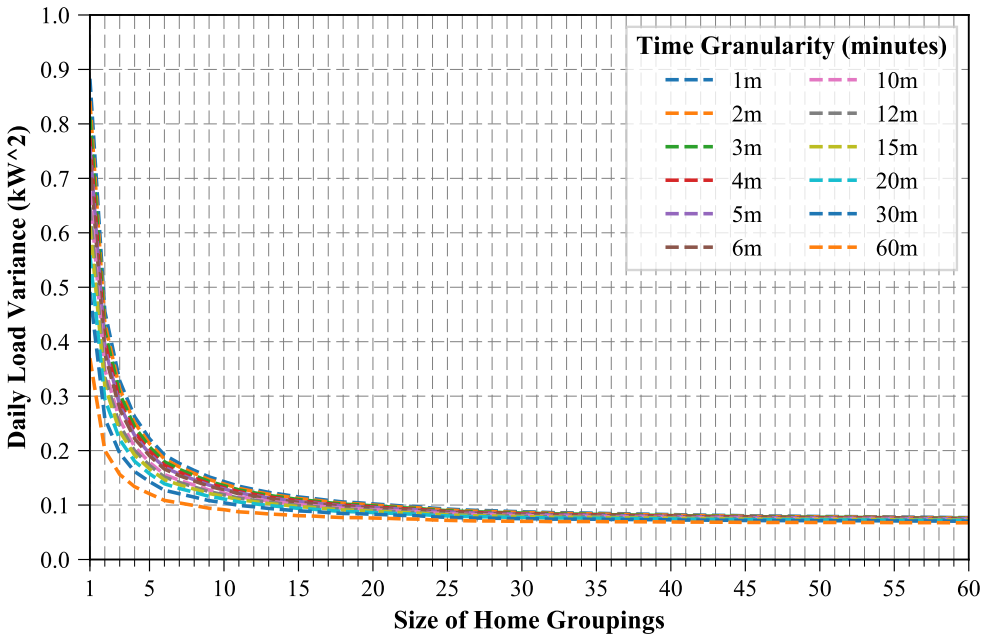

Figure 2.6: The daily load variance versus aggregation variations levels across different time granularities

effect that makes the aggregate load profile become significantly smoother and therefore resulting in a less variable profile.

By comparing the smoothness in the plots in Figures 2.4 and 2.6, it would imply the ADMD requires a larger number of Monte Carlo trials to effectively estimate when compared to load variance which is significantly smoother. Also, we can observe that at high customer grouping sizes, the variance is almost the same between the sampling intervals, whereas the sampling interval still has an impact on the ADMD even with 60 homes aggregation.

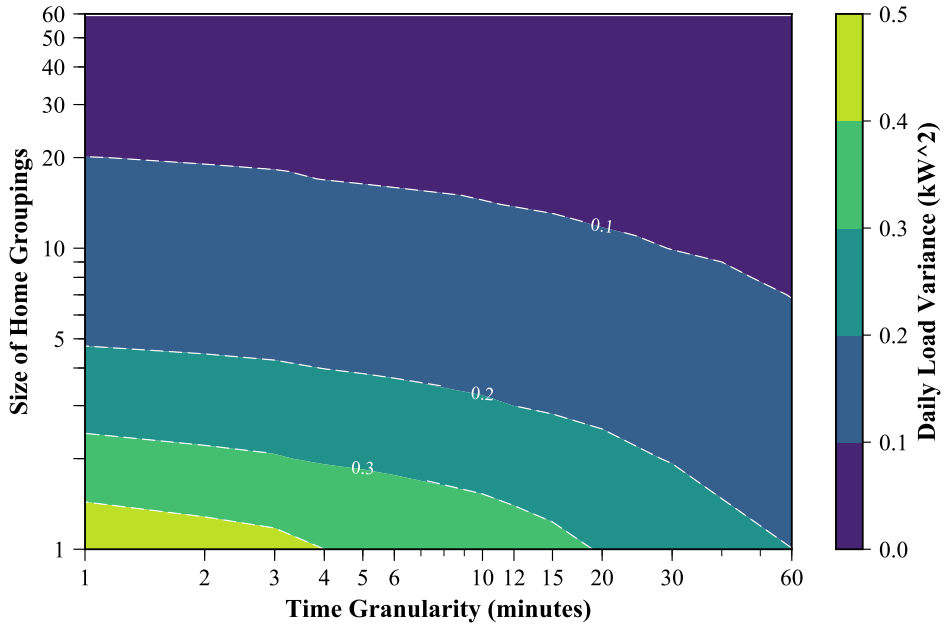

Figure 2.7: A characterisation of the demand variability when loads of different customer grouping sizes are aggregated across different time granularities

2.4 Concluding Remarks

This chapter proposes a methodology for characterising electrical load profiles over different time and aggregation scales. The main objective of this framework is to provide guidance for distribution network planners and operators in deriving design and operational parameters. As metrics for these two characterisation aspects, the after-diversity maximum demand (ADMD) and load variance were considered in this chapter. The characterisation is relevant for understanding both capacity and operational requirements when interconnecting different sizes of residential customer groupings. The temporal component of the characterisation helps with determining the optimal time granularity of data to be used in estimating design parameters, as well as the optimal control time scales to be used for active network management. The ADMD and load variance were both found to decrease when the size of customer groupings approached larger numbers. However, both the ADMD and load variance were found to saturate at a finite level when the size of customer groupings tended toward large numbers.

This work provides valuable insights into characterising design and operational parameters of distribution networks in relation to the number of customers connected on the network using data of different time granularities. The combination of using both the spatial aggregation and temporal aspects makes this framework a unique tool for distribution network planners and operators. The framework is not limited to the metrics considered in this study – it can be implemented in a variety of applications such as optimal placement and sizing of distributed generation and energy storage systems on the network in terms of penetration level (which can be deduced from the spatial aggregation component of the framework). Other applications could also include the derivations of optimal control time scales in active network management schemes.

A more detailed analysis will now be presented in Chapter 3, where real datasets from four different jurisdiction areas will be used. More time granularities and aggregation scales will be considered.

The goal is to turn data into information, and information into insight.

— CARLY FIORINA, *former executive, president, and chair of Hewlett-Packard (HP) Co.*

Chapter 3

Application of the Spatio-Temporal Characterisation Framework on Real Datasets from Different Jurisdiction Areas

Contents

3.1 Introduction

As mentioned in Chapter 2, this chapter presents a detailed analysis of the spatio-temporal framework for characterising electrical load profiles. In the previous chapter (Chapter 2), we introduced the first results of the framework, where we characterised the ADMD and variance of the load profiles. The load profiles used in the previous chapter were synthetic, generated from a model developed by the Centre for Renewable Energy Systems Technology (CREST) of Loughborough University.

The research question explored in this chapter is: *As a way of demonstrating the use of the spatio-temporal characterisation framework, how does the characterisation of the ADMD, load variance and load factor parameters vary across different jurisdiction areas when considering real customer load datasets?*

In this chapter, we now seek to apply the spatio-temporal characterisation framework on real datasets obtained from four different jurisdiction areas, viz. the United Kingdom (UK, Northern Grid), United States of America (USA, Texas), Belgium (Mons), and Australia (Ausgrid). Additional to the ADMD (a measure for diversity) and load variance (a measure for load variability) assessment metrics used in Chapter 2, we include a third metric of load factor, which is useful for calculating the expected network power losses. Additional to its usefulness in calculating the expected network power losses, the load factor is also useful for sizing a network or feeder, whereby, theoretically, we would like to have a load factor close to unity so that the system is not under-utilised. The lower the load factor, the more the system is likely to be under-utilised. This metric is defined as the ratio of the average energy consumed to the total energy that is delivered at peak demand over a given period of time. The load factor is discussed in detail in Section 3.2.2, Equation (3.2). The aim is to use these three assessment metrics for the respective jurisdiction areas, considering seasonal variations of these metrics.

The contribution of this chapter is a *new insight on the application of the proposed new methodology developed in Chapter 2 by using realistic customer load profiles datasets from four (4) different jurisdiction areas.*

This chapter is organised as follows: Section 3.2 presents descriptions of the datasets used in the analysis, as well as give a more detailed description of the methodology used in the analysis; Section 3.3 discusses the results obtained from the proposed methodology as applied to the different datasets; Section 3.4 provides key observations.

3.2 Methodology for using the Spatio-Temporal Characterisation Framework to Investigate a Number of Datasets

In this section, we will first describe the datasets used in this study, and then provide detailed descriptions and mathematical formulations pertaining to the proposed framework.

3.2.1 Datasets

Four distinctive datasets of real load profiles were used to validate the proposed framework for studying spatio-temporal implications on the ADMD, load variance, and load factor. These datasets were arbitrarily chosen on the basis of the availability of data and not necessarily for a special reason. The respective datasets are as follows:

3.2.1.1 UK Customer-Led Network Revolution (CLNR) Dataset [37]

This dataset was obtained through metering trials of residential customers connected to the Northern Powergrid in the United Kingdom (UK). A total of 155 residential homes was monitored, each of which had an installed solar PV generation unit. The daily load profiles were sampled at 1 minute intervals for the period ranging between 01/06/2012 and 31/03/2014. We will refer to this dataset as UK-CLNR.

3.2.1.2 USA Pecan Street Inc. Dataport (PSID) Dataset [38]

This dataset was sourced from the Pecan Street Inc. Dataport database, which contains 1-minutely sampled real electricity usage data for around 1436 homes, and the data collection project has been ongoing since 2011 for homes in Austin, Texas, United States of America (USA). This dataset will be referred to as USA-PSID.

3.2.1.3 Belgian (BE) Low Voltage (LV) Feeder Smart Meter (SM) Dataset

These daily load profiles were recorded using smart meters at a 15-minute sampling interval during the years 2013 and 2014. This dataset was sourced from a research

project conducted by the University of Mons in Belgium, and it will henceforth be referred to as BE-LVSM.

3.2.1.4 Australian (AU) Ausgrid Residential Rooftop-PV (ARPV) Dataset [39]

This dataset comprises of 300 randomly selected residential customers in the Ausgrid's electricity network area, who had a gross metered solar system installed for the period 01/07/2010 to 30/06/2013. All data records were sampled at half-hourly intervals. We will refer to this dataset as AU-ARPV.

For each dataset, we classify the data into four meteorological seasons, focusing on weekday load profiles only in order to restrict the analysis to a single modality of energy consumption patterns.

3.2.2 Methodology

A summary of this methodology is illustrated in Figure 3.1. The aim of this methodology is to produce representative trends in the ADMD, load variance, and load factor, when considering a network with multi-sized groupings of realistic customers monitored at different time intervals. It is therefore important to produce trends that are as representative of the considered datasets as accurately possible. For this reason, we employ a Monte Carlo based approach. Using Monte Carlo experiments allows us to cover a large number of independent possible combinations of homes that could occur at each aggregation scale in a given dataset. When the number of Monte Carlo trials increase, the sample means of the observed parameters will converge toward the true mean of the population (i.e., the respective jurisdiction areas of the datasets described in Section 3.2.1), and these sample means will become normally distributed [35, 36]. These repeated experiments of randomly picked variables (which are the load profiles in this case) will make it possible to estimate the true values of the parameters of interest, exploiting the benefit of the law of large numbers and the central limit theorem. In this sense, with a sufficient number of Monte Carlo iterations, the values of the ADMD, load variance, and load factor could be estimated for each dataset.

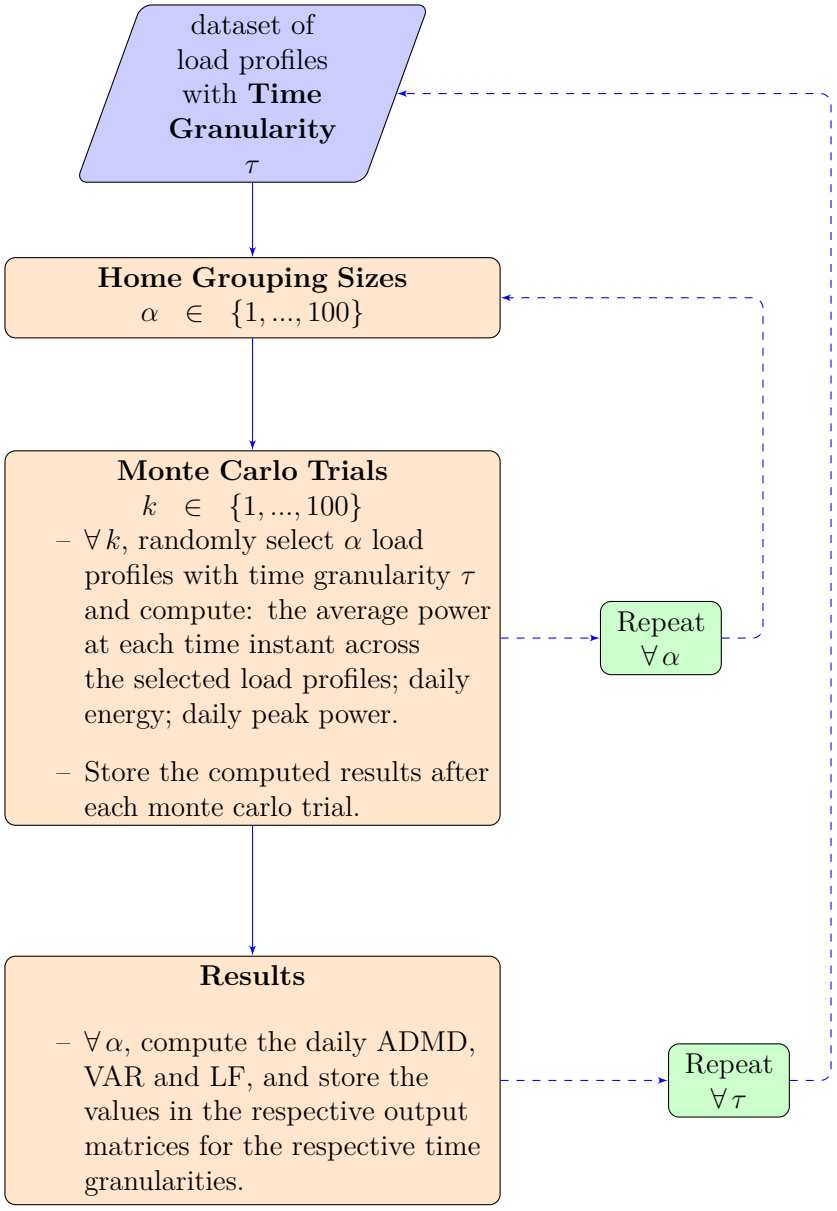

Figure 3.1: Monte Carlo based methodology for characterising the ADMD, load variance and load factor of aggregated load profiles with different time granularities.

We then run a Monte Carlo simulation for each seasonal pool of 24-hour period load profiles for all the considered datasets. The inputs to the algorithm are randomly drawn from the seasonal pools for the respective datasets to compute the three parameters of interest, namely: ADMD, load variance, and load factor. The idea of running Monte Carlo simulations is to estimate the representative values of the ADMD, load variance, and load factor. As we had indicated in Chapter 2, the

key question becomes: how many Monte Carlo iterations do we need to perform in order to be sufficiently confident that we have a close estimation of each parameter? We can do this by specifying the maximum acceptable percentage error of the mean value of the estimated parameter, and calculate the required iterations to be performed. If we chose a confidence level (with a confidence coefficient z_c) and a maximum percentage error (e), we can derive the required number of Monte Carlo iterations (n_k) for a parameter with a mean, $\widetilde{x}$, and a standard deviation, $\sigma_{\widetilde{x}}$, using Equation (3.1) [35, 40]. We use the sample mean, $\widetilde{x}$, and sample standard deviation, $\sigma_{\widetilde{x}}$, in Equation (3.1), with the assumption that both these statistical measures will tend toward the population values as we perform larger Monte Carlo iterations.

$$n_k = \left[\frac{100 z_c \sigma_{\widetilde{x}}}{e\widetilde{x}}\right]^2 \tag{3.1}$$

Equation (3.1) however gives rise to over-specified requirements of the number of trials to be run. For example, to achieve a 5% error estimation with 95% confidence level for the ADMD at 1 minute, 1 home grouping, we would require a total of 25 Monte Carlo trials. For the load variance and load factor, at the same error and confidence levels, we would require 2000 and 200 Monte Carlo trials, respectively. This means that, if a single trial were to be run to estimate all the three parameters at once, we would have to run 2000 trials for all averaging time interval and home grouping scales, and this would be very computationally intensive. We thus sought to derive error variation curves for estimating the three parameters, on the basis of which we would pick an appropriate error bound, and determine the number of Monte Carlo trial we may choose to run. The choice of error bounds will depend upon the degree of precision that the task at hand might demand. The error curves in Figure 3.2 were calculated for a 95% confidence level, using a re-arranged form of Equation (3.1) to solve for the maximum percentage error (e).

We chose a total of 100 Monte Carlo trials for this study, where, from Figure 3.2, we are able to estimate the ADMD, load variance, and load factor within 2.7%, 27.1%, and 6.7% at a 95% confidence level, respectively. For comparison, we then ran 2000 Monte Carlo trials at 1 minute, 1 home grouping category, and compare

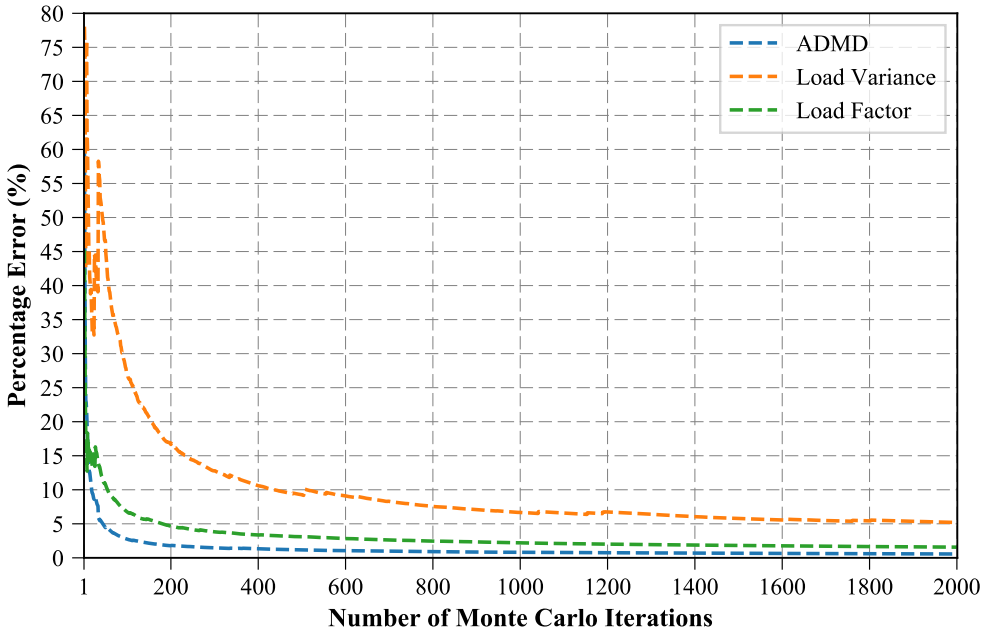

Figure 3.2: USA-PSID (1 minute averaging interval, 1 home grouping, summer): estimation errors versus the number of Monte Carlo iterations performed

the results with those obtained from 100 trials, from which we can state that the error bounds displayed on the error curves in Figure 3.2 appear to be conservative margins of the expected errors. From this comparison, we could observe that the ADMD, load variance, and load factor results obtained from 100 trials are within 7.1%, 4.0%, and 7.7% error difference of the results from 2000 trials, respectively. For every time granularity, a total of 10,000 Monte Carlo trials were performed, i.e., 100 trials for each of the 100 home grouping variations, which gives rise to 940,000 Monte Carlo simulations for the entire study. If we chose 2000 trials, as suggested by Equation (3.1), we would otherwise have had to run a total of 18,800,000 trials for the entire study.

The original data were converted to corresponding temporal time granularities, ranging from the original averaging time intervals to 1440 minutes. These time granularities were selected so that they are integer multiples of the original data time granularities, which would divide evenly into the total minutes of a full day (i.e., 1440 minutes). This is necessary for assessing the impact of temporal averaging time scales on the ADMD, load variance (denoted as VAR), and load factor (LF).

Table 3.1: Time Granularities (τ) for the Four Datasets

Dataset	Time Granularities, τ (mins)
UK-CLNR & USA-PSID	1, 2, 3, 4, 5, 6, 8, 9, 10, 12, 15, 16, 18, 20, 24, 30, 32, 36, 40, 45, 48, 60, 72, 80, 90, 96, 120, 144, 160, 180, 240, 288, 360, 480, 720, 1440
BE-LVSM	15, 30, 45, 60, 90, 120, 180, 240, 360, 480, 720, 1440
AU-ARPV	30, 60, 90, 120, 180, 240, 360, 480, 720, 1440

The considered datasets are thus converted to the viable temporal averaging time scales (in minutes) shown in Table 3.1.

Using the same approach followed in Chapter 2, we represent the pool of 24-hour period load profiles for each dataset for a given time granularity in minutes, τ, according to Equation (2.2).

A total of 100 Monte Carlo trials were conducted for each aggregation scale $\alpha \in \{1, ..., 100\}$. For the k^{th} Monte Carlo trial at aggregation scale α, a set of α homes, H_k^{α}, is randomly drawn by sampling homes without replacement. Then, the column vector of the average power at each time of day for the aggregated group of homes with a time granularity τ is given by Equation (2.3), as defined in Chapter 2.

The ADMD in kW and load variance (VAR) in kW^2 are thus computed according to Equations (2.4) and (2.5). Considering that the load factor, LF, is the ratio of the average energy consumed due to the average power demand, P, over a given time period, T, to the total energy that would have been delivered at peak demand, P_{max}, over the same time period (T) [41, 42], we can calculate the load factor as:

$$LF = \frac{\int_0^T P\, dt}{T \times P_{max}}. \tag{3.2}$$

The load factor can have many applications in designing and operating a power network. For example, we can estimate the expected average energy losses of a network or feeder over the time period T according to [41]:

$$W_{loss} = (LLF \times T \times P_{load\,loss}^{max}) + (T \times P_{no-load\,loss}), \tag{3.3}$$

where $P^{max}_{load\,loss}$ and $P_{no-load\,loss}$ are the power losses at maximum demand and at no load, respectively; whereas LLF is the loss load factor, defined as the ratio of the average energy losses to the energy losses at peak demand over the time period T [42]. The LLF can be approximated from the load factor (LF) by using methods proposed and tested in [41], where the Wolf, Junge, Sochinsky and Dewberry methods were found to yield the best approximation results. We do not explore the network losses in this chapter, but we instead focus on the trends in the load factor in relation to home grouping sizes and time granularities.

For a given time granularity and aggregation level, the load factor is computed in accordance with:

$$LF^{\tau}_{\alpha} = \frac{1}{100}\sum_{k=1}^{100}\left(\frac{E^{\tau}_{\alpha,k}}{24 \times D^{\tau}_{\alpha,k}}\right), \tag{3.4}$$

where $E^{\tau}_{\alpha,k}$ is the daily energy demand in kWh and $D^{\tau}_{\alpha,k}$ is the daily peak demand in kW, which are both defined in (3.5) and (3.6), respectively.

$$E^{\tau}_{\alpha,k} = \left(\sum_{t=1}^{T_{\tau}}\sum_{m\in H^{\alpha}_{k}}\left(P^{\tau}_{t,m}\right)\right)\frac{\tau}{60} \tag{3.5}$$

$$D^{\tau}_{\alpha,k} = max\Big|_{t=1}^{T_{\tau}}\left(\sum_{m\in H^{\alpha}_{k}}\left(P^{\tau}_{t,m}\right)\right) \tag{3.6}$$

3.3 Results and Discussions

This section presents the observations made in accordance with the spatio-temporal methodology described in Section 3.2. The methodology was applied to four datasets of real load data from four jurisdiction areas, within which seasonal modalities were considered. We will present the results in a three-tier format. Firstly, we give a summary of the general trends observed in the ADMD, load variance, and load factor, when load profiles with different temporal granularity are aggregated at different spatial scales. Secondly, we consider how the three parameters of interest compare across all four jurisdiction areas. Thirdly, we then consider the effect of seasonal variations for all the parameters of interest.

3.3.1 Observed trends in the after-diversity maximum demand (ADMD), load variance, and load factor

The trends observed in the ADMD, load variance, and load factor were found to be identical across all the case studies. For purposes of highlighting the general trends in the studied parameters, we therefore only consider the USA-PSID dataset, the results of which are representative of the trends observed for the BE-LVSM, UK-CLNR, and AU-ARPV datasets. Also notice that we will use the term *time granularity* interchangeably with *averaging time interval* to refer to the sampling time interval of the datasets.

3.3.1.1 After-diversity maximum demand

The use of real load data confirms the findings from synthetic data reported in Chapter 2 and in [33] that the calculated per-customer capacity requirement of the network decreases as both the size of customer groupings and time granularities increase. The ADMD tends to approach a settling level when the customer grouping size tends toward a large number. These observations are common to all jurisdiction datasets across all seasonal variations. The results for the USA-PSID dataset is shown in Figure 3.3, depicting the winter period. This diminishing trend in the ADMD is expected when increasing the size of customer groupings, since it becomes

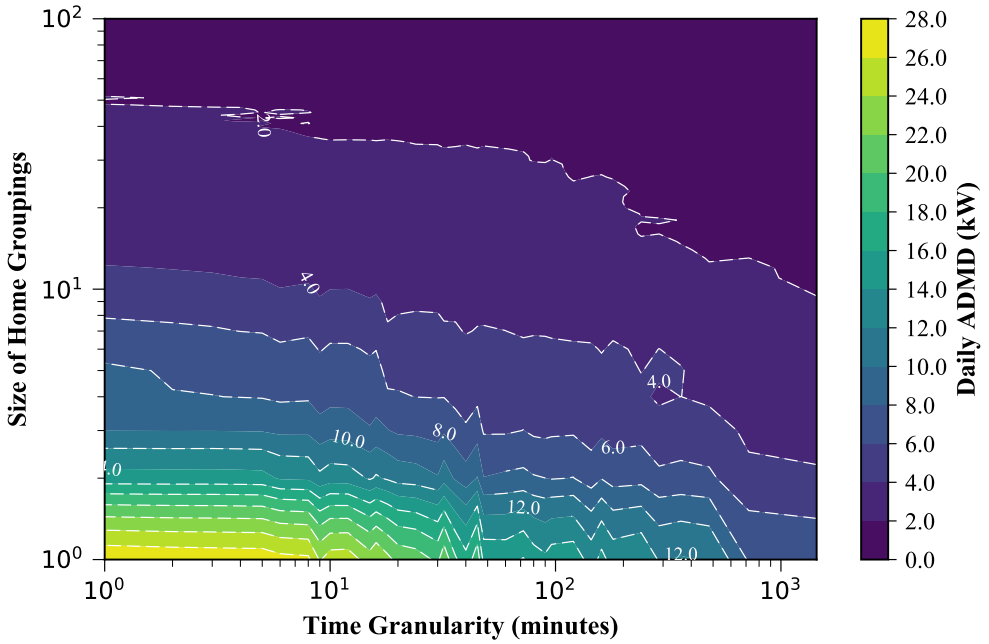

Figure 3.3: USA-PSID, winter: the per-customer capacity requirement as a function of the size of interconnected customer groupings and averaging time intervals

less likely for individual peak demands to occur at the same time across all the customers. The group peak demand thus converges toward the average demand of the population, which is a statistical expectation according to the central limit theorem. In terms of the sampling intervals, the observed trend is also not surprising due to the time averaging effects at longer averaging time intervals (for larger time granularities) masking out the potentially high individual peak demands.

3.3.1.2 Load variance

We observe that the trends in the variability of load demand, when interconnecting differently sized customer groupings, are in agreement with the findings of our initial work reported in Chapter 2 and in [33], where, as it can be seen in Figure 3.4, the aggregate demand becomes less variable as both the number of customer groupings and averaging time intervals increase. This is because the resultant aggregate demand comprises large customer groupings, whose loads are largely uncorrelated (due to the non-coincident nature of individual peaks) – thereby resulting in a smoother, less variable aggregate load profile. Similarly, the load variance decreases

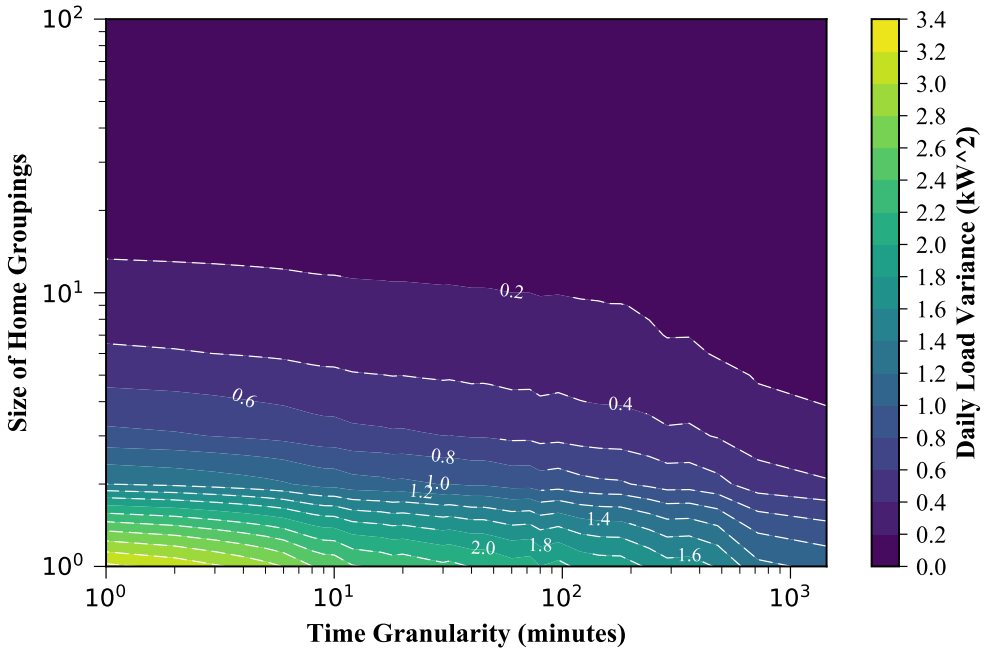

Figure 3.4: USA-PSID, winter: the load variance as a function of the size of interconnected customer groupings and averaging time intervals

at longer averaging time intervals due to larger time averaging effects. These observations are true for all the jurisdiction datasets. With reference to Figure 3.4, we observe that a combination of averaging time intervals and home grouping sizes can yield the same load variability. For instance, if we chose a 0.2 kW^2 load variability level, we notice that the following combinations yield the same load variability, viz. 10 homes at 96 minutes, 8 homes at 240 minutes, and 6 homes at 360 minutes. This suggests that the control design of the power system would need to change in reflection of the spatio-temporal load characteristics. For a given level of load variability and application, say reconciling power sharing contracts, we could send out control signals at 96-minute intervals on a network with 10 homes, which is equivalent to using a 360-minute interval for a network with 6 homes. Indeed, the choice of the granularity of control time scales will depend upon the control task at hand. However, the underlying observation is that it is important to choose appropriate time scales for updating control signals in relation to the spatial size of the network.

3.3.1.3 Load factor

The impact of both the temporal averaging time effects and the size of customer groupings on the load factor is the converse of what was observed in the ADMD and load variance. For all the datasets, the load factor was found to increase asymptotically toward a settling load factor level as the size of customer groupings increases. This trend is evident in Figure 3.5, displaying the winter results for the USA-PSID dataset. We have seen in Figure 3.3 that the coincident peak values saturate with the increasing home groupings, and we also then expect that the average demand approaches the population mean demand. This combination thus explains why the load factor levels off at large home groupings, since the ratio of the average and peak demands becomes less variable. Because finer averaging time periods produce much higher peak values, the load factor levels obtained from such temporal averaging periods are lower than those obtained at longer averaging time periods. For network losses estimation (such as using the formulation in Equation (3.3)), for instance, this highlights the importance of using data with correct temporal resolution in relation to the number of customers being supplied by the network or feeder. In particular, with less customers being aggregated, the load factor calculation is more sensitive to the time granularity.

3.3.2 Jurisdiction implications on the spatio-temporal load characterisation

Choosing the lowest common temporal averaging interval of 30 minutes, we show here how the results of the ADMD, load variance, and load factor compare across all the datasets. We consider the winter season in this section. Seasonal comparisons are presented in Section 3.3.3.

3.3.2.1 After-diversity maximum demand

We observe that, although the ADMD levels for smaller home groupings may be of widely different magnitudes across different jurisdiction datasets, the settling values all fall within the same region. A similar observation was found for synthetic load

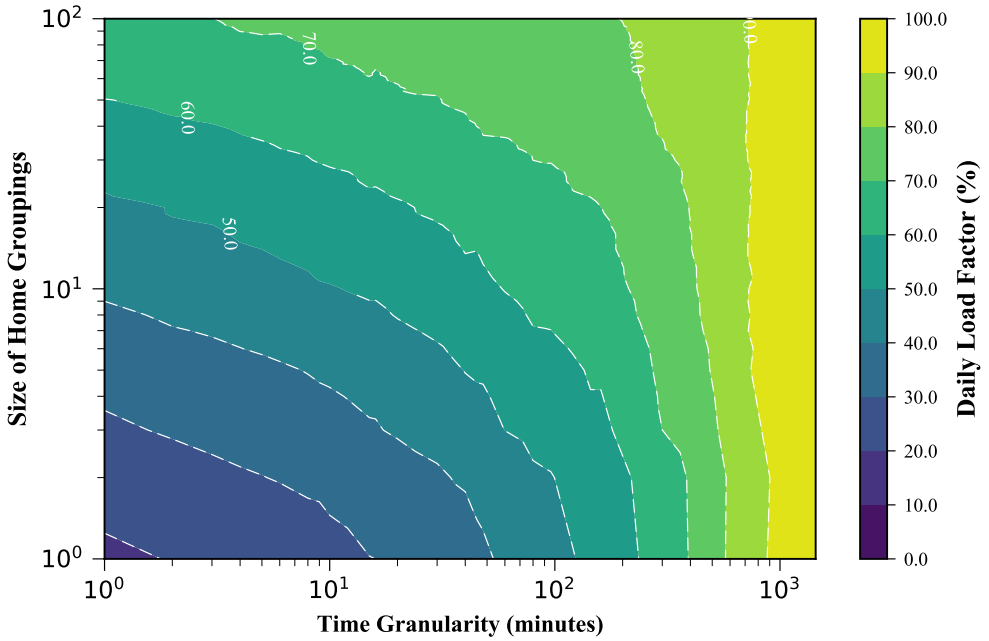

Figure 3.5: USA-PSID, winter: the load factor as a function of the size of interconnected customer groupings and averaging time intervals

data studies in [19, 33]. This could suggest that distribution networks with very large numbers of residential customers may be expected to have an ADMD level within a particular order of magnitude irrespective of a jurisdiction area. From Figure 3.6, we can observe that, at the 30 minute averaging time interval and 100 home grouping scales, the order of magnitudes in the ADMD is as follows (ascending order): UK-CLNR → USA-PSID → AU-ARPV → BE-LVSM.

3.3.2.2 Load variance

The order of magnitudes in the load variance across the four jurisdiction areas is the same as noted for the ADMD at the 30 minutes averaging time interval and 100 home grouping scales. Here, the temporal averaging effect is quite visible in Figure 3.7, with the datasets originally sampled at 1 minute (i.e., UK-CLNR and USA-PSID) settling off at a similar level, whereas the 15 and 30 minute (i.e., BE-LVSM and AU-ARPV, respectively) datasets settle off at a different level.

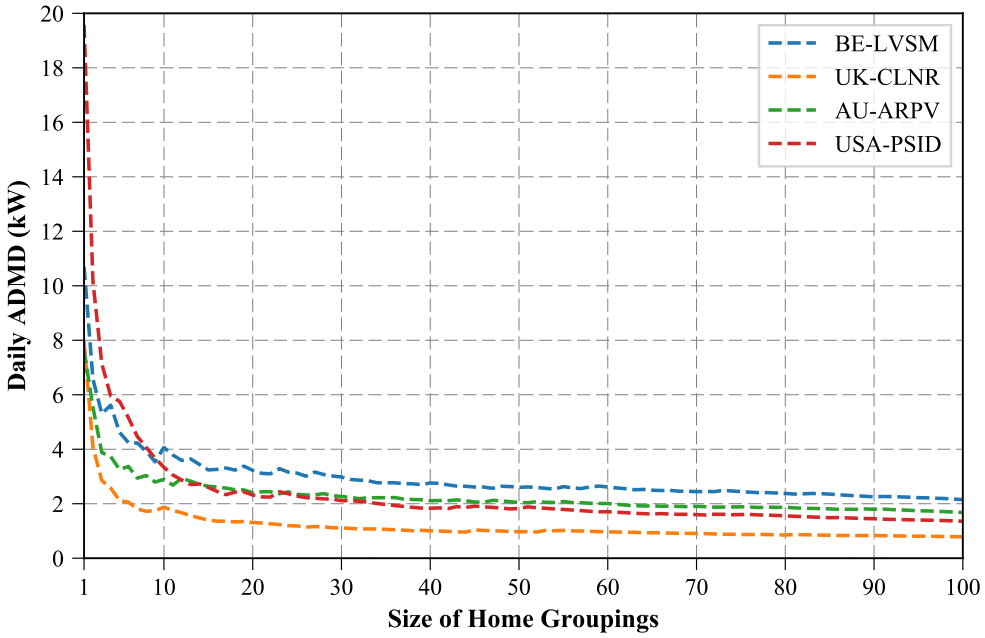

Figure 3.6: 30-minutes averaging interval: a comparison of the daily ADMD over the winter seasons of the different jurisdiction areas

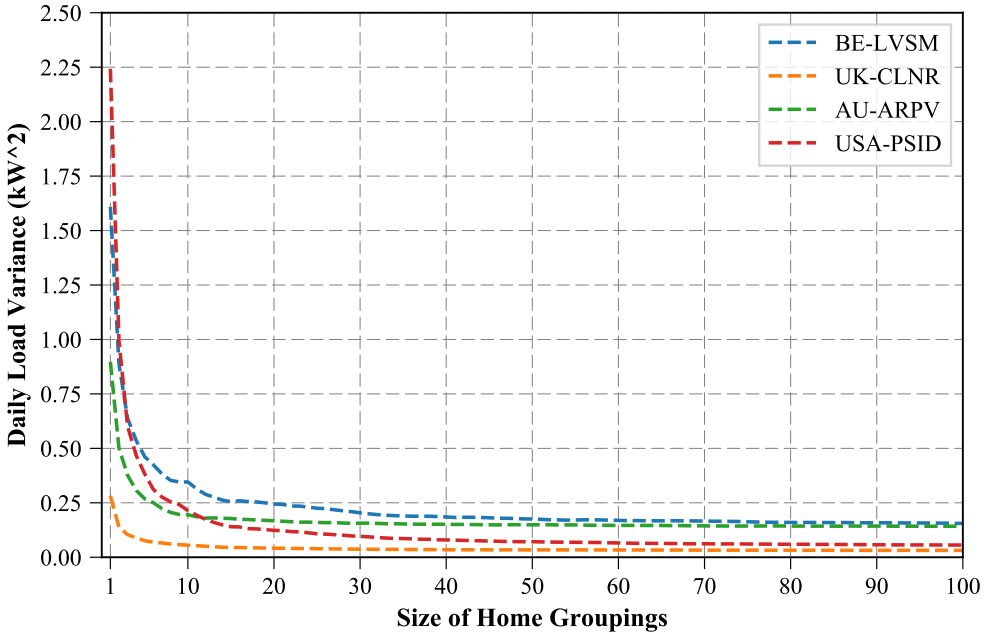

Figure 3.7: 30-minutes averaging interval: a comparison of the daily load variance over the winter seasons of the different jurisdiction areas

3.3.2.3 Load factor

While the load factor bears proxy to the expected network losses, it also reveals information about the flatness/spikiness of the load profiles. In this case, we observe

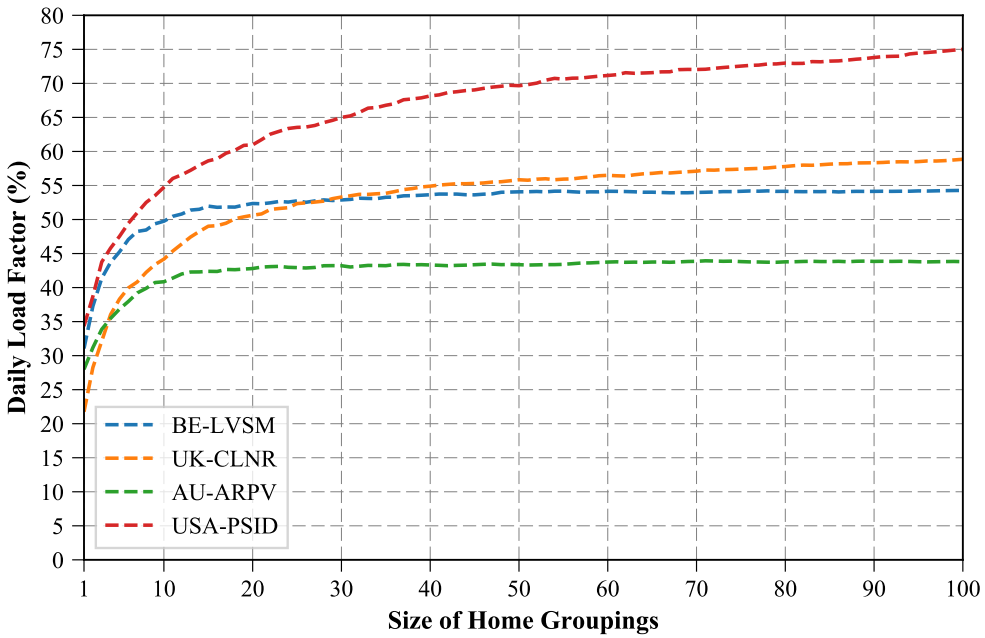

Figure 3.8: 30-minutes averaging interval: a comparison of the daily load factor over the winter seasons of the different jurisdiction areas

that the load factor shows a close correlation to the shape of the resulting aggregate load profile. A high load factor means that the load profile is significantly flat when compared to a low load factor, which suggests that the load has a peak which is widely varied from the base load. From the analyses of aggregate load profiles, we have observed that the USA-PSID dataset had a relatively flat load profile, with the AU-ARPV having the least flat profile at 100 home grouping level. This confirms the results depicted in Figure 3.8. It should be stated that an exact comparison cannot be made in relation to the expected network losses as that will depend on the calculated results from the formula defined in Equation (3.3) in Section 3.2.2.

3.3.3 Seasonal variations in the after-diversity maximum demand (ADMD), load variance, and load factor

Here, we show the USA-PSID results for the 100 home grouping level for several averaging time periods, where we observe that the ADMD, load variance, and load factor vary in accordance with seasonal influence, as illustrated in Figure 3.9, Figure 3.10, and Figure 3.11, respectively. In terms of the ADMD and load

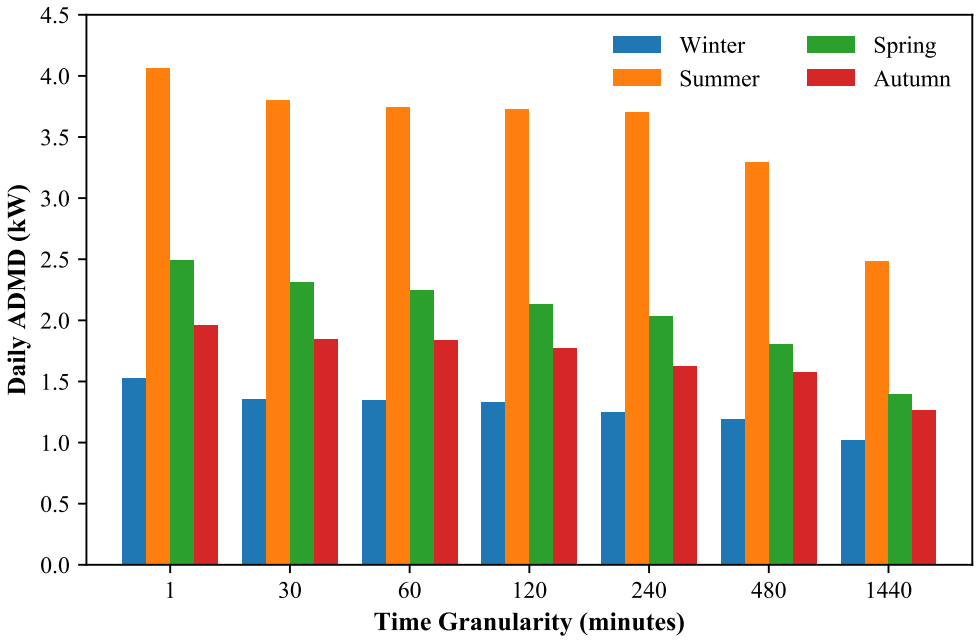

Figure 3.9: USA-PSID, 100-homes grouping: the seasonal variation of the ADMD at different averaging time intervals

variance, the order of magnitudes in ascending order is: *Winter* → *Autumn* → *Spring* → *Summer*. In terms of the load factor, the spring period shows the spikiest consumption pattern when compared to a fairly flatter consumption pattern in Winter.

The order of magnitudes of the ADMD and load variance for the BE-LVSM dataset is (ascending order): *Summer* → *Autumn* → *Spring* → *Winter*; whereas the AU-ARPV's is (ascending order): *Spring* → *Autumn* → *Summer* → *Winter*. The UK-CLNR dataset showed a somewhat identical order of magnitudes to that of the BE-LVSM dataset, but with an omission of the Autumn, as the dataset only encompassed months from January until July. This demonstrates that the energy cultures in specific jurisdiction areas differ across seasons.

These findings provide insight into a number of aspects, e.g., in which season to perform maintenance; how much the system is stressed; whether the transformers are overloaded a large percentage of the time, and so on. For instance, if the network losses are excessive or transformers overloaded, then this could indicate to the network operator that a system upgrade/reinforcement is imminent, etc.

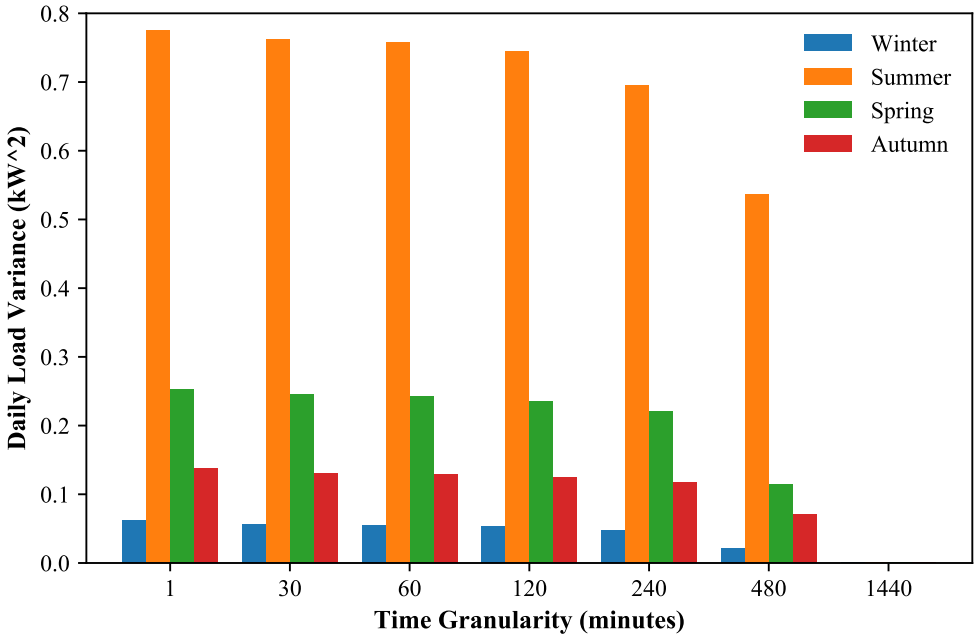

Figure 3.10: USA-PSID, 100-homes grouping: the seasonal variation of the load variance at different averaging time intervals

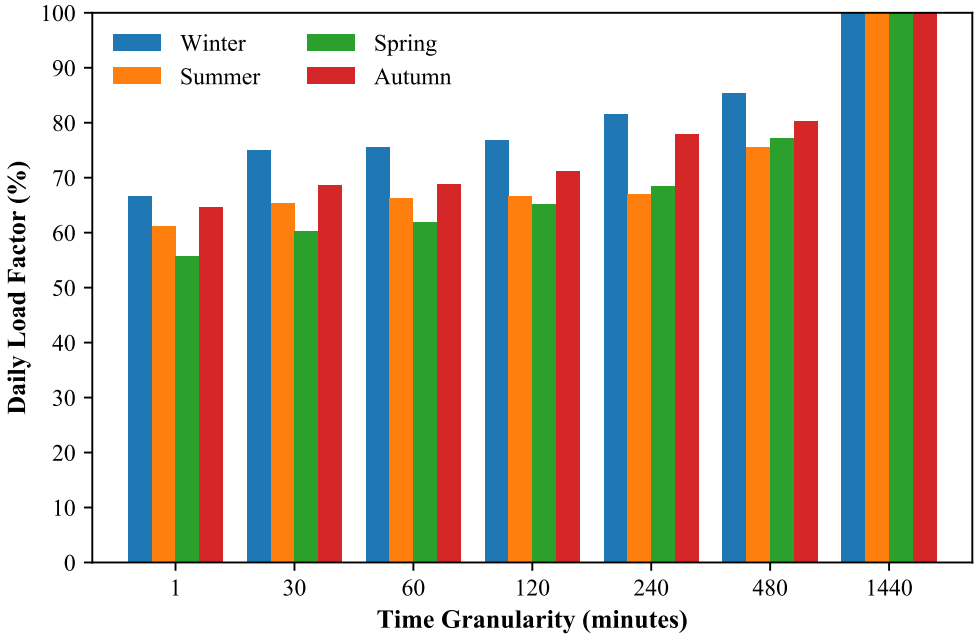

Figure 3.11: USA-PSID, 100-homes grouping: the seasonal variation of the load factor at different averaging time intervals

3.4 Concluding Remarks

This chapter proposes a spatio-temporal methodology for characterising the expected capacity and operational requirements, when customers or individual networks are interconnected at multi spatial scales. This characterisation is applied to datasets from four jurisdiction areas, which contain real load profiles sampled at different time granularities, and we are able to gain valuable insight into the required type of data to be used in estimating network design and operational parameters for planning purposes.

The after-diversity maximum demand (ADMD), load variance, and load factor have been studied in this chapter. Both the ADMD (i.e. per customer capacity requirement) and load variance asymptotically decrease toward a settling value, when both the size of customer groupings and averaging time intervals increase. Conversely, the load factor asymptotically increases toward a settling value, when both the size of home groupings and averaging intervals increase. These observations are true for all the considered jurisdiction areas. Within each of the jurisdiction areas, the ADMD, load variance, and load factor also vary from season to season, and this seasonal influence is jurisdiction-specific.

This methodology could serve as a valuable tool to network planners and operators in conducting planning and operational studies. The ADMD serves as a guidance for sizing the network infrastructure, the load variance gives insight into the selection of active network management schemes, and the load factor is useful for deriving parameters necessary for estimating the expected network losses, as well as sizing a network or feeder. As an area for future work, it will be important to explore the derivation of optimal time scales for estimating capacity and operational requirements of the network, including both grid-connected and islanded networks, in relation to load aggregation, especially in the presence of solar PV, electric vehicles, and energy storage systems.

Dependent upon the application, it is important that the time scales employed are optimally chosen in accordance with different spatial scales of the network. For

settlement of energy sharing contracts, for instance, smaller customer groupings would require longer time periods, since the variability of the aggregate load will be higher; whereas larger customer groupings may require shorter time periods as the variability of the aggregate load will be lower. Another example would be for active network management, such as voltage regulation, where shorter time scales would be required for a network with smaller customer groupings due to the resulting high variability of the aggregate load. These implications also apply to islanded networks.

Chapters 2 and 3 have provided a characterisation of customer load profiles. Chapter 4 will provide a base case characterisation of design and operational parameter of a distribution network.

The energy transition is possible and it is affordable. It is of utmost importance that we look at the transition not as a burden, but as an opportunity.

— RAINER BAAKE, *state secretary in the Economy Ministry of Germany*

Chapter 4

Characterisation of System Maximum Demand and Power Losses under Spatio-Temporal Load Aggregation on a Real Distribution Network

Contents

4.1 Introduction

The main research question for this chapter is: *Can the developed spatio-temporal characterisation framework be applied on the characterisation of design and operational parameters of a conventional electrical power system when such parameters are characterised at different customer aggregation levels when using time-series customer load data with different time granularities?*

In answering this research question, this chapter provides a demonstration of the spatio-temporal characterisation of the network ADMD, load variance, power losses, and the load-dependency loss factor of a conventional distribution network. This characterisation presents a base case scenario of these parameters when different sizes of home groupings are disconnected from the network at a time, using time-series customer load profiles with different time granularities.

Background to methods for determining network losses

There are various ways for determining the total network losses of a given power system. In a distribution network, the total network losses can be calculated as the difference between the energy injected into the network and the actual energy delivered to customers. These losses can be classified into two types, i.e., technical and non-technical losses. The former type constitutes the energy dissipated as heat in conductors and coils and from the excitation of the windings of transformers and other devices, whereas the latter is associated with discrepancies in metering and power pilferage [25, 26, 41, 43]. The different methods for determining both technical and non-technical losses have been summarised in [25, 26, 41, 43]. One of these methods computes the expected average energy losses of a network or feeder over the time period T on the basis of losses at peak demand over the time period T and the loss load factor (LLF), which is defined as the the ratio of the average energy losses to the energy losses at peak demand over the time period T [41–43]. The mathematical formulation for calculating the average energy losses is defined in Equation 3.3, Section 3.2.2. We will therefore focus on both losses and peak demand

of the power system in this chapter and in Chapter 5. The peak demand will have implications for network losses estimation in accordance with Equation 3.3, as well as a guiding parameter for determining power ratings of the network infrastructure such as transformers and circuit breakers. We characterise peak demand in a form of after-diversity maximum demand (ADMD), in the same way as we have done in Chapters 2 and 3.

Motivation for characterising network losses and peak demand

Unlike in the past, we now have the advantage of advanced techniques to accurately model real power networks for study purposes. Additionally, the modelling of customer energy consumption behaviours has also significantly improved, and we now increasingly have access to customers' smart meter data [25, 26], which we can leverage to perform planning and operational studies on real power networks. There is thus a great need to conduct a number of studies in the effort to investigate some of the issues that may arise around the effectiveness of the data used in network studies.

It is no doubt that gaining an in-depth understanding of the characterisation of how network losses vary both in relation to demand and time scales could help enable better assessments of efficient network configurations, especially when incorporating new energy resources and applications, and it could also help with implementing more agile operational techniques [44]. In addition, a thorough characterisation of distribution network losses could also offer useful insights into designing gainful ways of reducing network losses using distributed energy resources (e.g., solar photovoltaic (PV) and energy storage technologies), and other new applications such as electric vehicles [26, 45–50]. Although the characterisation of network losses and peak demand is the primary focus of this work, other major operational challenges may be more related to managing the spikes in power outputs from distributed variable energy resources and also through the use of energy storage technologies, the scope of which is not within the bounds of this thesis. One of such issues is the significance of the time granularity of load data used in performing network studies at different network load scales. Prior to the emergence of smart

meters, the energy consumption from each customer had been recorded over long time periods, even reaching up to 6-monthly or yearly time periods [44], and it is clear that this sort of slow-paced reporting time granularities will not be feasible in modern networks with active customers, whose patterns of energy consumption can change rapidly over any length of time periods.

Past works

To date, however, there is only a very limited number of studies that have attempted to consider this spatio-temporal aspect of network performance in the context of a real network with real customer load data. The authors of [24] have considered the implications of time granularity of customer load data on both planning and operational implications as case studies. The planning implications were studied in respect of the optimal selection of the conductors; whereas the operational implications were investigated in the form of benefits of load shifting to reduce peak demand. A real low voltage (LV) network model was used to study the load shifting benefits on peak reduction. Synthetic residential customer data were however used in their work. What is of interest in relation to our work is the application of the time granularity of customer load data to peak reduction on different feeders of the network. The question one would ask is that: what then happens to the conductor sizes and peak reduction on each of the feeders if we were to vary the number of customers at different time granularities? We however do not explicitly characterise the conductor sizes and peak reduction in this specific work, but we instead characterise the peak demand in relation to both reporting time granularity and load aggregation scales.

The work reported in [25] has attempted to quantify the errors that may result from using different demand data time resolutions to estimate distribution system energy losses. The key aspect is the extent to which the spikiness of the load profiles are preserved at different time resolutions due to the smoothing effect of arithmetic mean averaging. They hypothesise that an averaging period in the order of seconds would be more appropriate at a single customer level, while suggesting

that a half-hourly averaging period would be applicable for the 22 customers level. It is important to notice that this work focuses on the errors in loss estimation and not how much the losses change by when the network load is varied at different time granularities. The spikiness of the aggregate demand is also not studied in relation to variations in both the number of customers and sampling time intervals.

Another study that goes close to what we are interested in is the study published in [26], which analyses how domestic smart meter readings could be used to estimate the actual network losses, with emphasis on the time granularity of smart meter data reading intervals. Three datasets were used to investigate the accuracy of using a 30-minute reporting interval when compared to a 1-minute reporting interval. The study was performed on three different test networks, where it was found that the network losses were under-estimated by between 9% and 24% when using 30 minute data in comparison to 1 minute. The metrics for the accuracy was the absolute percentage error of the difference between the actual and predicted losses normalised over the actual losses. No variation of the size of network load was investigated. Also, no observation was made on the variation of the total system peak demand against both time granularity and network load size aspects.

Contributions of current work

The main contribution of this chapter is the *methodology to characterise the peak power and power losses on a conventional distribution network when the network customer composition is varied across different customer aggregation levels when using time-series customer load data with different time granularities.* An additional contribution of these chapters is the *new theoretical parameter, termed: load-dependency loss factor, which is introduced as a metric for characterising the variations in the power losses of a conventional distribution network in relation to the change in customer load composition of the network.*

Chapter structure

We define the study setup, including the test network and the datasets used, in

Section 4.2. The methodology used in the study is detailed out in Section 4.3, followed by the results and discussions in Section 4.4. Key observations will then be summarised in Section 4.5.

4.2 Test Network and Load Profiles Dataset

This section provides details of the study setup, including the test network and the time-series load profiles used in this study. We first present details of a typical UK low-voltage (LV) network used as a test network, and we then explain the characteristics of the load profiles added to the test network as a simulation of real customer energy consumption patterns.

4.2.1 Test network

Since the main objective of this work is to study the variation of specific network design and operation parameters, it was important to use a realistic network, comprising realistic customer behaviour. The load profiles descriptive of real customer behaviour are described in Section 4.2.2. We therefore chose to use one of the network topologies which represent real low voltage (LV) networks based in North West of England, under the jurisdiction of Electricity North West Limited (ENWL). A total of 25 LV networks (comprised of 131 LV distribution feeders, 5952 customers, and about 172km of LV cables) were developed as a part of the Low Carbon Network Fund Tier 1 project, referred to as the LV Network Solutions (LVNS) project [51]. The development of these network models was a joint project by ENWL and the University of Manchester, which ran between 2012 and 2014.

The University of Manchester built these LV network models from the GIS network and policy data (lengths, connectivity and impedances) and GIS customer data (types and locations) provided by ENWL. These GIS data were then implemented into the open-source distribution system simulator (OpenDSS) modelling platform to generate the LV network models, representative of typical UK LV networks. OpenDSS is a frequency-domain simulation software, whose special features allow researchers and engineers to create models for electric power distribution systems in order to carry out multi-phase power flow simulations for planning and operational analyses [52]. The models were validated using monitoring data obtained from the actual networks.

The test network used in this work is therefore the 11/0.4 kV LV feeder, which comprises 21 load connection points, and it is depicted in Figure 4.1. These designated 21 connection points will allow for the incorporation of real customer power consumption profiles.

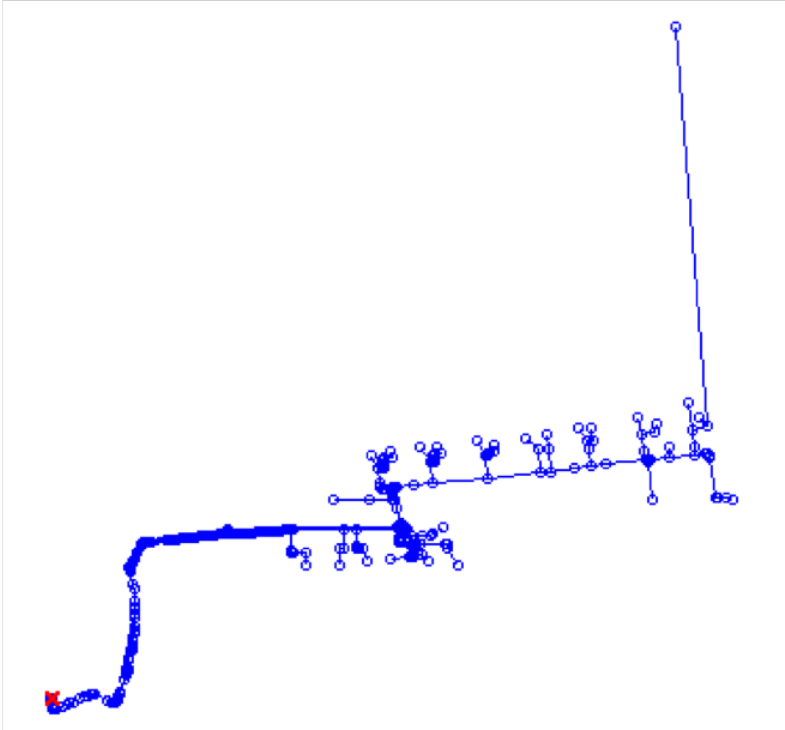

Figure 4.1: Graphical representation of the real low voltage (LV) test feeder, based on a typical UK distribution network [51].

4.2.2 Load profiles dataset

For purposes of demonstrating the proposed methodology in this chapter, a dataset representative of UK homes was used to mimic the real power consumption characteristics of customers to be connected onto the test network described in Section 4.2.1 (as shown in Figure 4.1). This dataset has a 1-minute original time granularity. The view is to use real customers load profiles on a real network, and, since the test network is representative of a UK feeder, it is fitting to adapt the UK-CLNR data for this study. Details about this dataset are given in Section 3.2.1.1 (Chapter 3, Page 37).

4.3 Methodology

In order to obtain the numerical results for the characterisation of the network ADMD, load variance, average power losses, and the load-dependency loss factor, we must model a representation of the network and the load characteristics that would mimic the power consumption patterns of the customers. Both the network model and load characteristics have already been described in Sections 4.2.1 and 4.2.2, respectively.

As already mentioned, the modelling of the low voltage test network, depicted in Figure 4.1, was implemented in the OpenDSS tool. This tool was mainly used to run the load flows to determine operational parameters of the network. Whereas OpenDSS' capability to implement customised control algorithms is limited, there is an advantage that control commands can be passed onto OpenDSS to drive a simulation via the COM interface functionality. OpenDSS simulations can be driven via the COM interface using external programs such as Matlab, Excel, C#, and Python [51]. We therefore used Python to implement the spatio-temporal algorithm to characterise the variations in peak demand and power losses when varying the total connected customers, using customer load profiles with different time granularities.

The block diagram representation of the OpenDSS-Python COM interface operation is illustrated in Figure 4.2, where the seamless processes that occur between OpenDSS and Python programs are demonstrated.

It is important to note that the integral methodology used in this specific study is based on the Monte Carlo based spatio-temporal framework outlined in both Figures 2.2 and 3.1 on Pages 26 and 39, respectively. The simulations were performed as detailed in the step-by-step algorithm below:

- ***Step 1: Input data pre-processing***

  Here, we prepare the load profiles dataset to ensure that only the time-series load profiles which are non-zero and non-negative all through the 24-hour period are preserved. Since this section pertains to the base case, where no renewable energy or smart appliances are connected to the network, we must

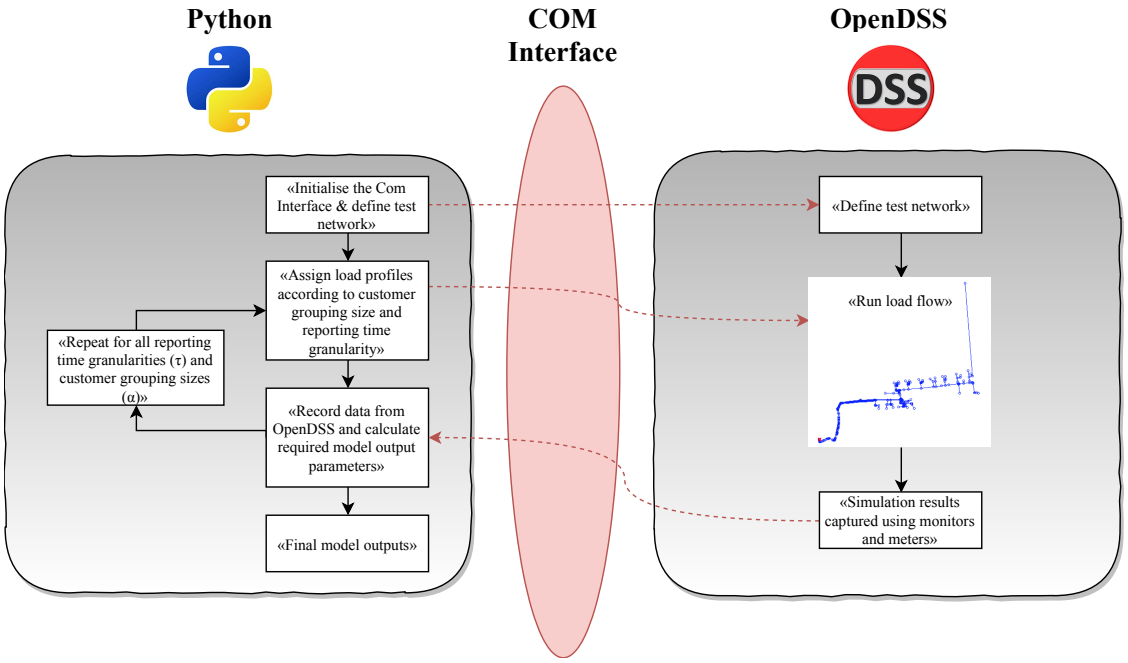

Figure 4.2: The high level visualisation of the COM interface operation between OpenDSS and Python programs

ensure that we are including customers who are active and without net energy generation. The pre-processed dataset is then converted to different reporting time granularities, equivalent to the 1-minute original time granularity datasets defined in Table 3.1 (Chapter 3, Page 42) for the UK-CLNR & USA-PSID datasets. These profiles will then constitute the dataset from which input to the algorithm will be drawn.

- ***Step 2: Consider different reporting time granularities,*** τ

  We now start the OpenDSS COM interface via the DSS text command from Python to define the test circuit and data measurement setup. For each reporting time granularity, τ, we randomly select a sub-dataset equal to the number of load points on the circuit, and assign these to all the load points on the network. We then run a time-series load flow with all loads connected, and record the total power supply, demand, and losses at each time instant, which we refer to as the time-series power supply, demand, and losses as $P_{S_o,t}^{(base),\tau}$, $P_{D_o,t}^{(base),\tau}$, and $P_{L_o,t}^{(base),\tau}$, respectively.

- ***Step 3: Consider different customer aggregation levels,*** α

  For every aggregation level, α, we consider disconnecting α loads at a time, and then re-run a load flow and measure the total power supply, demand, and losses for the respective reporting time granularities. In order to determine the number of possible combinations of such customer grouping size, we would need to calculate the possible number of combinations of α customers out of the total number of load points on the network, which, for a 21-loads network, we denote as C_{α}^{21}. In the particular case of a 21-loads network, an aggregation level of 1 customer would yield 21 possible combinations, whereas aggregation levels 3, 10, and 19 would yield 1330, 352716, and 210 possible combinations, respectively. For purposes of conserving computation time, we limit combinations to a maximum of 100 customer grouping possibilities (which have been found to give reasonable Monte Carlo errors), achieved by generating these combinations without repetition. This means that these possible combinations will represent the number of Monte Carlo trials, $k_{C_{\alpha}^{21}}$, for a given aggregation level, α, and we determined the number of trials as follows:

$$k_{C_{\alpha}^{21}} = \begin{cases} C_{\alpha}^{21} & C_{\alpha}^{21} < 100 \\ 100 & C_{\alpha}^{21} \geq 100 \end{cases}$$

  We calculate C_{α}^{21}, the number of combinations without repitition, as defined in Equation 4.1.

$$C_{\alpha}^{21} = \frac{21!}{\alpha(21-\alpha)!} \tag{4.1}$$

  We thus denote the measured parameters as $P_{S_{\alpha},t}^{(base),\tau}$, $P_{D_{\alpha},t}^{(base),\tau}$, and $P_{L_{\alpha},t}^{(base),\tau}$, respectively. At the end of the $k_{C_{\alpha}^{21}}$ Monte Carlo trials for a given aggregation level, α, at a reporting time granularity, τ, we obtain the matrices containing the measured parameters, which we denote as $P_{S_{\alpha},k,t}^{(base),\tau}$, $P_{D_{\alpha},k,t}^{(base),\tau}$ or $P_{L_{\alpha},k,t}^{(base),\tau}$. These matrices will take on the form defined below, as per the example of the total power supply, $P_{S_{\alpha},k,t}^{(base),\tau}$:

$$\left(\begin{array}{c|cccc} & k = \textit{Trial 1} & k = \textit{Trial 2} & \dots & k = \textit{Trial } k_{C_\alpha^{21}} \\ \hline t=1 & P_{S_\alpha,1,1}^{(base),\tau} & P_{S_\alpha,2,1}^{(base),\tau} & \dots & P_{S_\alpha,k_{C_\alpha^{21}},1}^{(base),\tau} \\ t=2 & P_{S_\alpha,1,2}^{(base),\tau} & P_{S_\alpha,2,2}^{(base),\tau} & \dots & P_{S_\alpha,k_{C_\alpha^{21}},2}^{(base),\tau} \\ \vdots & \vdots & \vdots & \vdots & \vdots \\ t=T_\tau & P_{S_\alpha,1,T_\tau}^{(base),\tau} & P_{S_\alpha,2,T_\tau}^{(base),\tau} & \dots & P_{S_\alpha,k_{C_\alpha^{21}},T_\tau}^{(base),\tau} \end{array}\right).$$

- ***Step 4: Compute the metrics of interest***

  The metrics of assessment are the daily values of the *ADMD*, *load variance*, *average losses*, and the *load-dependency loss factor*, and we compute a representative value of each of these metrics respectively for each reporting time granularity and aggregation level over a given day. The mathematical formulations for calculating these metrics are given in Equations 4.2, 4.3, 4.5 & 4.6, respectively.

  – *After-diversity maximum demand (ADMD)*

  Equation 4.2 defines the diversified peak of the total power that must be supplied to the customers connected on the network. Notice that ${}_{peak}S_\alpha^{(base),\tau}$ includes both the actual power demand by customers, plus the power losses associated with delivering power to the customer load points.

$${}_{peak}S_\alpha^{(base),\tau} = max\Big|_{k=1}^{k_{C_\alpha^{21}}}\left(max\Big|_{t=1}^{T_\tau}\left(P_{S_\alpha,k,t}^{(base),\tau}\right)\right) \tag{4.2}$$

  – *Load variance*

  The variability of the total demand on the network is defined in Equation 4.3. The interest here is to characterise the variability of the amount of power to be supplied by the distribution network to customers at various time scales and aggregation levels.

$$VAR_\alpha^{(base),\tau} = \frac{1}{k_{C_\alpha^{21}}}\sum_{k=1}^{k_{C_\alpha^{21}}}\left(\frac{1}{T_\tau}\sum_{t=1}^{T_\tau}\left(P_{S_\alpha,k,t}^{(base),\tau} - MEAN_\alpha^{(base),\tau}\right)^2\right), \tag{4.3}$$

  where $MEAN_\alpha^{(base),\tau}$ (in kW) is given by:

$$MEAN_\alpha^{(base),\tau} = \frac{1}{k_{C_\alpha^{21}}}\sum_{k=1}^{k_{C_\alpha^{21}}}\left(\frac{1}{T_\tau}\sum_{t=1}^{T_\tau}\left(P_{S_\alpha,k,t}^{(base),\tau}\right)\right). \tag{4.4}$$

– *Average power losses*

The next parameter to calculate is the power losses when different customer grouping sizes are considered at different time scales, which we denote as $L_{\alpha}^{(base),\tau}$, as defined in Equation 4.5. We calculate the total power losses as the difference between the total power injected into the network and the power delivered to the loads.

$$L_{\alpha}^{(base),\tau} = \frac{1}{k_{C_{\alpha}^{21}}} \sum_{k=1}^{k_{C_{\alpha}^{21}}} \left(\frac{1}{T_{\tau}} \sum_{t=1}^{T_{\tau}} \left(P_{S_{\alpha},k,t}^{(base),\tau} - P_{D_{\alpha},k,t}^{(base),\tau} \right) \right) \tag{4.5}$$

– *Load-dependency loss factor*

At a given time granularity, we can calculate the change in losses at various aggregation levels in relation to losses at full load. The power losses at full load are denoted as $L_{o}^{(base),\tau}$. The differential change in losses is thus given as a ratio to the total demand at full load, $D_{o}^{(base),\tau}$, in order to quantify how this change in losses implicitly compares to the differential change in network load when varying aggregation levels, and hence referring to this metric as the load-dependency loss factor.

We calculate the load-dependency loss factor, $\delta L_{\alpha}^{(base),\tau}$, in accordance with Equation 4.6.

$$\delta L_{\alpha}^{(base),\tau} = \left(\frac{L_{o}^{(base),\tau} - L_{\alpha}^{(base),\tau}}{D_{o}^{(base),\tau}} \right) \times 100 \tag{4.6}$$

where $L_{o}^{(base),\tau}$ and $D_{o}^{(base),\tau}$ are defined according to Equations 4.7 & 4.8, respectively.

$$L_{o}^{(base),\tau} = \frac{1}{T_{\tau}} \sum_{t=1}^{T_{\tau}} \left(P_{S_{o},k,t}^{(base),\tau} - P_{D_{o},k,t}^{(base),\tau} \right) \tag{4.7}$$

$$D_{o}^{(base),\tau} = \frac{1}{T_{\tau}} \sum_{t=1}^{T_{\tau}} \left(P_{D_{o},k,t}^{(base),\tau} \right) \tag{4.8}$$

- ***Step 5: Final results***

At the end of the simulation, covering all reporting time granularities and aggregation levels, we obtain the matrices of the daily diversified peak demand

$({}_{peak}S_{\alpha}^{(base),\tau})$, daily load variance $(VAR_{\alpha}^{(base),\tau})$, daily average power losses $(L_{\alpha}^{(base),\tau})$, and the load-dependency loss factor $(\delta L_{\alpha}^{(base),\tau})$ in the form:

$$\left(\begin{array}{c|cccc} & \alpha = \textit{Aggregation 1} & \alpha = \textit{Aggregation 2} & \dots & \alpha = \textit{Aggregation 20} \\ \hline \tau = \tau_1 & \blacksquare & \blacksquare & \dots & \blacksquare \\ \tau = \tau_2 & \blacksquare & \blacksquare & \dots & \blacksquare \\ \vdots & \vdots & \vdots & \vdots & \vdots \\ \tau = \tau_n & \blacksquare & \blacksquare & \dots & \blacksquare \end{array}\right),$$

where $\blacksquare$ will comprise ${}_{peak}S_{\alpha}^{(base),\tau}$, $VAR_{\alpha}^{(base),\tau}$, $L_{\alpha}^{(base),\tau}$ and $\delta L_{\alpha}^{(base),\tau}$, respectively.

4.4 Results and Discussions

In Chapters 2 and 3, we had calculated the specific metrics of assessment when aggregating load profiles with different time granularities using the spatio-temporal framework, where we used synthetic data in Chapter 2, and confirmed the same findings using real data from four different jurisdiction areas in Chapter 3. The results in Chapters 2 and 3 were obtained from studies based on load profiles alone. In this chapter, we are interested in examining how the specific metrics of assessment vary on a real network with real customers behaviour, under the same framework of temporal load aggregation. The aim is to consolidate the spatio-temporal framework with observations from realistic scenarios based on a real power network. The results for the specific parameters described in Section 4.3 are outlined in Sections 4.4.1 to 4.4.4.

4.4.1 After-diversity maximum demand

The characterisation of the network ADMD was performed on a network with 21 load points, where different sizes of home groupings were disconnected at a time, using load profiles with different time granularities. As evident in Figures 4.3 and 4.4, the ADMD variation trends are exactly as was observed in the previous chapters using load profiles studies. It is clear from these figures that the diversified maximum demand on the network decreases as both the size of home groupings on the network and the time granularity of load profiles used tend to larger magnitudes. This observation is summarised in the contour plot in Figure 4.5, where both the temporal and aggregation effects on the ADMD are illustrated. Looking at Figure 4.3, we can pick the uppermost trendline, which gives the ADMD variation against the size of home groupings for load profiles with a 1-minute time granularity. We can observe that when 20 homes were disconnected from the network, which represents a 1-home aggregation level, an ADMD level of about 7kW was obtained. However, when less homes are disconnected, meaning more homes connected at a time, the ADMD gradually drops to lower levels. For the same time granularity of 1 minute,

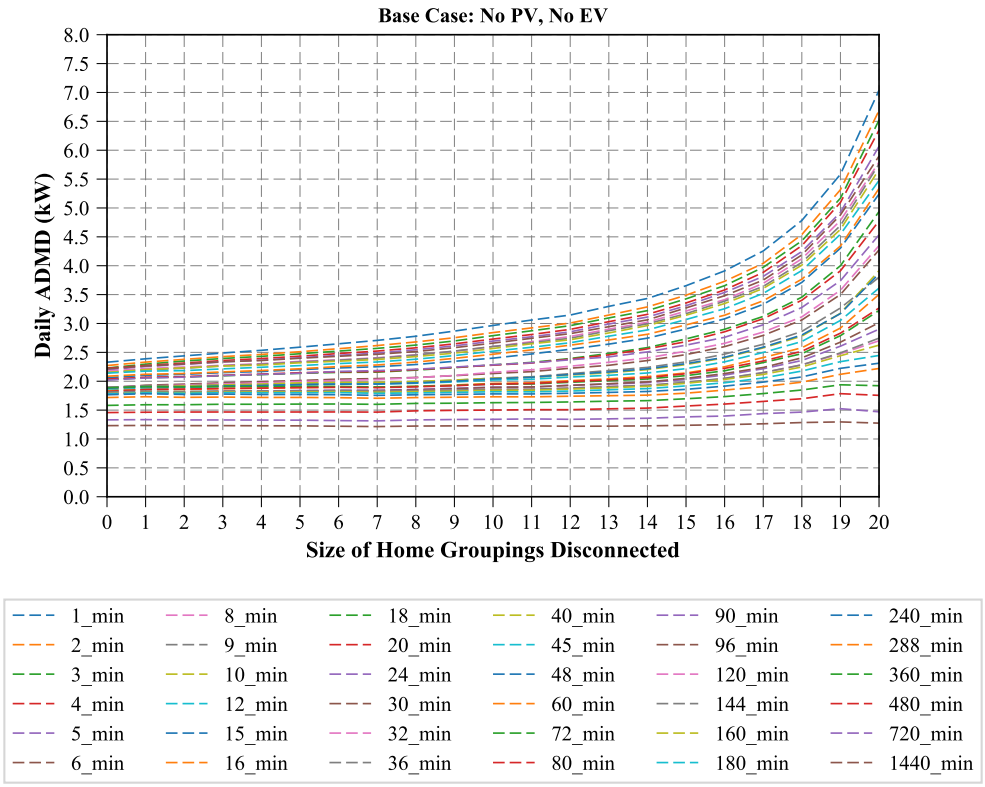

Figure 4.3: The network ADMD versus aggregation levels across different time granularities

an ADMD level of 2.3kW is attained when all the 21 homes are connected (i.e., when zero (0) homes are disconnected) on the network. This is a difference of about 66% in the ADMD figures between a network with 1 home and that with 21 homes.

For longer reporting time granularities, such as 360 minutes (6 hours), 480 minutes (8 hours), 720 minutes (half a day), and 1440 minutes (a day), we note that the ADMD levels remain almost invariant over the different sizes of home groupings. This highlights that using load data with long time granularities can yield to underestimated ADMD levels. In Figure 4.3, for instance, if we take the case of having 20 homes disconnected (i.e., having one (1) home connected on the network at a time), the ADMD level would be underestimated by a percentage of 81.9%, if we use the 1440-minute time granularity when compared to the 1-minute granularity. In fact, for this particular scenario of having one (1) home connected on the network at a time, from time granularities above 10 minutes, the ADMD values would be underestimated by over 20%.

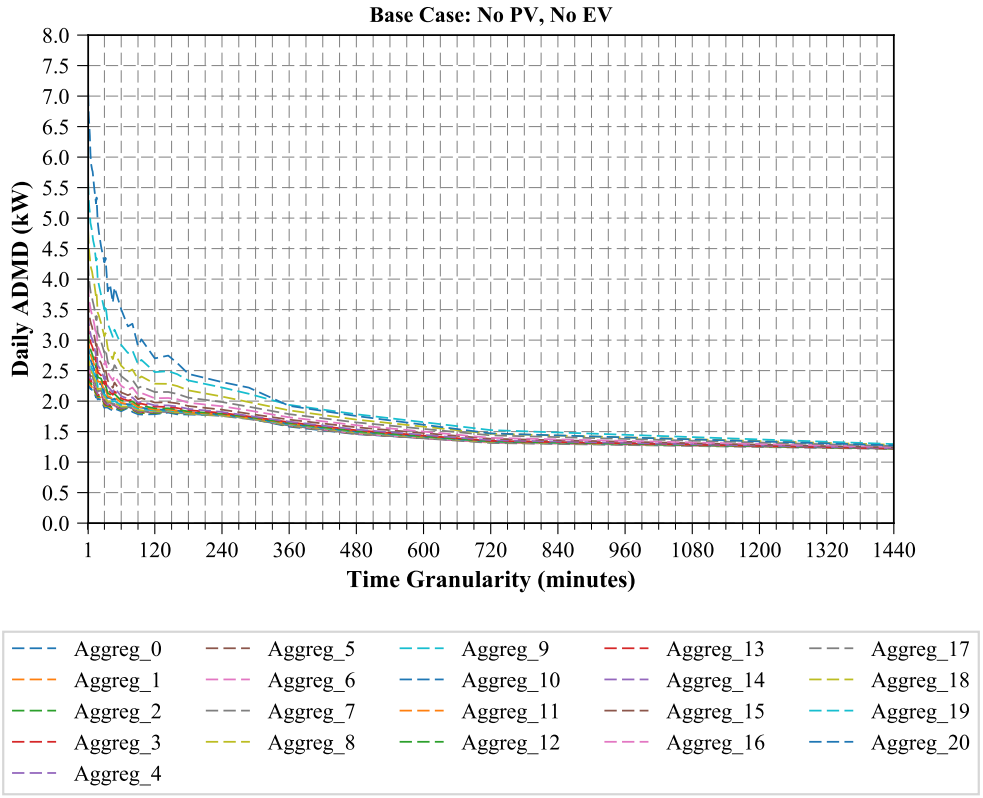

Figure 4.4: The network ADMD versus time granularities across different aggregation levels

For cases where a sizeable number of homes are connected on the network, the estimation errors are minimal. This is due to the law of large numbers allowing for the estimated values to converge toward the true value. The ADMD variation across time granularities however still remains the same, i.e., the values are underestimated (or lower) at longer reporting time granularities.

4.4.2 Load variance

Here we examine the variability of demand on the network when different sizes of home groupings are varied using load profiles with different time granularities. The results presented in Figure 4.6 show that the demand becomes less variable when the number of customers connected on the network increases. This trend is true for all the time granularities. As expected, the aggregate demand on the network becomes smoother as more customers become connected on the network, and the

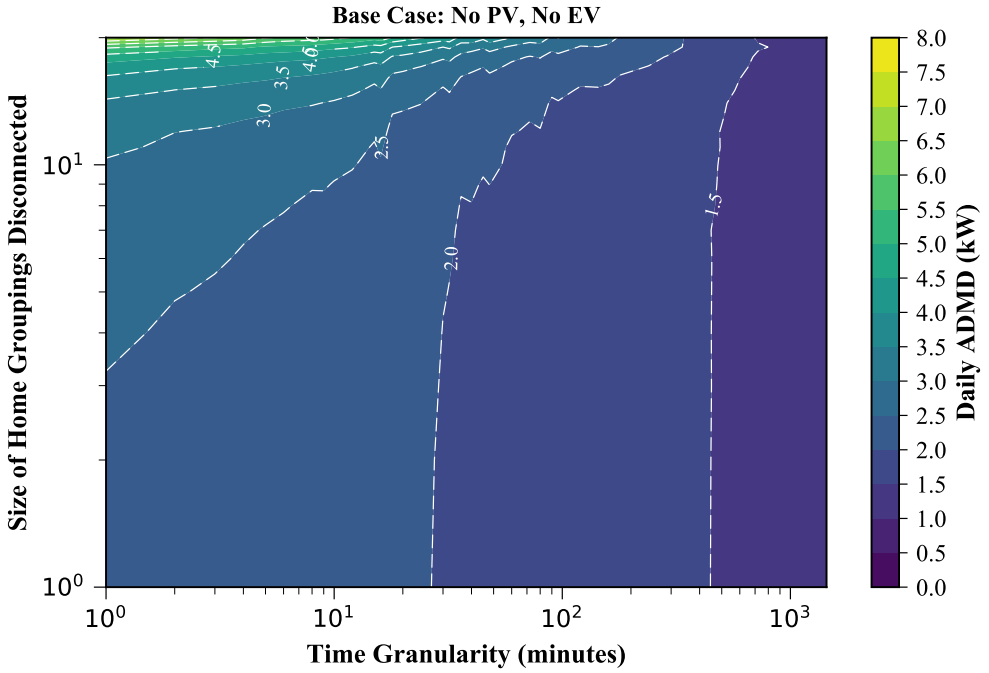

Figure 4.5: The diversified maximum demand as a function of the size of customer groupings connected on the network and the time granularity of load profiles

non-coincident occurrence of instances of high demands for individual homes cancel out; thereby resulting in a less variable aggregate load profile.

The effect of the time granularity of load profiles used is also visible in Figure 4.7, where the variability of the network demand gradually decreases with the increasing reporting time granularities. This is a result of the temporal averaging effect that masks out the higher demand instances.

For a given level of load aggregation, different load variability levels are obtained when different time granularity load profiles are used. For example, when twenty (20) homes are disconnected from the network (i.e., having one (1) home connected at a time), we obtain a load variance of 1.52kW^2 at a 1-minute granularity and 0.20kW^2 at a larger time granularity of 720 minutes (12 hours).

With reference to Figure 4.8, we also note that for a given contour line, which represents a particular level of demand variability, we get different time scales for different sizes of home groupings. This shows the significance of choosing optimal time scales for specific operational network schemes.

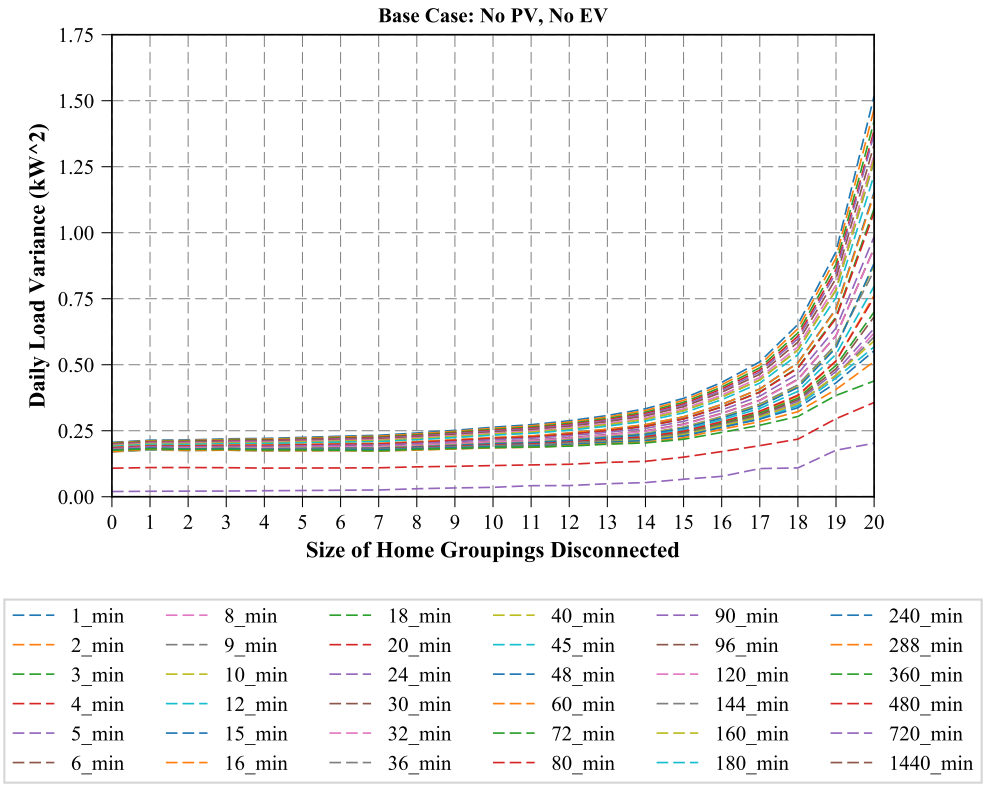

Figure 4.6: The network load variance versus aggregation levels across different time granularities

4.4.3 Average power losses

The results for the characterisation of average losses on the network are summarised in Figure 4.9 for the aggregation effects and in Figure 4.10 for the temporal effects.

In terms of the effect of the size of home groupings connected on the network, the results trends are as expected, i.e., obtaining higher losses when larger numbers of customers are connected on the network. This is evident from the graph shown in Figure 4.9, where we observe that the average losses decrease as more homes are disconnected from the network.

In Figure 4.10, we can see that lower levels of average losses are obtained when load profiles with larger time granularities are used. What comes out very prominently from this graph (Figure 4.10) is that the accuracy of determining network power losses can be compromised, if the correct time granularity load profiles are not used. For instance, if we take the zero (0) aggregation level

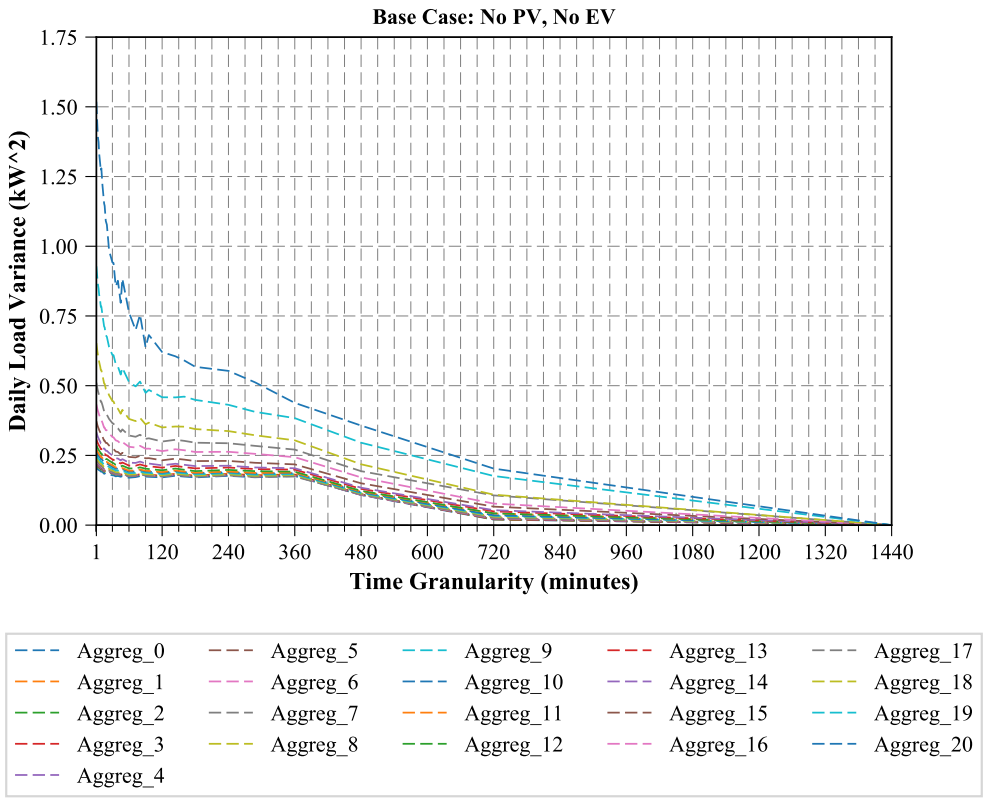

Figure 4.7: The network load variance versus time granularities across different aggregation levels

(i.e., having all the 21 loads connected on the network), we obtain 274W average losses when using a 1-minute time granularity and 200W for a 1440-minute time granularity. Considering that the 1-minute time granularity gives the best estimate of the losses, using the 1440-minute time granularity yields an underestimation of the losses by 27% for the scenario with full loads connected on the network. For the case of having one (1) home connected on the network, we obtain 7.2W for the 1-minute time granularity and 4.2W for the 1440-minute time granularity, which represents an underestimation of 42%.

What we observe is that significant underestimation of network losses occurs when we use load profiles with larger time granularities. However, we also note that the underestimation is even more pronounced when we do a calculation of network losses on a network with fewer customers connected on the network due to the corresponding higher variability in the demand, as we established in Section 4.4.2.

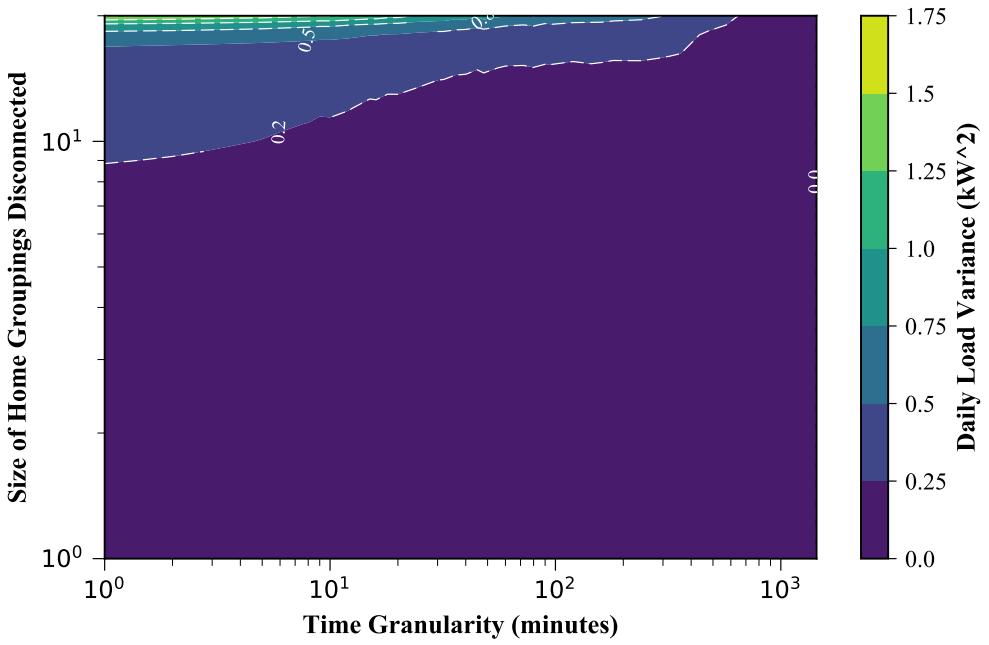

Figure 4.8: A characterisation of the demand variability when different customer grouping sizes are connected on the network using load profiles with different time granularities

Thus, if we use larger time granularities on a network with a high load variability, we will end up with pronounced underestimations of the network losses due to the masking out of significant demand occurrences.

4.4.4 Load-dependency loss factor

For this assessment metric, we are interested in the change in losses in relation to losses at full load when varying the size of home groupings of customers and when considering different time granularities. The key aspect is to quantify how much the differential change in demand contributes to the change in losses, as defined in Equation 4.6, which we term load-dependency loss factor. The characterisation of the load-dependency loss factor is given in Figures 4.11 and 4.12 for the aggregation and temporal effects, respectively.

From the characterisation of average losses explained in Section 4.4.3, we have observed that the more homes we connect on the network, the more average losses we obtain, which is a very intuitive observation. Therefore, in relation to Equation 4.6,

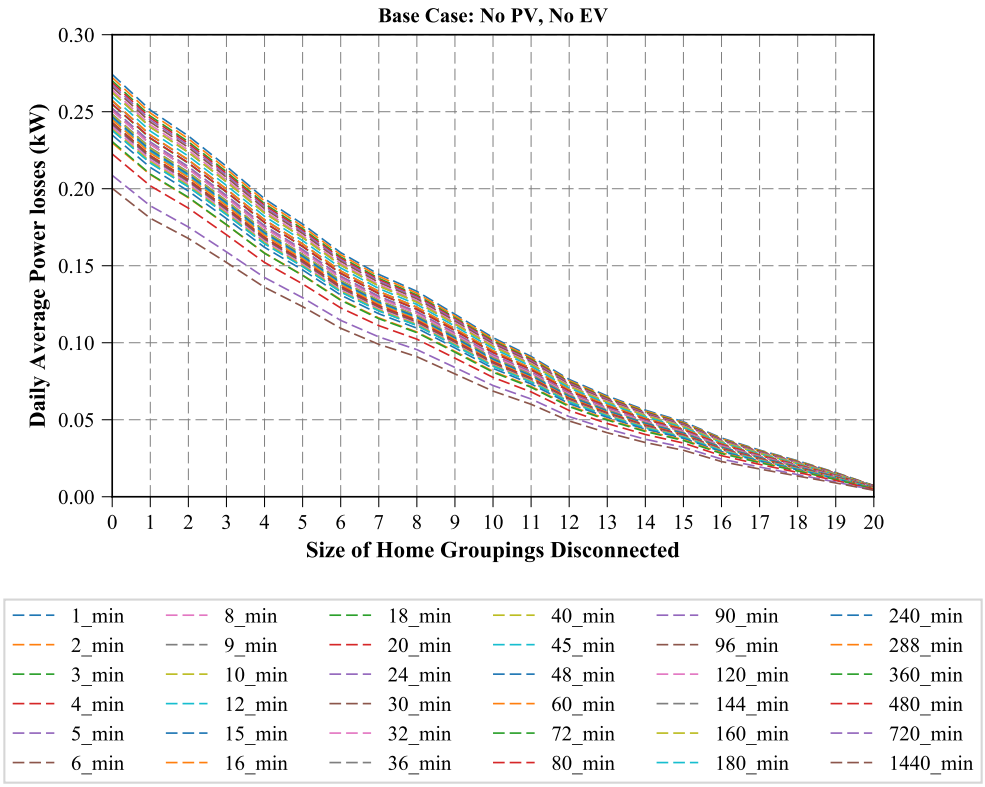

Figure 4.9: The network average losses versus aggregation levels across different time granularities

the $L_o^{b,\tau}$ term will constitute the highest losses when all loads are connected on the network, and the $L_\alpha^{b,\tau}$ term will always yield lower losses as the α magnitude increases. This means we get less losses when more homes are disconnected from the network. As a result, the numerator term of Equation 5.2 (i.e., $L_o^{b,\tau} - L_\alpha^{b,\tau}$) continues to increase with increasing α (number of homes disconnected from the network) values. This is what is depicted in Figure 4.11, where we observe that the load-dependency loss factor increases with the increasing size of home groupings disconnected from the network.

In practical terms, it is intuitive to expect a significant change in losses when a large amount of demand is shed from the network. At least this is true for a network with conventional energy resources. Chapter 5 investigates how this changes when we add new energy resources.

Again, the importance of time granularity is highlighted in Figure 4.12, where we see that lower load-dependency loss factors are obtained at larger time granularities,

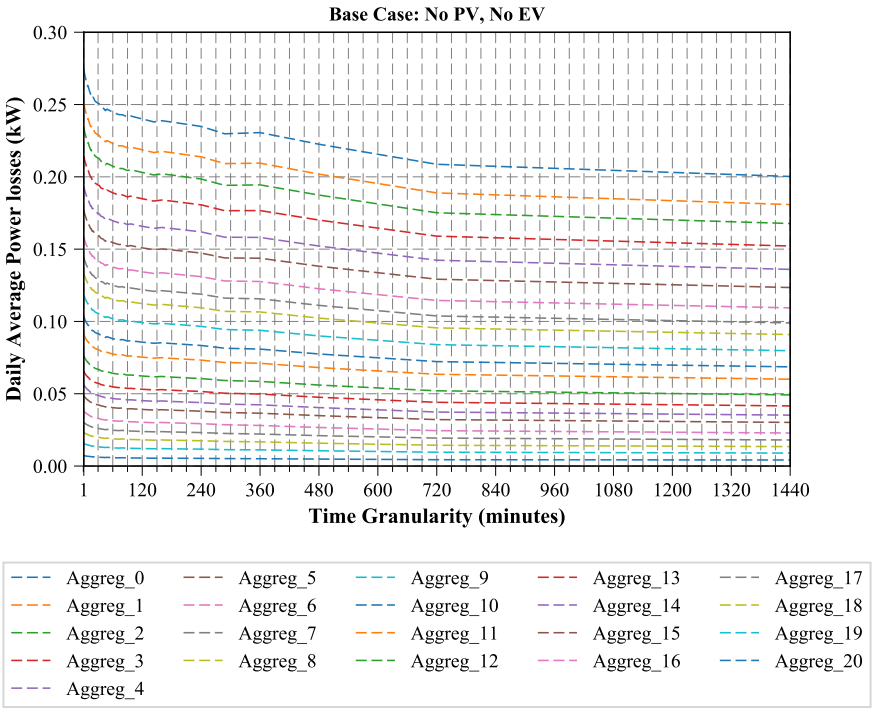

Figure 4.10: The network average losses versus time granularities across different aggregation levels

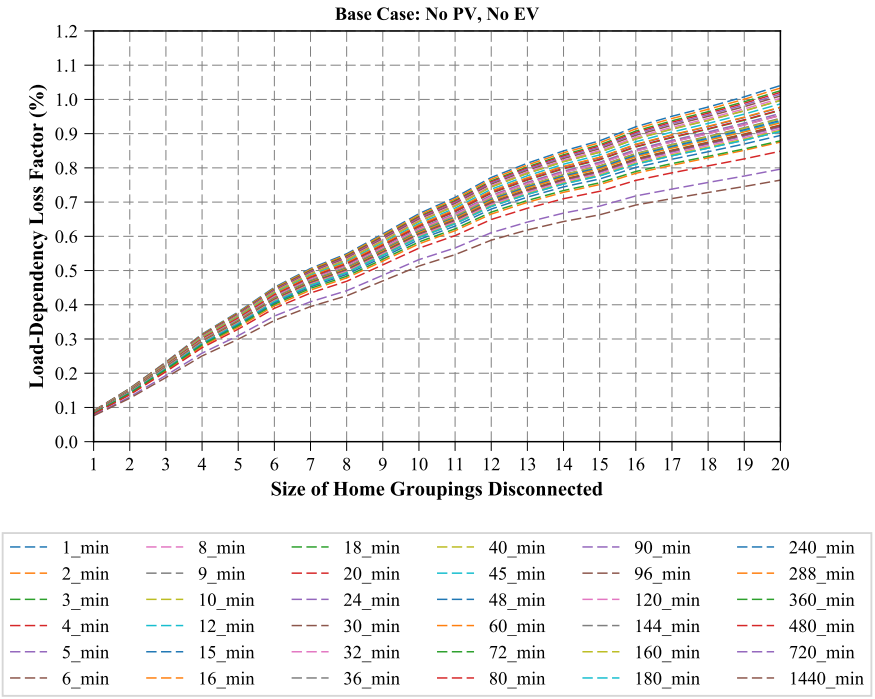

Figure 4.11: The network load-dependency loss factor versus aggregation levels across different time granularities

which represents an underestimation of the change in losses when the size of network demand is varied.

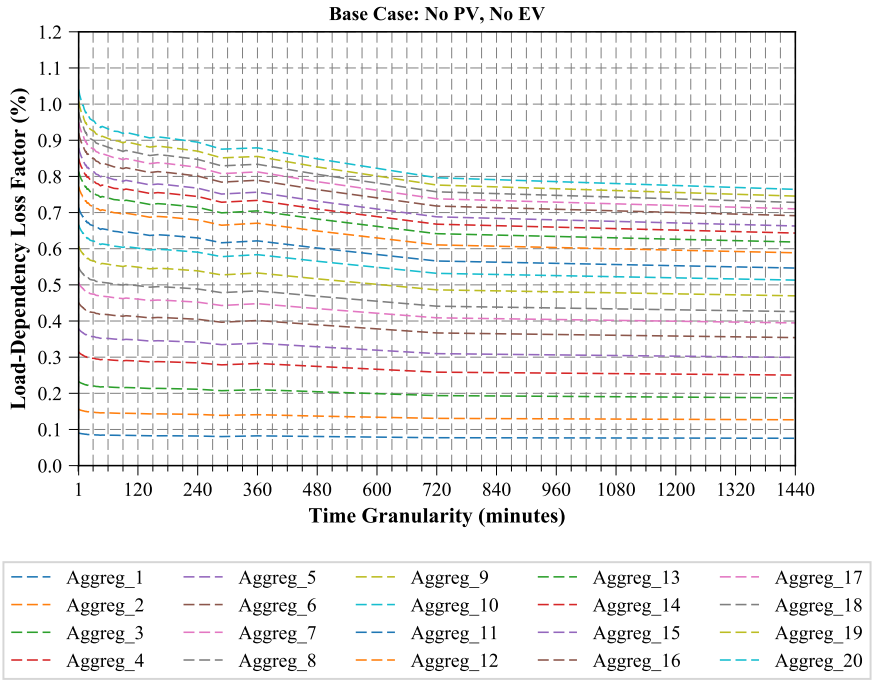

Figure 4.12: The network load-dependency loss factor versus time granularities across different aggregation levels

4.5 Concluding Remarks

This chapter provides a demonstration of the spatio-temporal framework on a network with 21 load points, where different sizes of home groupings were disconnected at a time, using load profiles with different time granularities. A characterisation of the network ADMD, load variance, average power losses, and the load-dependency loss factor was performed under temporal load aggregation.

Both the ADMD and load variance characterisations are in agreement with the observations made from the studies reported in Chapters 2 and 3. The per-customer capacity requirement (ADMD) and the load variability (load variance) both decrease with the increasing aggregation level of customers connected on the network and the time granularity of the load profiles used in performing the analysis.

The average power losses on the network increase with the increasing number of customers connected on the network, whereas the average power losses decrease with the increasing time granularity of the load profiles. This is an intuitive observation for a network with conventional energy resources.

We have also found that a large amount of change in demand yields a correspondingly high change in losses on the network, and this is what the load-dependency loss factor quantifies. The following chapter will investigate how this changes when we add new energy resources.

In all the observations made in respect of the considered parameters, the aspect of the time granularity of load profiles used has come out very prominently. High levels of underestimation of parameters occur when large time granularities are used. This calls for a reconsideration of the common practice of traditional time scales used in current power system applications, whether in billing, contract agreements, load scheduling or control, in view of significant errors in estimates that may occur.

This chapter sets the base for the analyses that will follow in Chapter 5, where we will consider the spatio-temporal characterisation of the network ADMD, average power losses, and the load-dependency loss factor under the presence of solar photovoltaic (PV) and electric vehicles. The load variance will not be considered in

Chapter 5 as this parameter can be implicitly observed in all the other parameters, whereby the variability in the load (and also in all the other parameters) decreases with increasing sizes of home groupings and longer averaging temporal effects. We will therefore only concentrate on the network ADMD, average power losses, and the load-dependency loss factor in the following chapter.

We need a system that "makes centralised resources, like power plants and bulk storage, and decentralised resources, like rooftop photovoltaics, truly complementary."

— VERA SILVA, *chief technology officer at GE Grid Solutions*

Chapter 5

Spatio-Temporal Characterisation of the Impacts of Solar Photovoltaic (PV) and Electric Vehicles (EVs) on the Distribution Network

Contents

5.1 Introduction

This chapter builds on the spatio-temporal characterisation of the network design and operational parameters described in Chapter 4, where we characterised the network after-diversity maximum demand (ADMD), load variance, average power losses, and the load-dependency loss factor, when different sizes of home groupings were disconnected from the network at a time, using load profiles with different time granularities. The characterisation presented in Chapter 4 considered the base case scenario, where all homes connected on the network had no renewable energy resources or new energy applications installed.

In this chapter, we will characterise the impact of integrating renewable energy resources and new energy applications onto the network. We will thus consider two case studies, namely: the impacts of the integration of (1) *solar PV* and (2) *electric vehicles (EVs)* onto the network in relation to both the design and operational aspects of the network. Under each of these case studies, we will consider two different scenarios.

As extension of the work presented in Chapter 4, this chapter explores the research question: *Can the spatio-temporal characterisation framework be useful for characterising peak power and power losses on a real electrical power system with a high presence of distributed variable energy resources and smart appliances?*

The main contribution of this chapter is the *methodology to characterise the peak power and power losses on a distribution network when the penetration level of distributed variable energy resources and smart appliances is varied across different customer aggregation levels when using time-series customer load data with different time granularities.* An additional contribution is *the use of the load-dependency loss factor, which is a new theoretical parameter, as a metric for characterising the impact of solar PV and plug-in electric vehicles on a distribution network.*

We first present a description of the study setup in Section 5.2, where we specify details about the test network, as well as the time-series profiles adopted for the simulation of the scenarios considered in the study. Case studies designations and

the methodologies for specific study scenarios are then explained in Section 5.3, followed by the discussion of the characterisation results in Section 5.4 and a summary of key observations in Section 5.5.

5.2 Test Network and Time-Series Profiles Dataset

The test network used for this work is the same as described in Section 4.2.1 (see Figure 4.1, Page 62). The load profiles dataset used in this work will also be the same as those utilised in Chapter 4 in Section 4.2.2. Since this chapter deals with characterising how the inclusion of solar PV and electric vehicles could impact on the design and operational parameters of a real network, it follows that we would need the time-series profiles of both solar PV and electric vehicle charging for each customer. Therefore, the dataset will now comprise these two additional profiles, representative of each of the considered customers on a typical UK network. The daily time-series profiles (i.e., base load profile (Figure 5.1(a)), solar PV generation profile (Figure 5.1(b)), electric vehicle charging profile (Figure 5.1(c)), and the resultant load profile (Figure 5.1(d))) for a typical home considered in the study are illustrated in Figure 5.1.

Whilst 1-minute time-series datasets were used in this chapter (and in the other chapters), it is important to mention that the use of datasets within the sub-1 minute granularity is an aspect that future power system planners and operators will need to consider. This is particularly important when the distributed variable energy resources continue to gain greater adoption on the power system. With the use of time-series datasets with a finer time granularity, the power system operators will be able to have a better idea of the actual power system conditions. Moreover, since the future power system will inevitably utilise advanced digital technologies where automation of various procedures in the power system management and control actions will be commonplace, there will be a growing need to maintain high levels of system reliability through data-driven decisions and this can be achieved by using more representative data within the sub-1 minute time resolution, despite existing privacy concerns that come with the use of these quasi real-time data [13].

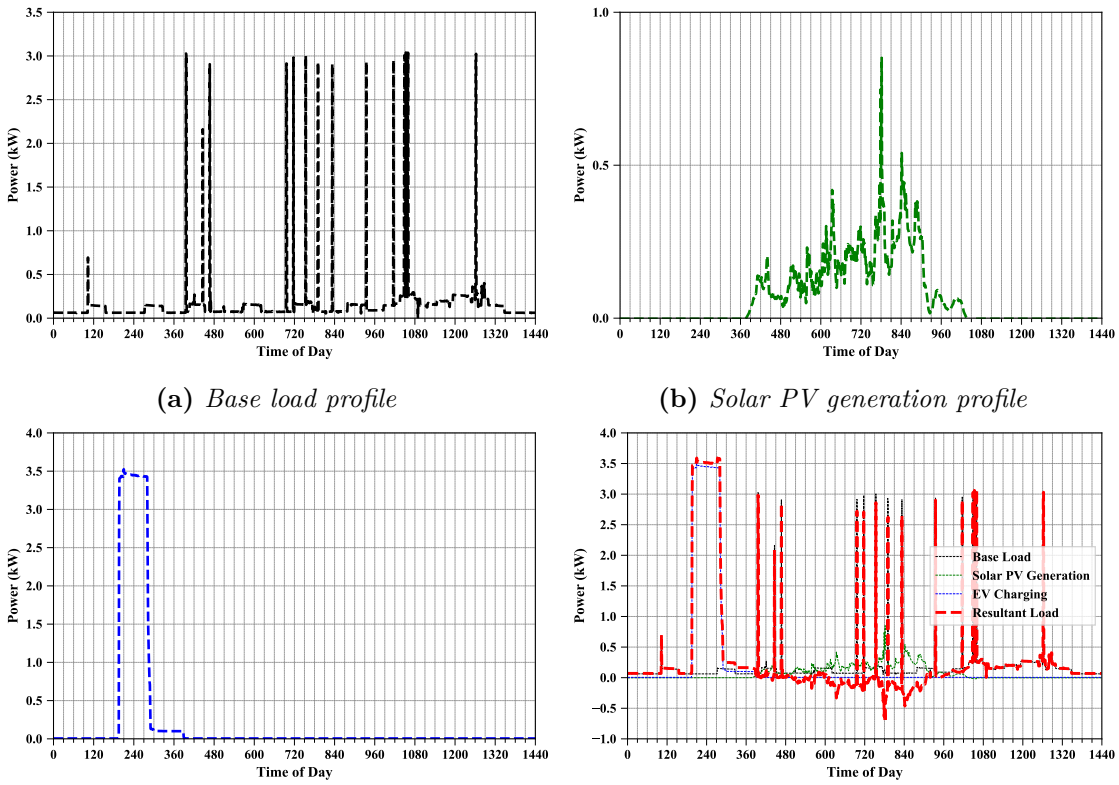

(a) *Base load profile*

(b) *Solar PV generation profile*

(c) *Electric vehicle charging profile*

(d) *Resultant daily time-series load profile*

Figure 5.1: This figure shows the typical daily time-series profiles for a typical home considered in this study.

5.3 Case Studies Designations and Methodologies

This work builds on the characterisation of the network design and operational parameters described in Chapter 4, where we characterised the network ADMD, load variance, average power losses, and the load-dependency loss factor, when different sizes of home groupings were disconnected from the network at a time, using load profiles with different time granularities. The characterisation presented in Chapter 4 considered the base case scenario, where all homes connected on the network had no renewable energy resources or new energy applications installed. In this chapter, we will go a step further to characterise the impact of integrating renewable energy resources and new energy applications onto the network, where we consider adding a solar PV generation and electric vehicle charging to each home. For this purpose, we designate two different scenarios under each of the two case

studies, viz. the solar PV case study, and electric vehicles case study.

The designations of the considered case studies, including the specific methodologies employed, are described in Sections 5.3.1 and 5.3.2. In both cases, we characterise the system diversified peak demand, average power losses, and the load-dependency loss factor. Each of these parameters will be defined under each case study in the following sections.

As already explained in Chapter 4, the load variance will not be considered in this chapter as this parameter is implicit in the observations noted for all the other parameters, whereby the variability in the load (and also in all the other parameters – i.e., the network ADMD, average power losses, and the load-dependency loss factor) decreases with increasing sizes of home groupings and longer averaging temporal effects. We will therefore only concentrate on the network ADMD, average power losses, and the load-dependency loss factor in this chapter.

5.3.1 PV CASE: Impact of solar PV based renewable energy

This case study focuses on the impact of distributed renewable energy on the distribution network. The approach used is with the view to characterise the variations in the three above-stated parameters of interest when the proportion of solar PV power is varied (i.e., added to or removed from the network) on the network at different sizes of customer groupings along with a consideration of different time granularities. Two scenarios are considered, namely: (i) a scenario where all households have existing solar PV installations, and (ii) another scenario where solar PV is incrementally added to the network. The respective methodologies for characterising the system diversified peak demand, average power losses, and the load-dependency loss factor are detailed under each scenario below.

(i) ***Disconnecting households with existing solar PV installation***

For this scenario, we consider that all customers have a rooftop solar PV installation, and they have no storage or electric vehicle charging applications. The main interest is to examine how the performance of a network with

such customer compositions varies in proportion to the number of customers connected at a time, and also considering such performance at different time granularities. Again, the Monte Carlo based spatio-temporal characterisation framework is applied here, and the detailed step-by-step algorithm is given below. We designate this scenario as *existing_pv*.

- ***Step 1: Input data pre-processing***
  - *general load consumption profiles*: Here, we prepare the load profiles dataset to ensure that only the time-series load profiles which are non-zero and non-negative throughout the 24-hour period are preserved.
  - *solar PV generation profiles*: Once we have all the active load profiles with no net power generation, we now select the solar PV generation profiles for the corresponding chosen customers to represent the on-site solar PV generation characteristics for those customers.
  - *resultant power profiles*: For this scenario, we are interested in a network with customers comprising existing solar PV installation. Therefore, we now compute the resultant power profiles for each of the customers in the dataset. The resulting pre-processed dataset is then converted to different time granularities, equivalent to the 1-minute original time granularity datasets defined in Table 3.1 (see Page 42, Chapter 3) for the UK-CLNR & USA-PSID datasets. These resultant power profiles will now constitute the dataset from which inputs to the algorithm will be drawn.
- ***Step 2: Consider different time granularities, τ***

  We now start the OpenDSS COM interface via the DSS text command from Python to define the test circuit and data measurement setup. For each reporting time granularity, τ, we randomly select a sub-dataset of resultant load profiles equal to the number of load points on the circuit, and assign these to all the load points on the network. We then run a time-series load flow with all customers connected, and record the total

power supply, demand, and losses at each time instant, which we refer to as the time-series power supply, demand, and losses as $P_{S_o,t}^{(existing\_pv),\tau}$, $P_{D_o,t}^{(existing\_pv),\tau}$, and $P_{L_o,t}^{(existing\_pv),\tau}$, respectively. Notice that we assign a superscript ($^{existing\_pv}$) to make reference to this scenario in order to differentiate between the two scenarios of the solar PV case study.

- ***Step 3: Consider different customer aggregation levels,*** α

  For every aggregation level, α, we consider disconnecting α customers at a time, and then re-run a load flow and measure the total power supply, demand, and losses for the respective time granularities. Unlike in the base case (refer to Section 4.3, Chapter 4), where neither solar PV panels nor electric vehicles were connected, it is important to notice that the customer power profiles being utilised here now comprise the resultant power of the general power consumption and the solar PV power generation of the customer. The choice of the number of Monte Carlo trials (which is equivalent to the possible combinations of customer grouping sizes, denoted as C_α^{21} for a 21-loads network, achieved by generating these combinations without repetition) remains as established in Section 4.3, Chapter 4, limiting the maximum number of Monte Carlo trials to 100.

  We thus denote the measured parameters as $P_{S_\alpha,t}^{(existing\_pv),\tau}$, $P_{D_\alpha,t}^{(existing\_pv),\tau}$, and $P_{L_\alpha,t}^{(existing\_pv),\tau}$, respectively. At the end of the $k_{C_\alpha^{21}}$ Monte Carlo trials for a given aggregation level, α, at a time granularity, τ, we obtain the matrices containing the measured parameters, which we denote as$P_{S_\alpha,k,t}^{(existing_pv),\tau}$, $P_{D_\alpha,k,t}^{(existing\_pv),\tau}$ or $P_{L_\alpha,k,t}^{(existing\_pv),\tau}$. These matrices will take on the form defined below, as per the example of the total power supply, $P_{S_\alpha,k,t}^{(existing\_pv),\tau}$:

$$\left(\begin{array}{c|cccc} & k = Trial\ 1 & k = Trial\ 2 & \dots & k = Trial\ k_{C_\alpha^{21}} \\ \hline t=1 & P_{S_\alpha,1,1}^{(existing\_pv),\tau} & P_{S_\alpha,2,1}^{(existing\_pv),\tau} & \dots & P_{S_\alpha,k_{C_\alpha^{21}},1}^{(existing\_pv),\tau} \\ t=2 & P_{S_\alpha,1,2}^{(existing\_pv),\tau} & P_{S_\alpha,2,2}^{(existing\_pv),\tau} & \dots & P_{S_\alpha,k_{C_\alpha^{21}},2}^{(existing\_pv),\tau} \\ \vdots & \vdots & \vdots & \vdots & \vdots \\ t=T_\tau & P_{S_\alpha,1,T_\tau}^{(existing\_pv),\tau} & P_{S_\alpha,2,T_\tau}^{(existing\_pv),\tau} & \dots & P_{S_\alpha,k_{C_\alpha^{21}},T_\tau}^{(existing\_pv),\tau} \end{array}\right).$$

- ***Step 4: Compute the metrics of interest***

  The metrics of assessment are the daily values of the *ADMD*, *average losses*, and the *load-dependency loss factor*, and we compute a representative value of each of these metrics respectively for each time granularity and aggregation level over a given day. The mathematical formulations for calculating these metrics are similar to those used in Chapter 4, Section 4.3, in Equations 4.2, 4.5 & 4.6, respectively. The only variation is the usage of different superscripts to denote specific scenarios, such as $\square^{(base)}$ for the *base scenario* and $\square^{(existing\_pv)}$ for the *existing_pv scenario*.

  – *After-diversity maximum demand (ADMD)*

    Equation 4.2 (defined on Page 66, Chapter 4) defines the peak of the total power that must be supplied to the customers connected on the network; the customers each of which would have an existing installation of solar PV. The ${}_{peak}S_\alpha^{(existing\_pv),\tau}$ includes both the actual power demand by customers, plus the power losses associated with delivering power to the customer load points.

  – *Average power losses*

    The power losses when different customer grouping sizes are considered at different time scales, which we denote as $L_\alpha^{(existing\_pv),\tau}$, are calculated according to the definition presented in Equation 4.5 (see Page 67, Chapter 4), where we calculate the total power losses as the difference between the total power injected into the network and the power delivered to the loads.

– *Load-dependency loss factor*

At a given time granularity, we can calculate the change in losses at various aggregation levels in relation to losses at full load with existing solar PV generation. In this scenario, the power losses at full load are denoted as $L_o^{(existing\_pv),\tau}$. The differential change in losses is thus given as a ratio to the total demand at full load with existing solar PV generation, $D_o^{(existing\_pv),\tau}$, in order to quantify how this change in losses implicitly compares to the differential change in network load when varying aggregation levels, and hence referring to this metric as the load-dependency loss factor, $\delta L_\alpha^{(existing\_pv),\tau}$. We calculate this metric in accordance with Equation 4.6, as defined in Section 4.3, Chapter 4.

- ***Step 5: Final results***

At the end of the simulation, covering all time granularities and aggregation levels, we obtain the matrices of the daily peak demand ($_{peak}S_\alpha^{(existing\_pv),\tau}$), daily average power losses ($L_\alpha^{(existing\_pv),\tau}$), and the load-dependency loss factor ($\delta L_\alpha^{(existing\_pv),\tau}$) in the form:

$$\begin{pmatrix} & \alpha = Aggregation\ 1 & \alpha = Aggregation\ 2 & \dots & \alpha = Aggregation\ 20 \\ \tau = \tau_1 & \blacksquare & \blacksquare & \dots & \blacksquare \\ \tau = \tau_2 & \blacksquare & \blacksquare & \dots & \blacksquare \\ \vdots & \vdots & \vdots & \vdots & \vdots \\ \tau = \tau_n & \blacksquare & \blacksquare & \dots & \blacksquare \end{pmatrix},$$

where ■ will comprise $_{peak}S_\alpha^{(existing\_pv),\tau}$, $L_\alpha^{(existing\_pv),\tau}$ and $\delta L_\alpha^{(existing\_pv),\tau}$, respectively.

(ii) ***Incrementally adding new solar PV installation***

This scenario considers a case where we have a network comprising customers with no existing solar PV installation. The initial customer composition of the network is exactly the same as the one considered in the base case. Every time we simulate an aggregation level, it will mean that we add such number of

customers with solar PV installation, whilst the rest of the customers will have their normal base load. In Scenario 5.3.1-(i), *existing_pv*, each aggregation level meant that such many customers with existing solar PV installation were disconnected from the network at a time. So, in this scenario (i.e., Scenario 5.3.1-(ii)), which we refer to as *new_pv*, we are essentially studying what would happen if customers were to randomly add solar PV installations on their rooftops at different time and aggregation scales. The step-by-step Monte Carlo based spatio-temporal characterisation algorithm is outlined below:

- ***Step 1: Input data pre-processing***
  - *general load consumption profiles*: Here, we prepare the load profiles dataset to ensure that only the time-series load profiles which are non-zero and non-negative all through the 24-hour period are preserved. There profiles will represent the customers with no solar PV installation.
  - *solar PV generation profiles*: Once we have all the active load profiles with no net power generation, we now select the solar PV generation profiles for the corresponding chosen customers to represent the on-site solar PV generation characteristics for those customers.
  - *resultant power profiles*: We now compute the resultant power profiles for each of the customers in the dataset. The resulting pre-processed dataset will represent cases where a customer would have a solar PV installation. Both the general load consumption and resultant power profiles are then converted to different time granularities, equivalent to the 1-minute original time granularity datasets defined in Table 3.1 (see Page 42, Chapter 3) for the UK-CLNR & USA-PSID datasets. A pool of these profiles will now constitute the input data to the algorithm, where the general load consumption profiles will represent

customers without solar PV installation, and the resultant power profiles will represent customers with new solar PV installation.

- ***Step 2: Consider different time granularities,*** τ

  We now start the OpenDSS COM interface via the DSS text command from Python to define the test circuit and data measurement setup. For each time granularity, τ, we randomly select a sub-dataset of general load consumption profiles equal to the number of load points on the circuit, and assign these to all the load pints on the network. We do this to have an initial customer composition which is representative of the case where all customers connected on the network have no solar PV installed. We then run a time-series load flow with all customers connected, and record the total power supply, demand, and losses at each time instant, which we refer to as the time-series power supply, demand, and losses as $P_{S_o,t}^{(base),\tau}$, $P_{D_o,t}^{(base),\tau}$, and $P_{L_o,t}^{(base),\tau}$, respectively. It is important to notice that this step will be similar to that of the base case, described in the previous chapter in Section 4.3, and we thus assign the same notations for the initial measured results in this scenario as those used in the base case.

- ***Step 3: Consider different customer aggregation levels,*** α

  For every aggregation level, α, we consider adding α customers with solar PV installation at a time, i.e, assigning corresponding profiles drawn from the resultant power profiles pool, and then re-run a load flow and measure the total power supply, demand, and losses for the respective time granularities. All other customers will remain connected to the network, but without solar PV installation, where corresponding general load consumption profiles are assigned to these customers. The choice of the number of Monte Carlo trials (which is equivalent to the possible combinations of customer grouping sizes, denoted as C_{α}^{21} for a 21-loads network, achieved by generating these combinations without repetition)

remains as established in Section 4.3 in Chapter 4, limiting the maximum number of Monte Carlo trials to 100.

We thus denote the measured parameters as $P_{S_\alpha,t}^{(new\_pv),\tau}$, $P_{D_\alpha,t}^{(new\_pv),\tau}$, and $P_{L_\alpha,t}^{(new\_pv),\tau}$, respectively. At the end of the $k_{C_\alpha^{21}}$ Monte Carlo trials for a given aggregation level, α, at a time granularity, τ, we obtain the matrices containing the measured parameters, which we denote as$P_{S_\alpha,k,t}^{(new_pv),\tau}$, $P_{D_\alpha,k,t}^{(new\_pv),\tau}$ or $P_{L_\alpha,k,t}^{(new\_pv),\tau}$. These matrices will take on the form defined below, as per the example of the total power supply, $P_{S_\alpha,k,t}^{(new\_pv),\tau}$:

$$\left(\begin{array}{c|cccc} & k = Trial\ 1 & k = Trial\ 2 & \dots & k = Trial\ k_{C_\alpha^{21}} \\ \hline t=1 & P_{S_\alpha,1,1}^{(new\_pv),\tau} & P_{S_\alpha,2,1}^{(new\_pv),\tau} & \dots & P_{S_\alpha,k_{C_\alpha^{21}},1}^{(new\_pv),\tau} \\ t=2 & P_{S_\alpha,1,2}^{(new\_pv),\tau} & P_{S_\alpha,2,2}^{(new\_pv),\tau} & \dots & P_{S_\alpha,k_{C_\alpha^{21}},2}^{(new\_pv),\tau} \\ \vdots & \vdots & \vdots & \vdots & \vdots \\ t=T_\tau & P_{S_\alpha,1,T_\tau}^{(new\_pv),\tau} & P_{S_\alpha,2,T_\tau}^{(new\_pv),\tau} & \dots & P_{S_\alpha,k_{C_\alpha^{21}},T_\tau}^{(new\_pv),\tau} \end{array}\right).$$

- ***Step 4: Compute the metrics of interest***

  The metrics of assessment are the daily values of the *ADMD*, *average losses*, and the *load-dependency loss factor*, and we compute a representative value of each of these metrics respectively for each time granularity and aggregation level over a given day. The mathematical formulations for calculating the ADMD and average losses are similar to those used in Chapter 4, Section 4.3, in Equations 4.2, & 4.5, respectively. The only variation is the usage of different superscripts to denote specific scenarios, such as $\square^{(base)}$ for the *base scenario* and $\square^{(new\_pv)}$ for the *new_pv scenario*. The load-dependency loss factor is calculated according to Equation 5.1.

  – *After-diversity maximum demand (ADMD)*

    Equation 4.2 (defined on Page 66, Chapter 4) defines the peak of the total power that must be supplied to the customers connected on the network at different penetration levels of solar PV, when considering such penetration levels at various time granularities. The ${}_{peak}S_\alpha^{(new\_pv),\tau}$ includes both the actual power demand by customers,

plus the power losses across the network, which is a result of either delivering power to the load points or due to the reverse current emanating from periods of excess solar PV generation.

– *Average power losses*

We now calculate the average power losses of the network when different solar PV penetration levels (i.e., customer groupings with new solar PV installation) are added onto the network using different time granularities, and we will denote this as $L_{\alpha}^{(new\_pv),\tau}$. This parameter will be computed using the mathematical formulation similar to the one defined in Equation 4.5 (see Page 67, Chapter 4). The power losses at each time instant of the day is calculated as the difference between the total power injected into the network and the power delivered to the loads.

– *Load-dependency loss factor*

At a given reporting time granularity, we can calculate the change in losses at various aggregation levels in relation to losses at full load. Since no solar PV was installed at the initial load flow where all customers were connected, we will denote the power losses at full load as $L_{o}^{(base),\tau}$. The differential change in losses is thus given as a ratio to the total demand at full load, $D_{o}^{(base),\tau}$, in order to quantify how much this change in losses implicitly compares to the differential change in network load when adding solar PV at different penetration levels, and hence referring to this metric as the load-dependency loss factor. This metric is calculated in accordance with Equation 5.1.

$$\delta L_{\alpha}^{(new\_pv),\tau} = \left(\frac{L_{o}^{(base),\tau} - L_{\alpha}^{(new\_pv),\tau}}{D_{o}^{(base),\tau}} \right) \times 100, \qquad (5.1)$$

where $L_{o}^{(base),\tau}$ and $D_{o}^{(base),\tau}$ are defined according to Equations 4.7 & 4.8, respectively, as defined in Section 4.3, Chapter 4.

- ***Step 5: Final results***

  At the end of the simulation for incrementally adding new solar PV installation, covering all time granularities and aggregation levels, we obtain the matrices of the daily peak demand (${}_{peak}S_{\alpha}^{(new\_pv),\tau}$), daily average power losses ($L_{\alpha}^{(new\_pv),\tau}$), and the load-dependency loss factor ($\delta L_{\alpha}^{(new\_pv),\tau}$) in the form:

$$\left(\begin{array}{c|cccc} & \alpha = Aggregation\ 1 & \alpha = Aggregation\ 2 & \dots & \alpha = Aggregation\ 20 \\ \hline \tau = \tau_1 & \blacksquare & \blacksquare & \dots & \blacksquare \\ \tau = \tau_2 & \blacksquare & \blacksquare & \dots & \blacksquare \\ \vdots & \vdots & \vdots & \vdots & \vdots \\ \tau = \tau_n & \blacksquare & \blacksquare & \dots & \blacksquare \end{array}\right),$$

  where ■ will comprise ${}_{peak}S_{\alpha}^{(new\_pv),\tau}$, $L_{\alpha}^{(new\_pv),\tau}$ and $\delta L_{\alpha}^{(new\_pv),\tau}$, respectively.

5.3.2 EV CASE: Impact of a combination of electric vehicles (EVs) based flexible demand with Solar PV based renewable energy

This case study focuses on the impact of the inclusion of flexible demand on the distribution network, both in the presence of solar PV and also in the case where no solar PV is present on the network. The purpose of this case study is to characterise the system peak demand, average power losses, and the load-dependency loss factor when we vary the proportion of flexible demand on the network at different sizes of customer groupings along with a consideration of different time granularities. Although there is a wider variety of flexible load types, such as washing machines, tumble dryers, geysers, etc., we will represent flexible demand in the form of electric vehicle charging profiles. We will consider two scenarios under which electric vehicles will be added onto the network in different settings; firstly in a setting where (i) new electric vehicles are added to households with no solar PV installation, and, secondly, in another setting where (ii) new electric vehicles are added to households with existing solar PV installation. The respective methodologies employed under each of these two scenarios are described below.

(i) ***Adding new EVs to households with no solar PV installation***

In this scenario, we explore the impacts of incrementally adding electric vehicles onto a network that does not comprise solar PV installation. The scenario mimics what would happen if we were to have a network with customers who do not have installation of solar PV systems at their homes, and then over time acquire electric vehicles, which they will then need to plug into their sockets for charging. Our interest is to characterise the assessment metrics of this study when the different proportions of electric vehicles are added to the network, and we also explore how such characterisation varies when we consider different time granularities. Every time we simulate an aggregation level (i.e., the grouping size of homes with electric vehicles), we will add such number of customers with ownership of electric vehicles, whilst keeping the rest of the customers with their normal base load. The view is to give insight into what might be expected when more and more electric vehicles are integrated into a network with no solar PV. We will also gain an appreciation of how the assessment metrics could be affected by the different time granularities employed. The step-by-step Monte Carlo based spatio-temporal characterisation algorithm is now outlined below.

- ***Step 1: Input data pre-processing***
  - *general load consumption profiles*: Here, we prepare the load profiles dataset to ensure that only the time-series load profiles which are non-zero and non-negative all through the 24-hour period are preserved. These profiles will represent the customers with no solar PV installation.
  - *EV charging profiles*: We now select EV charging profiles and match them to corresponding active general load consumption profiles with no net power generation, which then defines the respective EV charging profiles of the individual customers in the dataset.

  - *resultant power profiles*: In order to obtain the resultant power profiles for each of the customers in the dataset, we add the charging profile values to the general load consumption profile. The resulting pre-processed dataset will represent a customer with EV charging activities. Both the general load consumption and resultant power profiles are then converted to different time granularities, equivalent to the 1-minute original time granularity datasets defined in Table 3.1 (see Page 42, Chapter 3) for the UK-CLNR & USA-PSID datasets.

- ***Step 2: Consider different time granularities,*** τ

  We now start the OpenDSS COM interface via the DSS text command from Python to define the test circuit and data measurement setup. For each time granularity, τ, we randomly select a sub-dataset of general load consumption profiles equal to the number of load points on the circuit, and assign these to all the load points on the network. We do this to have an initial customer composition which is representative of the case where all customers connected on the network have no solar PV system installed. We then run a time-series load flow with all customers connected, and record the total power supply, demand, and losses at each time instant, which we refer to as the time-series power supply, demand, and losses as $P_{S_o,t}^{(base),\tau}$, $P_{D_o,t}^{(base),\tau}$, and $P_{L_o,t}^{(base),\tau}$, respectively. It is important to notice that this step will be similar to that of the base case, described in the previous chapter in Section 4.3, and we thus assign the same notations for the initial measured results in this current scenario. This step is also similar to the *new_pv* scenario (i.e., Scenario 5.3.1-(ii)).

- ***Step 3: Consider different customer aggregation levels,*** α

  For every aggregation level, α, we consider adding EVs to α customers at a time (which means assigning resultant power profiles to these customers), and then re-run a load flow and measure the total power supply, demand, and losses for the respective time granularities. All other customers will remain connected to the network, but comprising the general load

consumption profiles only. The choice of the number of Monte Carlo trials (which is equivalent to the possible combinations of customer grouping sizes, denoted as C_{α}^{21} for a 21-loads network, achieved by generating these combinations without repetition) remains as established in Section 4.3, Chapter 4, limiting the maximum number of Monte Carlo trials to 100. We thus denote the measured parameters as $P_{S_\alpha,t}^{(ev),\tau}$, $P_{D_\alpha,t}^{(ev),\tau}$, and $P_{L_\alpha,t}^{(ev),\tau}$, respectively. At the end of the $k_{C_\alpha^{21}}$ Monte Carlo trials for a given aggregation level, α, at a time granularity, τ, we obtain the matrices containing the measured parameters, which we denote as $P_{S_\alpha,k,t}^{(ev),\tau}$, $P_{D_\alpha,k,t}^{(ev),\tau}$ or $P_{L_\alpha,k,t}^{(ev),\tau}$. These matrices will take on the form defined below, as per the example of the total power supply, $P_{S_\alpha,k,t}^{(ev),\tau}$:

$$\left(\begin{array}{c|cccc} & k = \textit{Trial 1} & k = \textit{Trial 2} & \dots & k = \textit{Trial } k_{C_\alpha^{21}} \\ \hline t=1 & P_{S_\alpha,1,1}^{(ev),\tau} & P_{S_\alpha,2,1}^{(ev),\tau} & \dots & P_{S_\alpha,k_{C_\alpha^{21}},1}^{(ev),\tau} \\ t=2 & P_{S_\alpha,1,2}^{(ev),\tau} & P_{S_\alpha,2,2}^{(ev),\tau} & \dots & P_{S_\alpha,k_{C_\alpha^{21}},2}^{(ev),\tau} \\ \vdots & \vdots & \vdots & \vdots & \vdots \\ t=T_\tau & P_{S_\alpha,1,T_\tau}^{(ev),\tau} & P_{S_\alpha,2,T_\tau}^{(ev),\tau} & \dots & P_{S_\alpha,k_{C_\alpha^{21}},T_\tau}^{(ev),\tau} \end{array}\right).$$

- ***Step 4: Compute the metrics of interest***

  The metrics of assessment are the daily values of the *ADMD*, *average losses*, and the *load-dependency loss factor*, and we compute a representative value of each of these metrics respectively for each time granularity and aggregation level over a given day. The mathematical formulations for calculating the ADMD and average losses are similar to those used in Chapter 4, Section 4.3, in Equations 4.2 & 4.5, respectively. The only variation is the usage of different superscripts to denote specific scenarios, such as $\square^{(base)}$ for the *base scenario* and $\square^{(ev)}$ for the *ev scenario*. The load-dependency loss factor is calculated according to Equation 5.2.

  – *After-diversity maximum demand (ADMD)*

    Equation 4.2 (defined on Page 66, Chapter 4) defines the peak of the total power that must be supplied to the customers connected on the network at different penetration levels of EVs when considering

such penetration levels at various time granularities. The ${}_{peak}S_{\alpha}^{(ev),\tau}$ includes both the actual power demand by customers, plus the power losses culminating from the I^2R associated with delivering power to the load points.

– *Average power losses*

We now calculate the average power losses of the network when we add EVs at different penetration levels onto the network using different time granularities, and we denote that as $L_{\alpha}^{(ev),\tau}$. This parameter will be computed using the mathematical formulation similar to the one defined in Equation 4.5 (see Page 67, Chapter 4). The interesting question is how these losses will compare to the case where we begin to have local generation in the form of solar PV system in Scenario 5.3.2-(ii). The power losses at each time instant of the day is calculated as the difference between the total power injected into the network and the power delivered to the loads.

– *Load-dependency loss factor*

At a given reporting time granularity, we can calculate the change in losses at various aggregation levels in relation to losses at full load. Since neither solar PV nor EVs were installed at the initial load flow where all customers were connected, we will denote the power losses at full load as $L_{o}^{(base),\tau}$. The differential change in losses is thus given as a ratio to the total demand at full load, $D_{o}^{(base),\tau}$, in order to quantify how much this change in losses implicitly compares to the differential change in network load when adding EVs at different penetration levels, and hence referring to this metric as the load-dependency loss factor. This metric is calculated in accordance with Equation 5.2.

$$\delta L_{\alpha}^{(ev),\tau} = \left(\frac{L_{o}^{(base),\tau} - L_{\alpha}^{(ev),\tau}}{D_{o}^{(base),\tau}} \right) \times 100, \tag{5.2}$$

where $L_o^{(base),\tau}$ and $D_o^{(base),\tau}$ are defined according to Equations 4.7 & 4.8, respectively, as defined in Section 4.3, Chapter 4.

- ***Step 5: Final results***

  At the end of the simulation for incrementally adding new EVs to a network without solar PV generation, covering all time granularities and aggregation levels, we obtain the matrices of the daily peak demand (${}_{peak}S_\alpha^{(ev),\tau}$), daily average power losses ($L_\alpha^{(ev),\tau}$), and the load-dependency loss factor ($\delta L_\alpha^{(ev),\tau}$) in the form:

$$\left(\begin{array}{c|cccc} & \alpha = Aggregation\ 1 & \alpha = Aggregation\ 2 & \dots & \alpha = Aggregation\ 20 \\ \hline \tau = \tau_1 & \blacksquare & \blacksquare & \dots & \blacksquare \\ \tau = \tau_2 & \blacksquare & \blacksquare & \dots & \blacksquare \\ \vdots & \vdots & \vdots & \vdots & \vdots \\ \tau = \tau_n & \blacksquare & \blacksquare & \dots & \blacksquare \end{array}\right),$$

  where ■ will comprise ${}_{peak}S_\alpha^{(ev),\tau}$, $L_\alpha^{(ev),\tau}$ and $\delta L_\alpha^{(ev),\tau}$, respectively.

(ii) ***Adding new EVs to households with existing solar PV installation***

In contrast to the *ev_scenario*, Scenario 5.3.2-(i), this scenario considers a network where all customers have existing solar PV generation installed at their homes. The interest is then to compare the results of this scenario to the case where we have no solar PV generation on the network in relation to the impacts that would occur when EVs are added onto the network at different penetration levels using different time granularities. This will particularly highlight the role that local solar PV generation could have on the design and operation of the distribution network. The step-by-step Monte Carlo based spatio-temporal characterisation algorithm for this scenario is described below.

- ***Step 1: Input data pre-processing***
  - *general load consumption profiles*: Here, we prepare the load profiles dataset to ensure that only the time-series load profiles which are non-zero and non-negative all through the 24-hour period are preserved.

These profiles will represent the customers with neither solar PV installation nor EV ownership.

- *resultant power profiles – existing solar PV generation*: At this point, we calculate the resultant power profiles when all customers have solar PV systems installed at their homes. This constitutes the power profiles to represent the initial customer composition of the network for this scenario.
- *resultant power profiles – existing solar PV generation with EV charging*: We will now need to calculate the resultant power profiles to signify cases when an EV is added onto the network in the presence of existing local solar PV generation. Both the resultant power profiles with existing solar PV generation and also with EV ownership in the presence of existing local solar PV generation are then converted to different time granularities, equivalent to the 1-minute original time granularity datasets defined in Table 3.1 (see Page 42, Chapter 3) for the UK-CLNR & USA-PSID datasets.

- ***Step 2: Consider different time granularities,*** τ

We now start the OpenDSS COM interface via the DSS text command from Python to define the test circuit and data measurement setup. For each time granularity, τ, we randomly select a sub-dataset of resultant power profiles with existing solar PV generation equal to the number of load points on the circuit, and assign these to all the load points on the network. We do this to have an initial customer composition which is representative of the case where all customers connected on the network have local solar PV generation at their homes. We then run a time-series load flow with all customers connected, and record the total power supply, demand, and losses at each time instant, which we refer to as the time-series power supply, demand, and losses as $P_{S_o,t}^{(existing\_pv),\tau}$, $P_{D_o,t}^{(existing\_pv),\tau}$, and $P_{L_o,t}^{(existing\_pv),\tau}$, respectively. Notice that we annotate the measurements from the initial load flow in the same way as those

obtained in Step 2 of Scenario 5.3.1-(i) (see Page 85). This is because both scenarios have the same initial customer composition with existing local solar PV generation.

- ***Step 3: Consider different customer aggregation levels,*** α

  For every aggregation level, α, we consider adding EVs to α customers at a time (which means assigning resultant power profiles with existing solar PV generation and EV charging to these customers), and then re-run a load flow and measure the total power supply, demand, and losses for the respective time granularities. All other customers will remain connected to the network, but only comprising the resultant power profiles with existing solar PV generation. The choice of the number of Monte Carlo trials (which is equivalent to the possible combinations of customer grouping sizes, denoted as C_{α}^{21} for a 21-loads network, achieved by generating these combinations without repetition) remains as established in Section 4.3, Chapter 4, limiting the maximum number of Monte Carlo trials to 100.

  We thus denote the measured parameters as $P_{S_\alpha,t}^{(pv\_ev),\tau}$, $P_{D_\alpha,t}^{(pv\_ev),\tau}$, and $P_{L_\alpha,t}^{(pv\_ev),\tau}$, respectively. At the end of the $k_{C_\alpha^{21}}$ Monte Carlo trials for a given aggregation level, α, at a time granularity, τ, we obtain the matrices containing the measured parameters, which we denote as $P_{S_\alpha,k,t}^{(pv\_ev),\tau}$, $P_{D_\alpha,k,t}^{(pv\_ev),\tau}$ or $P_{L_\alpha,k,t}^{(pv\_ev),\tau}$. These matrices will take on the form defined below, as per the example of the total power supply, $P_{S_\alpha,k,t}^{(pv\_ev),\tau}$:

$$\left(\begin{array}{c|cccc} & k = \textit{Trial 1} & k = \textit{Trial 2} & \dots & k = \textit{Trial } k_{C_\alpha^{21}} \\ \hline t = 1 & P_{S_\alpha,1,1}^{(pv\_ev),\tau} & P_{S_\alpha,2,1}^{(pv\_ev),\tau} & \dots & P_{S_\alpha,k_{C_\alpha^{21}},1}^{(pv\_ev),\tau} \\ t = 2 & P_{S_\alpha,1,2}^{(pv\_ev),\tau} & P_{S_\alpha,2,2}^{(pv\_ev),\tau} & \dots & P_{S_\alpha,k_{C_\alpha^{21}},2}^{(pv\_ev),\tau} \\ \vdots & \vdots & \vdots & \vdots & \vdots \\ t = T_\tau & P_{S_\alpha,1,T_\tau}^{(pv\_ev),\tau} & P_{S_\alpha,2,T_\tau}^{(pv\_ev),\tau} & \dots & P_{S_\alpha,k_{C_\alpha^{21}},T_\tau}^{(pv\_ev),\tau} \end{array}\right).$$

- ***Step 4: Compute the metrics of interest***

  The metrics of assessment are the daily values of the *ADMD*, *average*

losses, and the *load-dependency loss factor*, and we compute a representative value of each of these metrics respectively for each time granularity and aggregation level. The mathematical formulations for calculating the ADMD and average losses are similar to those used in Chapter 4, Section 4.3, in Equations 4.2, & 4.5, respectively. The only variation in these mathematical formulations is the usage of different superscripts to denote specific scenarios, such as $\square^{(base)}$ for the *base scenario* and $\square^{(pv\_ev)}$ for the *pv_ev scenario*. The load-dependency loss factor is calculated according to Equation 5.3.

- *After-diversity maximum demand (ADMD)*

  Equation 4.2 (defined on Page 66, Chapter 4) defines the peak of the total power that must be supplied to the customers connected on the network at different penetration levels of EVs in the presence of local solar PV when considering such penetration levels at various time granularities. Notice that ${}_{peak}S_{\alpha}^{(pv\_ev),\tau}$ includes both the actual power demand by customers, plus the power losses culminating from the I^2R associated with either delivering power to the load points or due to the reverse current emanating from periods of excess solar PV generation.

- *Average power losses*

  Noting that the network will contain solar PV generation, we now calculate the average power losses of the network when we add EVs at different penetration levels onto the network using different time granularities, which we denote as $L_{\alpha}^{(pv\_ev),\tau}$. This parameter will be computed using the mathematical formulation similar to the one defined in Equation 4.5 (see Page 67, Chapter 4). The power losses at each time instant of the day is calculated as the difference between the total power injected into the network and the power delivered to the loads.

– *Load-dependency loss factor*

At a given reporting time granularity, we can calculate the change in losses at various aggregation levels in relation to losses at full load. We denote the power losses at full load as $L_o^{(existing\_pv),\tau}$, since, for this scenario, we begin with all customers suited with existing local solar PV generation. The differential change in losses is thus given as a ratio to the total demand at full load, $D_o^{(existing\_pv),\tau}$, in order to quantify how much this change in losses implicitly compares to the differential change in network load when adding EVs at different penetration levels, and hence referring to this metric as the load-dependency loss factor. This metric is calculated in accordance to Equation 5.3.

$$\delta L_\alpha^{(pv\_ev),\tau} = \left(\frac{L_o^{(existing\_pv),\tau} - L_\alpha^{(pv\_ev),\tau}}{D_o^{(existing\_pv),\tau}} \right) \times 100 \qquad (5.3)$$

where $L_o^{(existing\_pv),\tau}$ and $D_o^{(existing\_pv),\tau}$ are defined according to Equations 4.7 & 4.8, respectively, as defined in Section 4.3, Chapter 4.

- ***Step 5: Final results***

At the end of the simulation for incrementally adding new EVs onto a network comprising solar PV generation, covering all time granularities and aggregation levels, we obtain the matrices of the daily peak demand ($_{peak}S_\alpha^{(pv\_ev),\tau}$), daily average power losses ($L_\alpha^{(pv\_ev),\tau}$), and the load-dependency loss sensitivity factor ($\delta L_\alpha^{(pv\_ev),\tau}$) in the form:

$$\begin{pmatrix} & \alpha = Aggregation\ 1 & \alpha = Aggregation\ 2 & \dots & \alpha = Aggregation\ 20 \\ \tau = \tau_1 & \blacksquare & \blacksquare & \dots & \blacksquare \\ \tau = \tau_2 & \blacksquare & \blacksquare & \dots & \blacksquare \\ \vdots & \vdots & \vdots & \vdots & \vdots \\ \tau = \tau_n & \blacksquare & \blacksquare & \dots & \blacksquare \end{pmatrix},$$

where ■ will comprise $_{peak}S_\alpha^{(pv\_ev),\tau}$, $L_\alpha^{(pv\_ev),\tau}$ and $\delta L_\alpha^{(pv\_ev),\tau}$, respectively.

5.4 Results and Discussions

As explained in Section 5.3, this chapter builds on the characterisation of the network design and operational parameters covered in Chapter 4, where we characterised the network after-diversity maximum demand (ADMD), load variance, average power losses, and the load-dependency loss factor, when different sizes of home groupings were disconnected at a time, using load profiles with different time granularities. The characterisation of these parameters, as presented in Chapter 4, considered the base case scenario, where all homes connected on the network had no renewable energy resources or any new energy applications installed. This chapter now presents a characterisation of the same (excluding load variance, as afore-explained) design and operational parameters, but under different case studies.

In the following sections, we will present the results obtained under the two case studies considered in this chapter, viz. the solar PV and electric vehicles case studies. Each of these case studies has two specific scenarios, as defined in Section 5.3. The solar PV case study, defined in Section 5.3.1, has two scenarios defined in Sections 5.3.1-(i) & 5.3.1-(ii), which, respectively, represent the scenario where households with existing solar PV installations are incrementally disconnected from the network, and the scenario where solar PV installations are incrementally added to households connected onto the network. The electric vehicles case study, defined in Section 5.3.2, also includes two different scenarios defined in Sections 5.3.2-(i) & 5.3.2-(ii), which, respectively, represent the scenario where new electric vehicles are added to households with no solar PV installation, and the scenario where new electric vehicles are added to households with existing solar PV installation.

The spatio-temporal characterisation results obtained under the above-cited specific scenarios are presented in Sections 5.4.1.1, 5.4.1.2, 5.4.2.1, & 5.4.2.2. In all the scenarios, we will characterise the network diversified peak demand (i.e., the ADMD), average power losses, and the load-dependency loss factor.

5.4.1 Impact of solar PV based renewable energy

This section presents the results of the spatio-temporal characterisation of the impact of distributed solar PV on the distribution network described in Section 4.2.1 (see Chapter 4, Figure 4.1, Page 62). The solar PV case study was performed with the view to characterise the variations in the three afore-stated parameters of interest when the proportion of solar PV power is varied (i.e., added to or removed from the network) on the network at different sizes of customer groupings along with a consideration of different time granularities. We now present the results for each of the two considered scenarios in Sections 5.4.1.1 and 5.4.1.2.

5.4.1.1 Disconnecting households with existing solar PV installation

In line with the methodology defined in Section 5.3.1-(i) for the scenario where households with existing solar PV installation are incrementally disconnected from the network, we will now present the characterisation results of the ADMD, average power losses, and load-dependency loss factor in Sections 5.4.1.1: (a), (b), and (c), respectively.

(a) ***After-diversity maximum demand***

In comparison to the results for the base scenario (presented in Section 4.4.1, Chapter 4) where households did not have solar PV installation, the trends in the variation of the ADMD are the same for the scenario we are reporting on in this section. It is evident in Figures 5.2 - 5.4 that the network ADMD decreases as both the size of home groupings on the network and the time granularity of load profiles used tend to larger magnitudes. The ADMD variations against the size of home groupings and the time granularities are depicted in Figures 5.2 & 5.3, respectively; whereas, a summary of the combined effect of both the size of home groupings and time granularities is presented as a contour plot in Figure 5.4.

The interesting observation is that the magnitudes of the ADMD are lower in the presence of solar PV when compared to the base case scenario. Let us

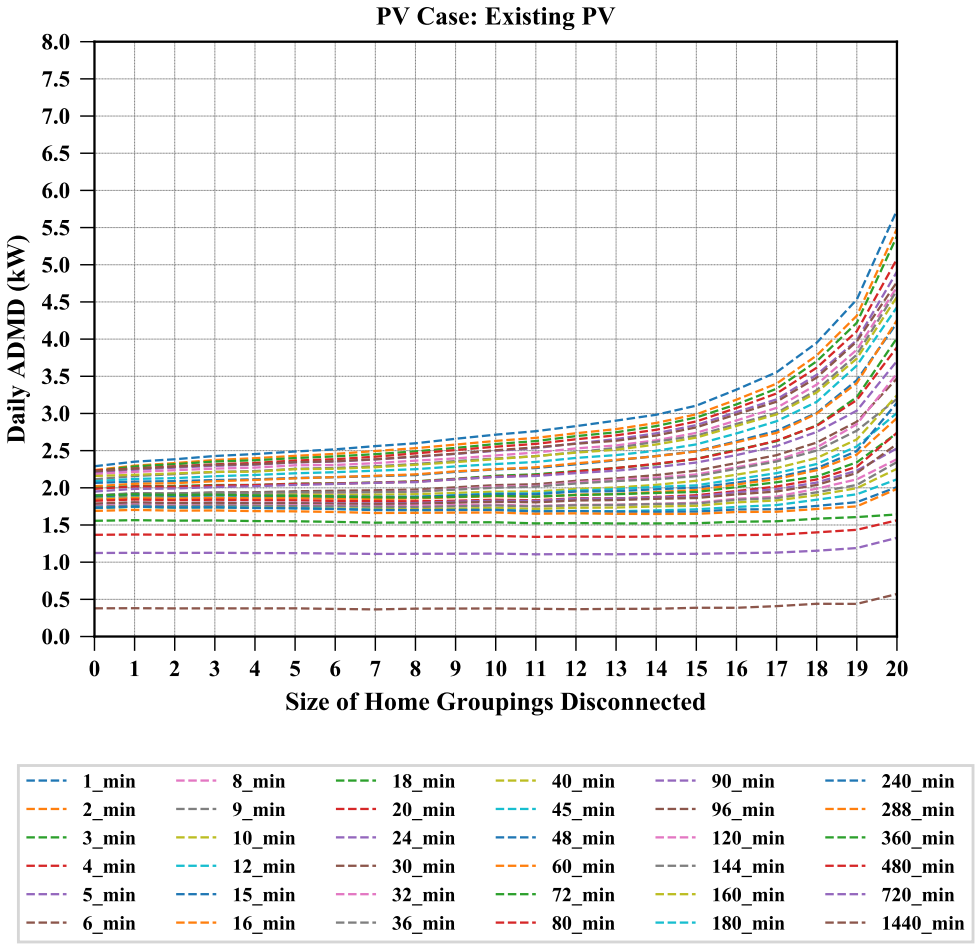

Figure 5.2: The network ADMD versus aggregation levels across different time granularities when incrementally disconnecting existing solar PV installation from the network

compare the results presented in Figure 5.2 against the results for the base case scenario presented in Figure 4.3 (Chapter 4, Page 70). If we consider the uppermost trendline, which gives the ADMD variation against the size of home groupings for load profiles with a 1-minute time granularity, we can observe that when 20 homes were disconnected from the network, which represents a 20-home aggregation level, ADMD levels of 7.04kW and 5.73kW are obtained for the base case and the case with existing solar PV installation, respectively. Similarly, for the same time granularity of 1 minute when no home is disconnected from the network, we get 2.33kW and 2.29kW for the base case scenario and for the case with existing solar PV installation, respectively.

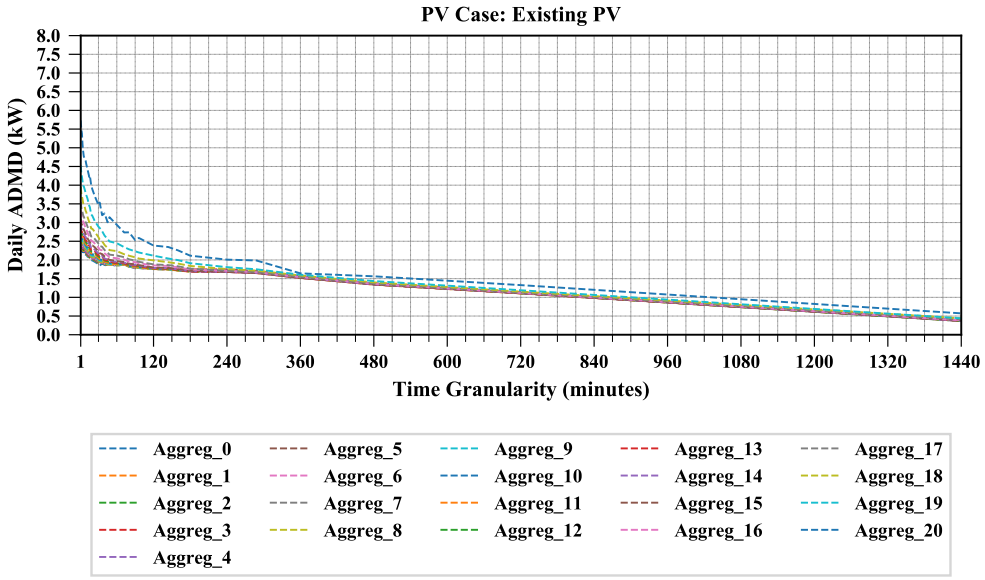

Figure 5.3: The network ADMD versus time granularities across different aggregation levels when incrementally disconnecting existing solar PV installation from the network

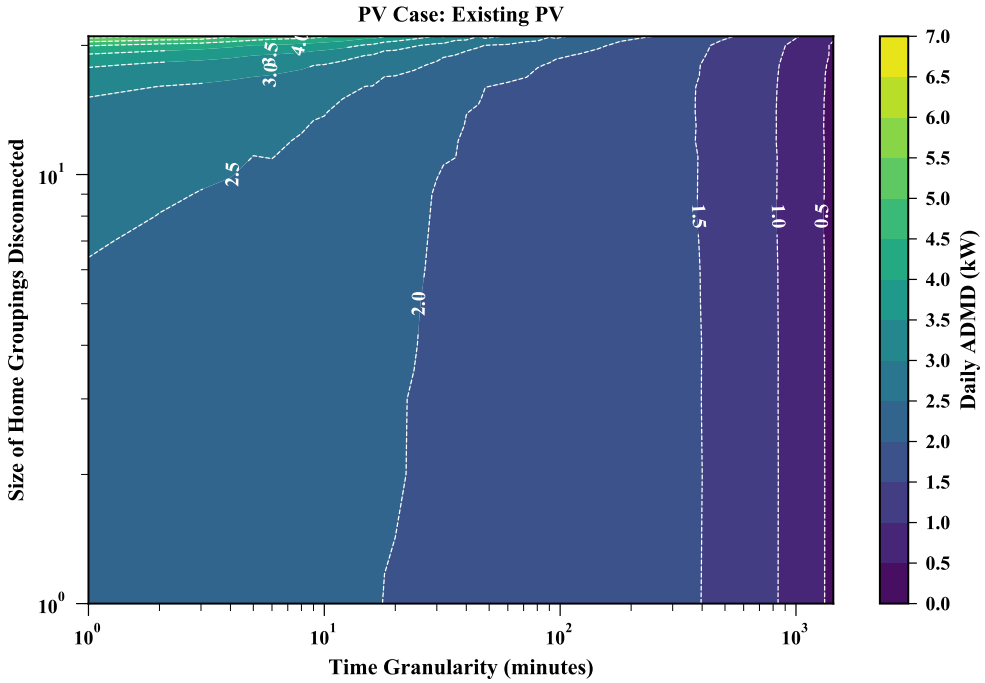

Figure 5.4: The diversified maximum demand as a function of the size of customer groupings and the time granularity when incrementally disconnecting existing solar PV installation from the network

In both of these scenarios (and for all the other sizes of home groupings and time granularities), we can observe that the inclusion of solar PV installation

reduces the per customer capacity requirements of the network. The lower ADMD levels in the scenario with existing solar PV installation are a result of the resultant load profiles exhibiting lower power requirements to be supplied from the network as a result of the off-setted local solar PV generation.

(b) ***Average power losses***

The results for the characterisation of average power losses on the network are summarised in Figure 5.5 for the aggregation effects and in Figure 5.6 for the temporal effects.

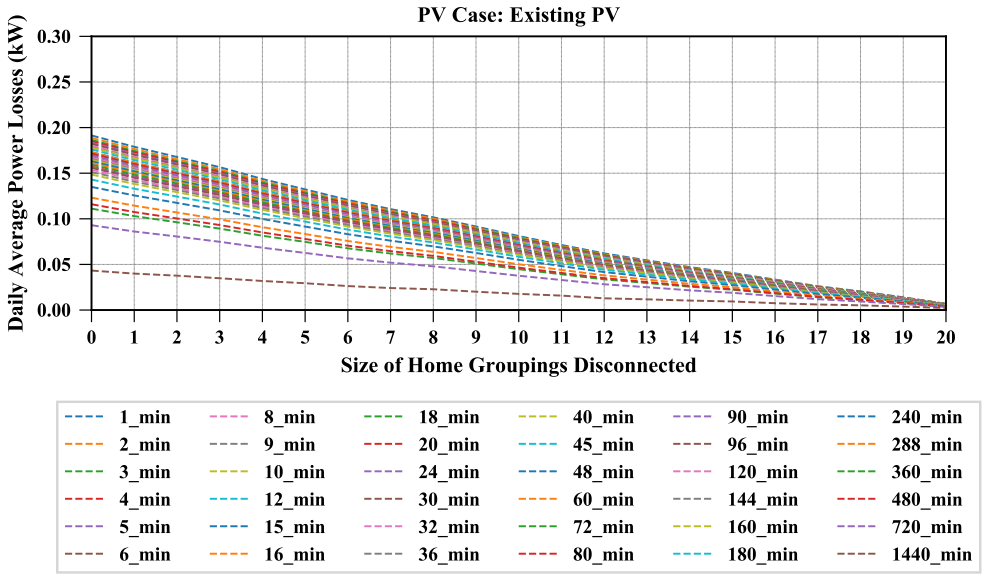

Figure 5.5: The network average losses versus aggregation levels across different time granularities when incrementally disconnecting existing solar PV installation from the network

The characterisation of the variation in the network average power losses is in agreement with the characterisation results presented in Section 4.4.3 (Chapter 4, Page 73) and the discussions given in that section squarely apply to the observations for this scenario of disconnecting homes with existing solar PV installation.

As evident from Figures 5.5 & 5.6, the variation in the network average power losses is as expected, where, respectively, we obtain higher losses when larger

numbers of customers are connected on the network at once, and lower levels of average power losses when load profiles with larger time granularities are used.

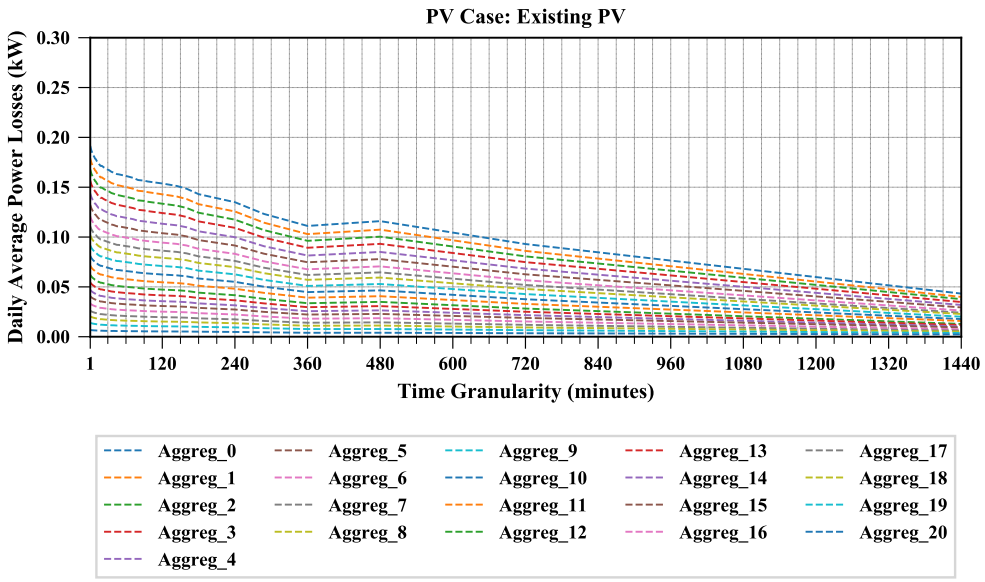

Figure 5.6: The network average losses versus time granularities across different aggregation levels when incrementally disconnecting existing solar PV installation from the network

In comparison to the results for base case scenario, the average power losses are lower for the scenario with existing solar PV installation, and this is true for all the aggregation levels and across all the time granularities. Considering a 1-home aggregation level (which means having 20 homes connected onto the network), we respectively obtain 251W, 217W, and 181W network average power losses at 1, 144, and 1440 minute time granularities for the base case scenario; whereas, we obtain 179W, 141W, and 40W network average power losses at 1, 144, and 1440 minute time granularities for the scenario with existing solar PV installation. For both scenarios, we can observe that it is important to choose data with the right time granularity in order to avoid undesirable temporal averaging effects. For instance, in the case of the existing solar PV scenario, the estimated network average power losses at the 1440-minute time granularity are about 78% lower than at the 1-minute time

granularity. This underestimation error can be detrimental to planning and design considerations of the network.

(c) ***Load-dependency loss factor***

Similarly to the base case scenario in Section 4.4.4 (Chapter 4, Page 75), for this parameter, we are interested in the change in losses in relation to losses at full load (with all loads fitted with a solar PV installation in this scenario) when varying the size of home groupings of customers and when considering different time granularities. The main reason is to quantify how much the differential change in network demand contributes to the change in losses, as defined in Equation 4.6 (Chapter 4, Page 67). In this scenario, we disconnect homes fitted with a solar PV installation according to different aggregation levels, using different time granularities. It is these changes in the network demand that we seek to correlate to the corresponding changes in the network losses.

The characterisation of the load-dependency loss factor for this scenario is summarised in Figures 5.7 and 5.8 for the aggregation and time granularity effects, respectively.

As we have noted in Section 5.4.1.1-(b), higher network losses are obtained as more customers are connected on the network at once for the scenario with existing solar PV installation. It, therefore, follows that in relation to Equation 4.6 (using the parameters for the scenario with existing solar PV installation), the $L_o^{(existing\_pv),\tau}$ term will constitute the highest losses (albeit lower than the power losses for the base case scenario) when all loads are connected on the network, and the $L_\alpha^{(existing\_pv),\tau}$ term will always yield lower losses as the α magnitude increases. This means that we obtain less network power losses when more homes with existing solar PV installation are disconnected from the network. As a result, the numerator term of Equation 4.6 (i.e., $L_o^{(existing\_pv),\tau} - L_\alpha^{(existing\_pv),\tau}$) continues to increase with increasing α (number of homes disconnected from the network) values. This

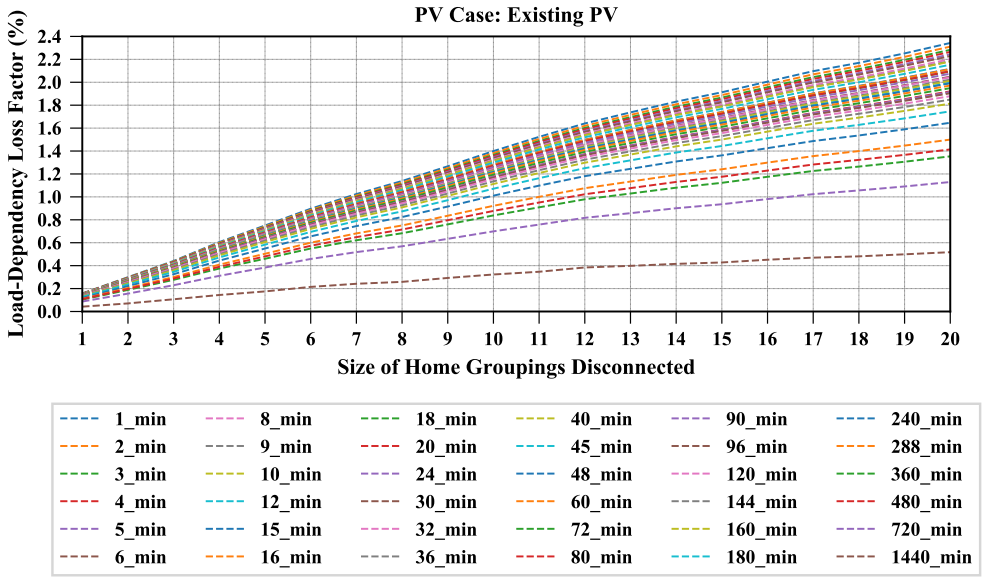

Figure 5.7: The network load-dependency loss factor versus aggregation levels across different time granularities when incrementally disconnecting existing solar PV installation from the network

variation in the changes in losses in relation to the changes in network demand is what is depicted in Figure 5.7, and we can observe that the load-dependency loss factor increases with the increasing size of home groupings disconnected from the network.

For the time granularity effects highlighted in Figure 5.8, it can be seen that lower load-dependency loss factors are obtained at larger time granularities. This is in line with the observation that the estimated network power losses tend to be underestimated at larger time granularities – thereby yielding less variable results, and hence lower load-dependency loss factors.

The observed trends in the load-dependency loss factor variations described in this scenario are applicable to the trends obtained for the scenario of adding new solar PV installation, the results of which are displayed in Section 5.4.1.2-(c).

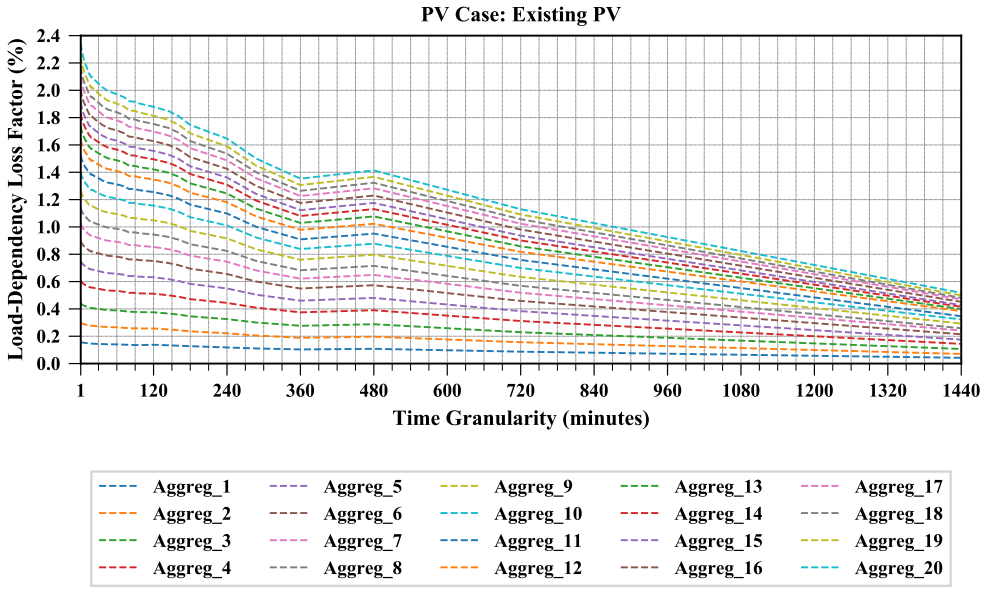

Figure 5.8: The network load-dependency loss factor versus time granularities across different aggregation levels when incrementally disconnecting existing solar PV installation from the network

5.4.1.2 Adding new solar PV installation

In this section, we will discuss the results for the characterisation of the ADMD, average power losses, and load-dependency loss factor in Sections 5.4.1.2: (a), (b), and (c), respectively. These results are in line with the methodology defined in Section 5.3.1-(ii) for the scenario where new solar PV installation is incrementally added onto households with no existing solar PV installation. Here, we examine the impact of adding new solar PV installation onto the network at different aggregation levels and using load profiles with different time granularities; whereas in Section 5.4.1.1, we examined the impact of random disconnection of households with existing solar PV installation.

(a) ***After-diversity maximum demand***

As was noted for the scenario with existing solar PV installation in Section 5.4.1.1-(a) and in all the ADMD observations in the previous chapters, the trend in the network ADMD remains the same – decreasing as both the size of home groupings on the network and the time granularity of load

profiles used tend to larger magnitudes. In the scenario of adding new solar PV installations onto the network, a given size of home groupings represents a penetration level of solar PV on the network, which means that a 1-home grouping size signifies a case where a solar PV installation is added to one (1) home at a time. The ADMD variations against the size of home groupings and the time granularities are presented in Figures 5.9 & 5.10, respectively; whereas, a summary of the combined effect of both the size of home groupings and time granularities is presented as a contour plot in Figure 5.11.

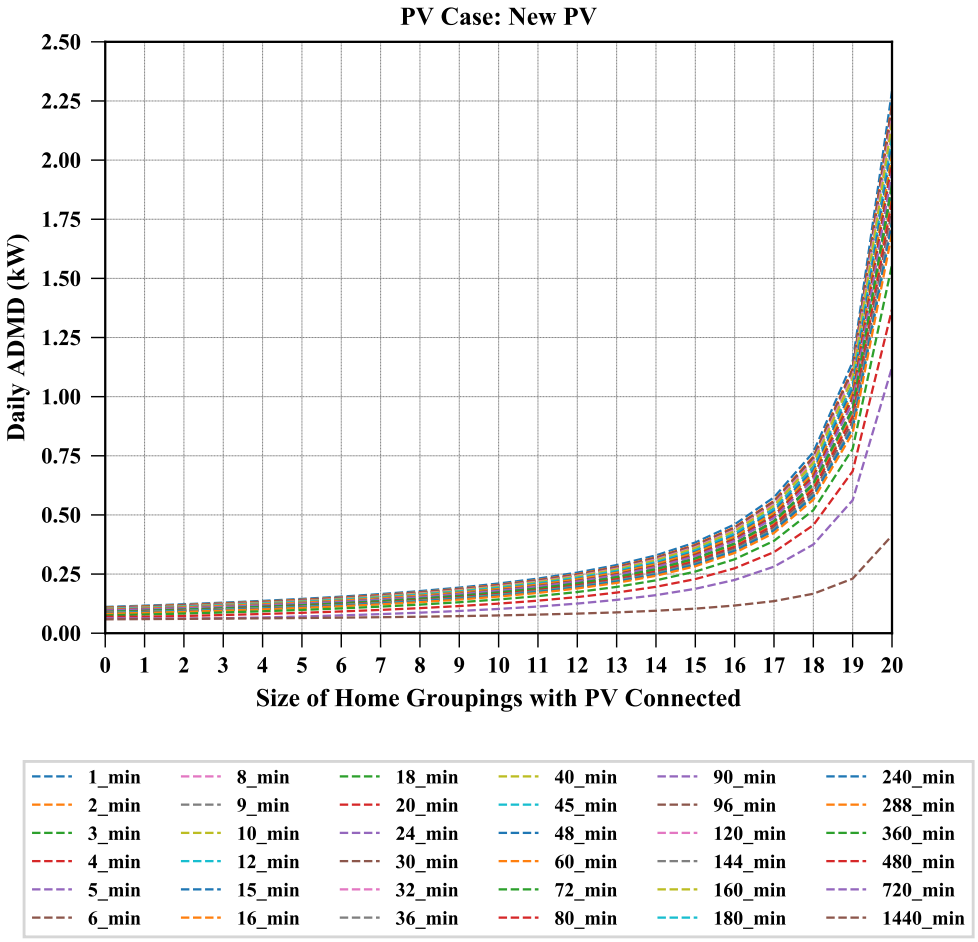

Figure 5.9: The network ADMD versus aggregation levels across different time granularities when incrementally adding new solar PV installation onto the network

In reference to Figures 5.9-5.11, we can observe that the highest ADMD value is obtained for the highest solar PV penetration level, where solar PV installation is added onto twenty (20) homes at a time. This means that only

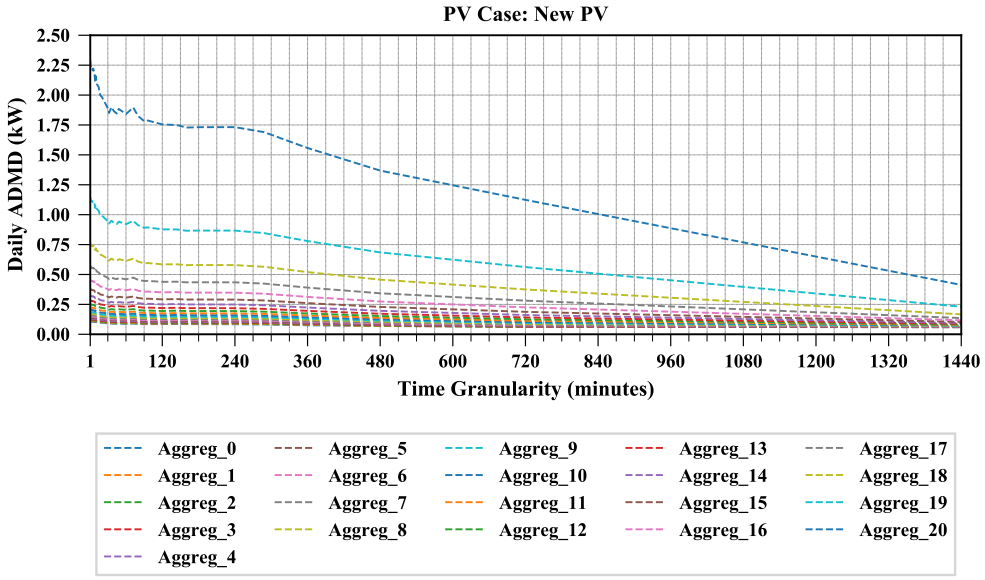

Figure 5.10: The network ADMD versus time granularities across different aggregation levels when incrementally adding new solar PV installation onto the network

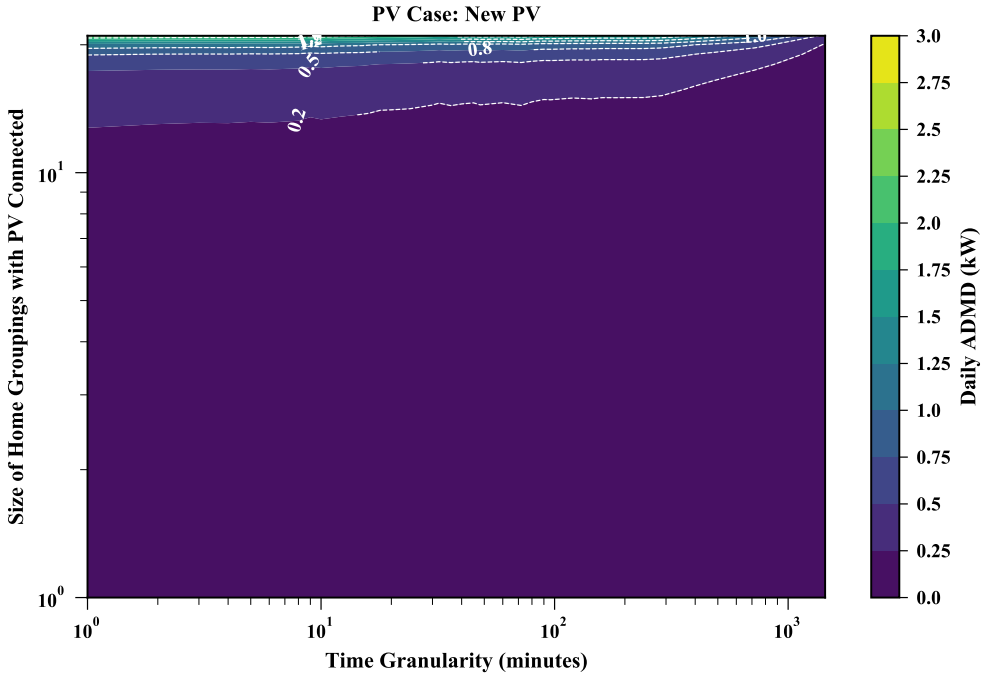

Figure 5.11: The diversified maximum demand as a function of the size of customer groupings and the time granularity when incrementally adding new solar PV installation onto the network

one home would have no solar PV installation in this case. Lower ADMD values are obtained at the lower solar PV penetration level.

The results for this scenario require a further investigation on the impact of solar PV penetration onto the distribution network performance, especially such aspects relating to intermittency levels, harmonics and reverse power flow in relation to design and operational parameters of the distribution network. These aspects are however not within the scope of this work. A comprehensive study about the impact of energy efficiency and renewable energy on electricity master planning and design parameters is presented in [53] and [54].

(b) ***Average power losses***

For this scenario, we obtain higher losses when fewer numbers of customers with solar PV installation are connected on the network at once, and lower levels of average power losses when load profiles with larger time granularities are used. The effects of solar PV penetration onto the network are summarised in Figure 5.12, whereas the temporal effects are presented in Figure 5.13.

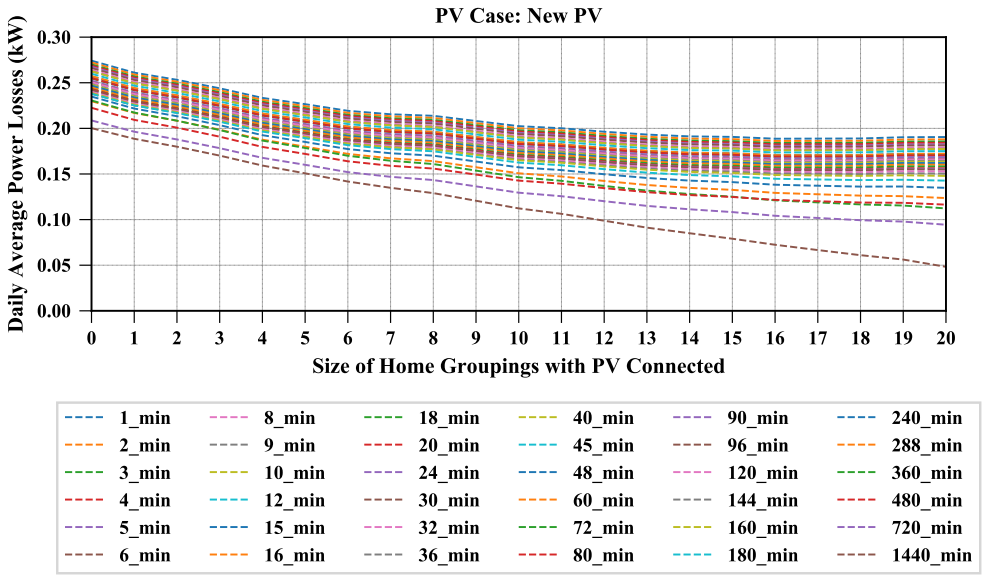

Figure 5.12: The network average losses versus aggregation levels across different time granularities when incrementally adding new solar PV installation onto the network

As expected, the network losses on the network decrease as more solar PV is added onto the network. This is evident in Figure 5.12, where, if we take the uppermost trendline of 1-minute time granularity, we obtain 274W, 202W,

and 191W network average losses for the zero-home, 10-homes, and 20-homes solar PV penetration levels, respectively.

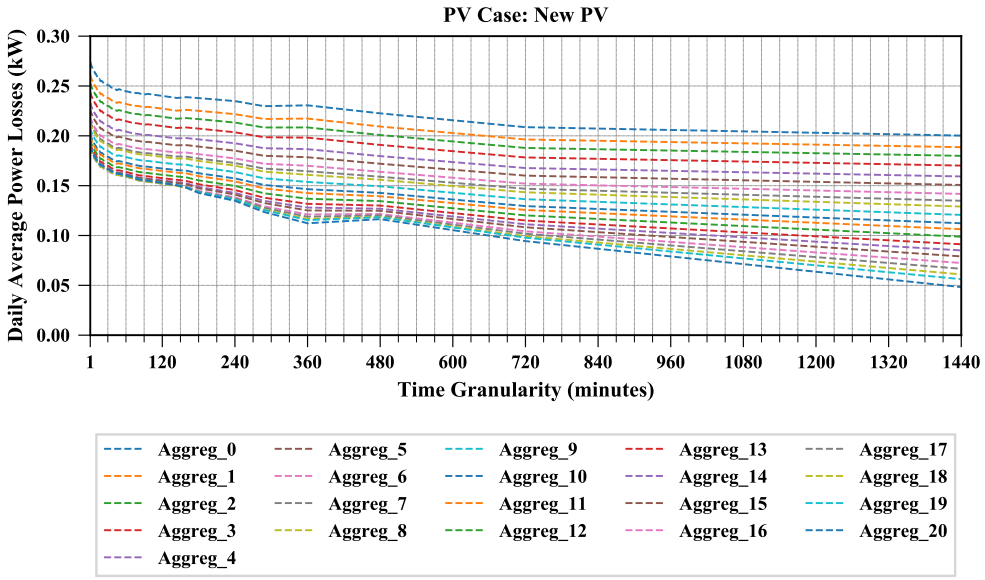

Figure 5.13: The network average losses versus time granularities across different aggregation levels when incrementally adding new solar PV installation onto the network

With reference to Figure 5.13, and taking the uppermost trendline of zero-home solar PV penetration level, we can observe that the temporal effects are as noted for the base case and existing solar PV scenarios, where the estimated network average losses decrease as time granularities become larger. For example, in the case of the uppermost trendline in Figure 5.13, we respectively obtain 274W, 238W, and 200W network average losses at the 1, 144, and 1440 minute time granularities, with an underestimation error of about 27% at the 1440-minute time granularity.

(c) ***Load-dependency loss factor***

The variations in the load-dependency loss factor for this scenario are the same as those observed for the scenario with existing solar PV installation, as described in Section 5.4.1.1-(c).

The load-dependency loss factor characterisation for this scenario is summarised in Figure 5.14.

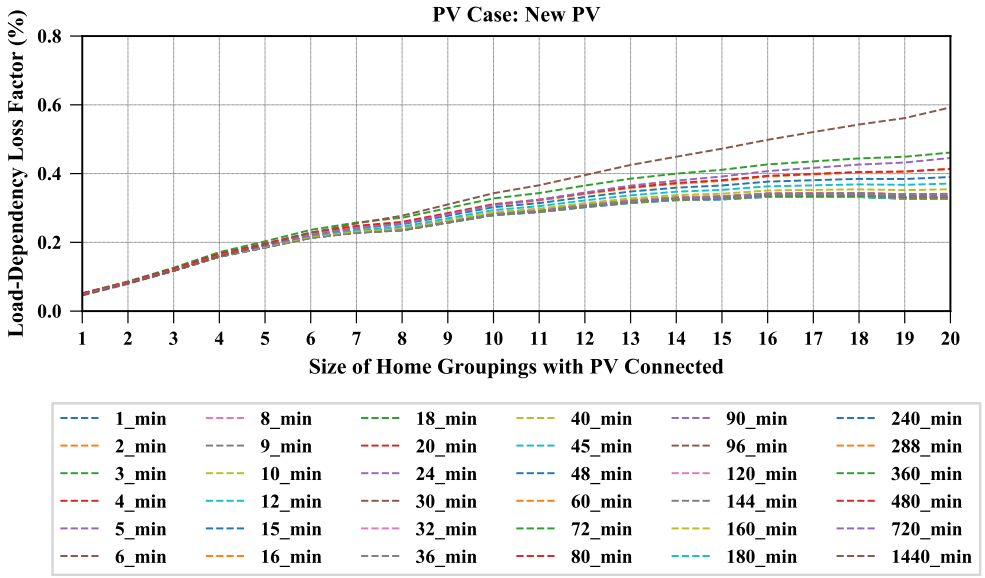

Figure 5.14: The network load-dependency loss factor versus aggregation levels across different time granularities when incrementally adding new solar PV installation onto the network

5.4.2 Impact of a combination of solar PV based renewable energy with electric vehicles (EVs) based flexible demand

The results discussions presented in this section build on the results presented for the base case scenario in Section 4.4 (Chapter 4, Page 69) and the scenario with existing solar PV installation as presented Section 5.4.1-(i). The spatio-temporal characterisation results of the combined impact of solar PV based renewable energy and electric vehicles (EVs) on the distribution network will be presented in the following sub-sections, 5.4.2.1 & 5.4.2.2, detailing out the observations under two scenarios, viz. the scenario where new electric vehicles are added to households with no existing solar PV installation, and the scenario where new electric vehicles are added to households with existing solar PV installation, respectively.

5.4.2.1 Adding new EVs to households without solar PV installation

As per the methodology defined in Section 5.3.2-(i) for the scenario where vehicles are added to households with no solar PV installation, the characterisation results

of the ADMD, average power losses, and load-dependency loss factor are presented in Sections 5.4.2.1: (a), (b), and (c), respectively.

(a) ***After-diversity maximum demand***

As we will also note for the second scenario results presented in Section 5.4.2.2-(a), the trend in the network ADMD remains unchanged – decreasing as both the size of home groupings on the network and the time granularity of load profiles used tend to larger magnitudes. In this scenario of adding new EVs to households with no existing solar PV installation, a given size of home groupings represents a penetration level of EVs on the network, which means that a 1-home grouping size signifies a case where an EV is added to one (1) home at a time. The ADMD variations against the size of home groupings and the time granularities are presented in Figures 5.15 & 5.16, respectively; whereas, a summary of the combined effect of both the size of home groupings and time granularities is presented as a contour plot in Figure 5.17. From these graphs, it can be observed that the ADMD increases as the penetration level of EVs increases.

In particular, we can observe in Figures 5.15-5.17 that the highest ADMD value is obtained for the highest EV penetration level, where EVs are added onto twenty (20) homes at a time. This means that only one home would have no EV added to it in this case. The temporal effect on the ADMD variation remains the same as noted for all the previous scenarios.

(b) ***Average power losses***

As respectively summarised in Figures 5.18 & 5.19, we obtain higher losses when larger numbers of customers with an EV ownership are connected onto the network at once, and lower levels of average power losses when load profiles with larger time granularities are used.

In this scenario where new EVs are added to households with no existing solar PV generation, the magnitudes of the network average power losses

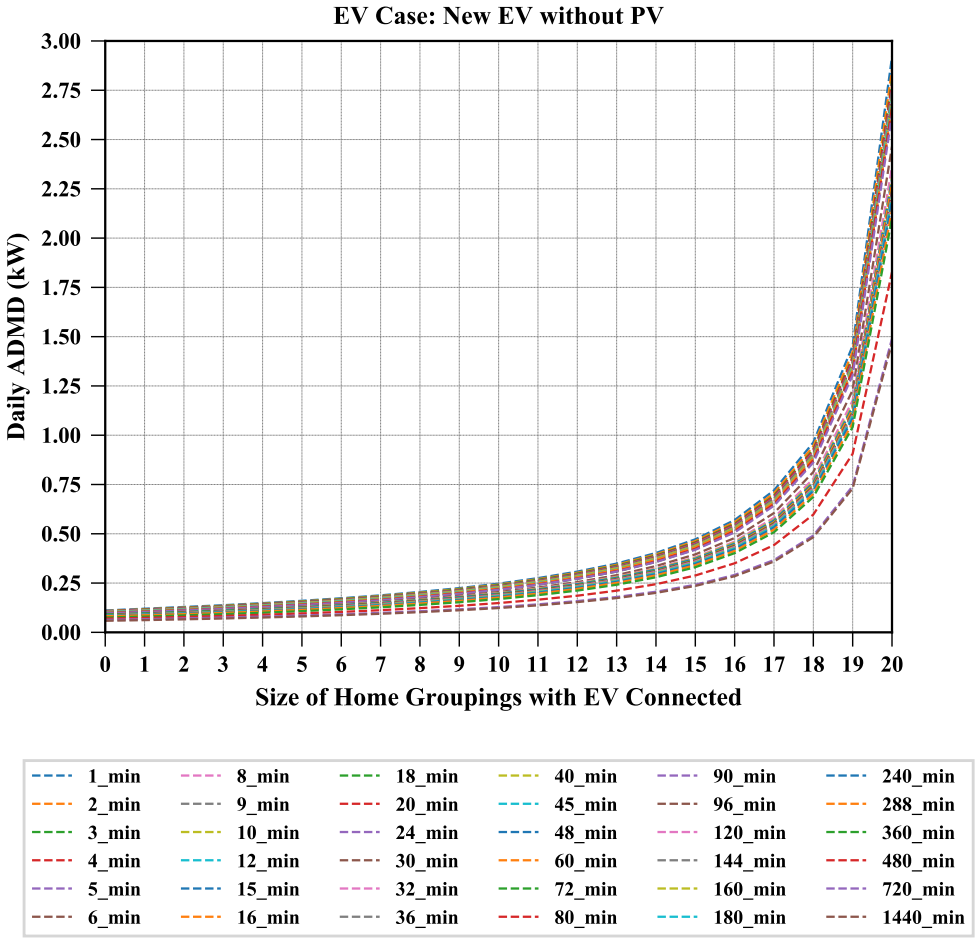

Figure 5.15: The network ADMD versus aggregation levels across different time granularities when incrementally adding new EVs to households without solar PV installation

are the highest when compared to all the considered scenarios. This is an expected network losses characterisation result as the addition of more EVs to the network translates into increased power demand on the network, and hence resulting in a corresponding increase in the network I^2R losses.

(c) ***Load-dependency loss factor***

In contrast to the solar PV case study in Section 5.4.1, the differential changes in the network average power losses increase with the increasing EV penetration level on the network. This is true for both scenarios considered under the EV case study, both in the scenario of adding EVs to homes with no existing

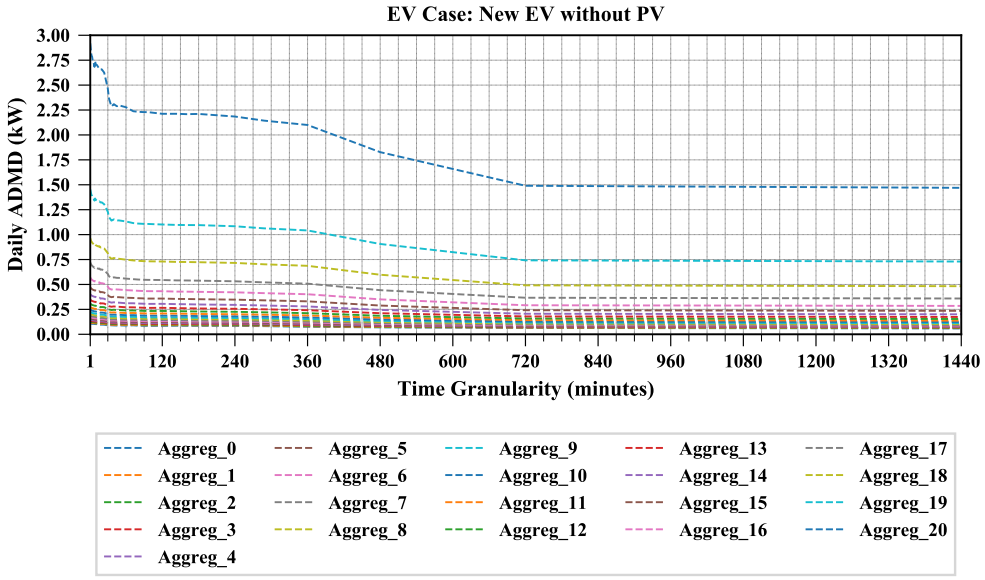

Figure 5.16: The network ADMD versus time granularities across different aggregation levels when incrementally adding new EVs to households without solar PV installation

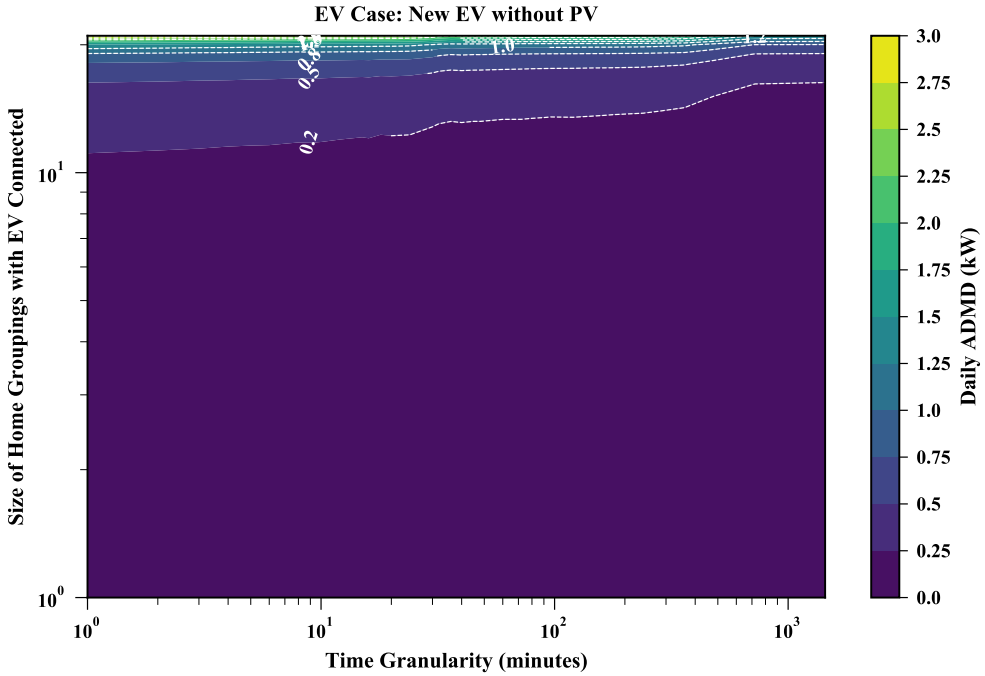

Figure 5.17: The diversified maximum demand as a function of the size of customer groupings and the time granularity when incrementally adding new EVs to households without solar PV installation

solar PV generation and the scenario of adding EVs to homes with existing solar PV generation (the results of which are presented in Section 5.4.2.2-(c)).

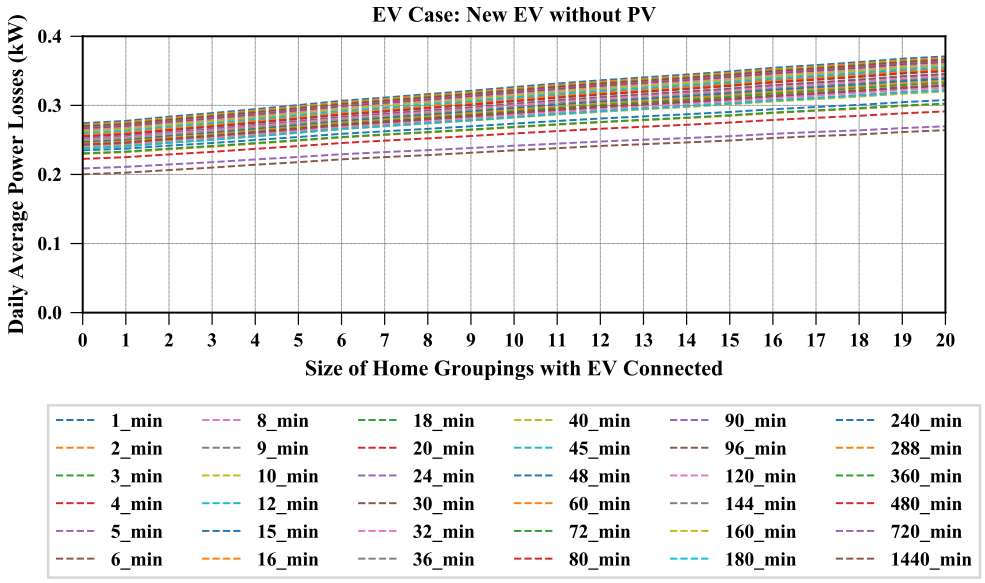

Figure 5.18: The network average losses versus aggregation levels across different time granularities when incrementally adding new EVs to households without solar PV installation

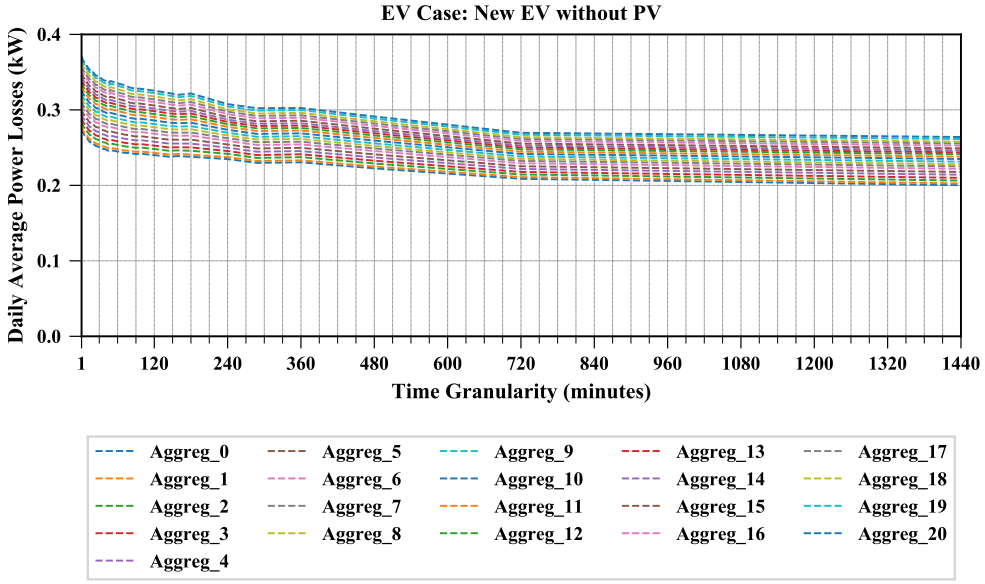

Figure 5.19: The network average losses versus time granularities across different aggregation levels when incrementally adding new EVs to households without solar PV installation

The characterisation of the load-dependency loss factor for the scenario of adding EVs to homes with no existing solar PV generation is summarised in Figures 5.20 and 5.21 for the aggregation and time granularity effects,

respectively.

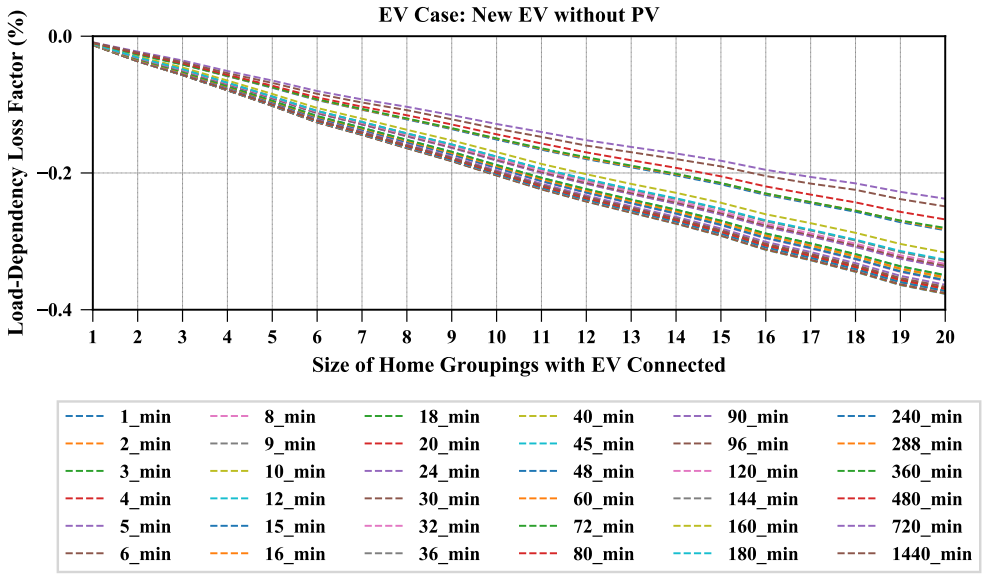

Figure 5.20: The network load-dependency loss factor versus aggregation levels across different time granularities when incrementally adding new EVs to households without solar PV installation

With reference to Equation 5.2, the $L_o^{(base),\tau}$ (which is the same network power losses obtained when all loads are connected on the network for the base case scenario) term will constitute the lowest losses when all loads are connected on the network, and the $L_\alpha^{(ev),\tau}$ term will always yield higher losses as the α magnitude increases. This means we obtain more network power losses when more homes acquire an EV. As a result, the numerator term of Equation 5.2 (i.e., $L_o^{(base),\tau} - L_\alpha^{(ev),\tau}$) continues to decrease with increasing α (number of homes disconnected from the network) values. In fact, this numerator term yields negative results, which is why we observe that the load-dependency loss factors for the EV case study yield characterisation curves below the zero-axis, as displayed in Figures 5.20 and 5.21 for the scenario with no existing solar PV, and in Figures 5.27 and 5.28 for the scenario with existing solar PV installation (refer to Page 127). This variation in the changes in losses, in relation to the changes in network demand, is depicted in Figure 5.20, and we

can observe that the load-dependency loss factor decreases with the increasing size of home groupings added onto the network.

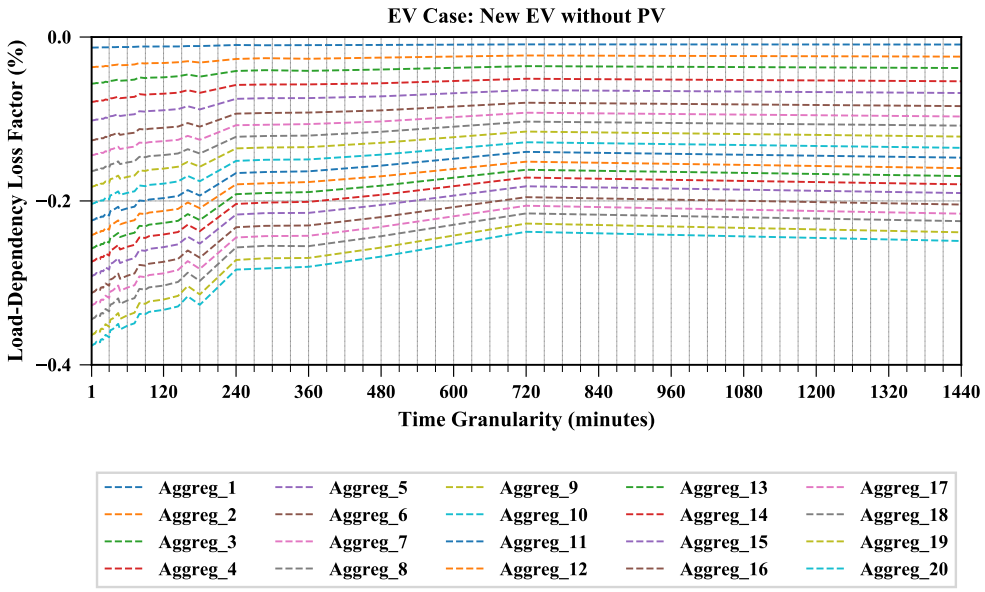

Figure 5.21: The network load-dependency loss factor versus time granularities across different aggregation levels when incrementally adding new EVs to households without solar PV installation

The observed trends in the load-dependency loss factor variations described in this scenario are applicable to the trends obtained for the scenario of adding new EVs to homes with existing solar PV generation, the results of which are displayed in Section 5.4.2.2-(c).

5.4.2.2 Adding new EVs to households with existing solar PV installation

The results presented in this section are in line with the methodology defined in Section 5.3.2-(ii) for the scenario where electric vehicles are added to households with existing solar PV installation. The characterisation results of the ADMD, average power losses, and load-dependency loss factor are presented in Sections 5.4.2.2: (a), (b), and (c), respectively.

(a) ***After-diversity maximum demand***

As was the case for all the scenario results presented thus far, the scenario of adding EVs to households with existing solar PV installation yields same the

trend in the network ADMD, where the ADMD decreases as both the size of home groupings on the network and the time granularity of load profiles used tend to larger magnitudes. For this scenario, a given size of home groupings represents a penetration level of EVs on the network with existing solar PV installation, which means that a 1-home grouping size signifies a case where an EV is added to one (1) home with solar PV installation at a time. The ADMD variations against the size of home groupings and the time granularities are presented in Figures 5.22 & 5.23, respectively; whereas, a summary of the combined effect of both the size of home groupings and time granularities is presented as a contour plot in Figure 5.24.

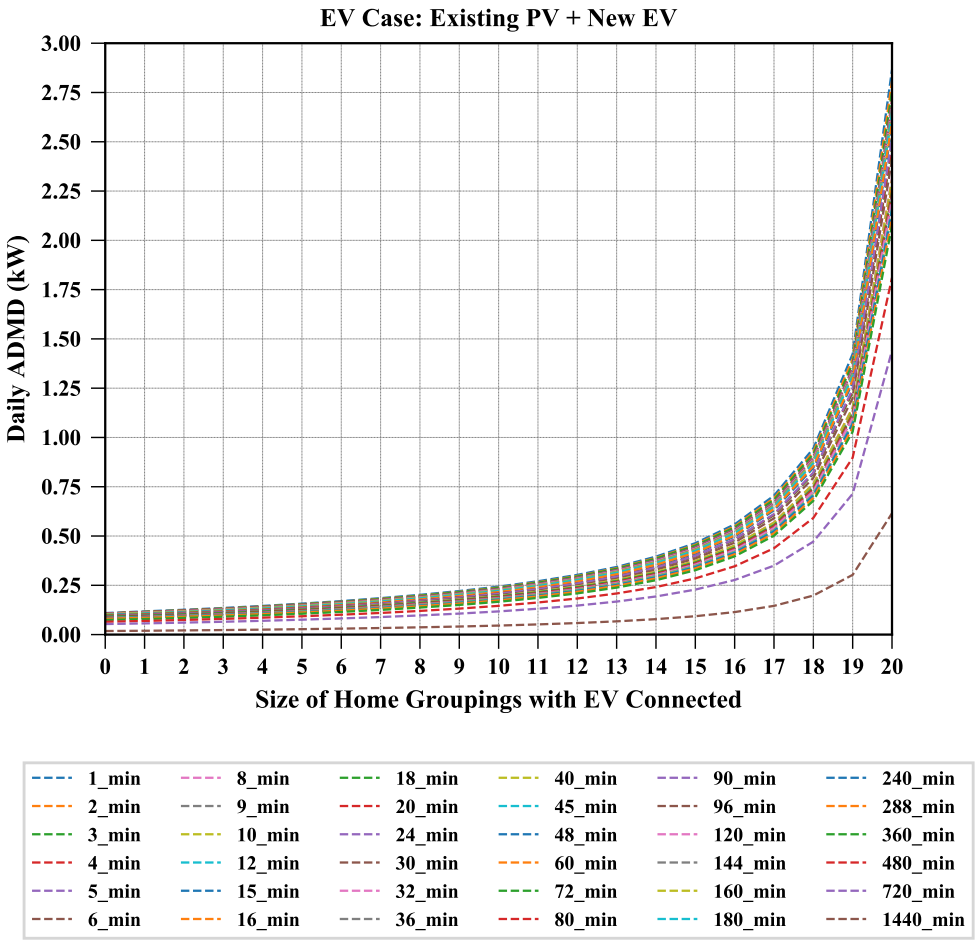

Figure 5.22: The network ADMD versus aggregation levels across different time granularities when incrementally adding new EVs to households with existing solar PV installation

Unlike the scenario in Section 5.4.2.1-(a), this scenario considers adding EVs to households which already contain solar PV installation. Therefore, the initial results for the zero-home aggregation level (i.e., when all homes fitted with solar PV generation are connected onto the network) are exactly the same as those obtained for the scenario where households with existing solar PV installation were incrementally disconnected from the network (refer to Section 5.4.1.1-(a)). The ADMD values for the zero-home aggregation at 1, 144, and 1440 minute time granularities are 2.29kW, 1.75kW, and 0.38kW, respectively, all of which are lower than the scenario with no existing solar PV installation.

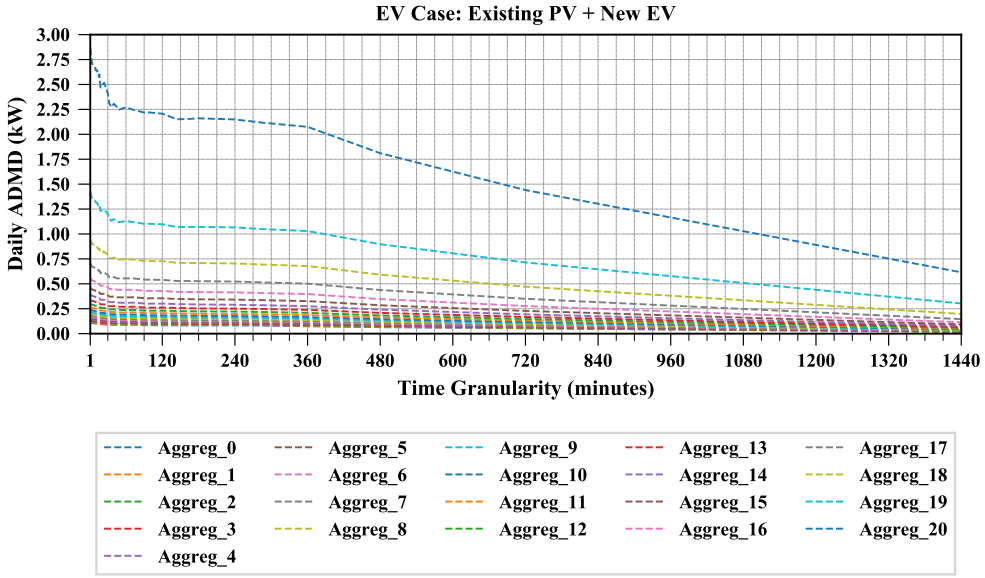

Figure 5.23: The network ADMD versus time granularities across different aggregation levels when incrementally adding new EVs to households with existing solar PV installation

Similarly to the scenario with no existing solar PV installation in Section 5.4.2.1-(a), the ADMD increases as the penetration level of EVs increases. The ADMD values are however lower for aggregation levels greater than zero across all time granularities for the EV scenario with existing solar PV installation. This is an expected result due to the lower power requirements from the network which is off-setted by the existing local solar PV generation.

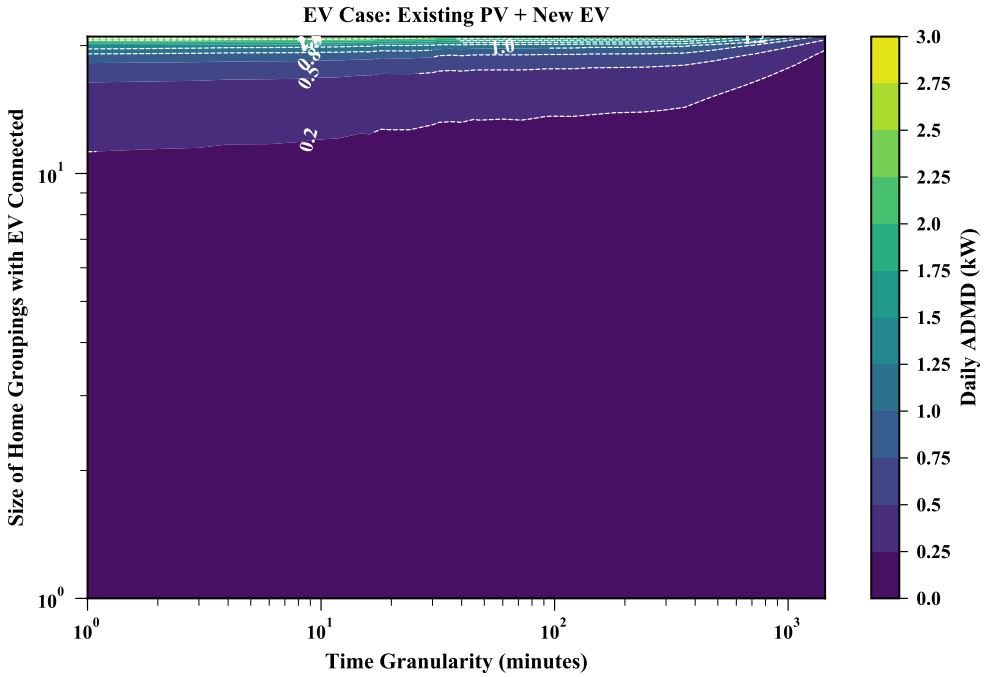

Figure 5.24: The diversified maximum demand as a function of the size of customer groupings and the time granularity when incrementally adding new EVs to households with existing solar PV installation

(b) ***Average power losses***

The characterisation trends in the variation of network average power losses in relation to both the aggregation and time granularity levels are exactly the same as noted for all the other scenarios discussed thus far. The results for the characterisation of the average power losses on the network are summarised in Figure 5.25 for the aggregation effects and in Figure 5.26 for the temporal effects.

In comparison to the scenario with existing solar PV, presented in Section 5.4.1.1-(b), we obtain the same power losses at the zero-home aggregation level, i.e., when no EV is added to any home. However, higher power losses are obtained at higher EV penetration levels for the EV scenario in the presence of existing solar PV, but still lower than those obtained for the EV scenario with no existing solar PV. This is true for all the aggregation and time granularity levels.

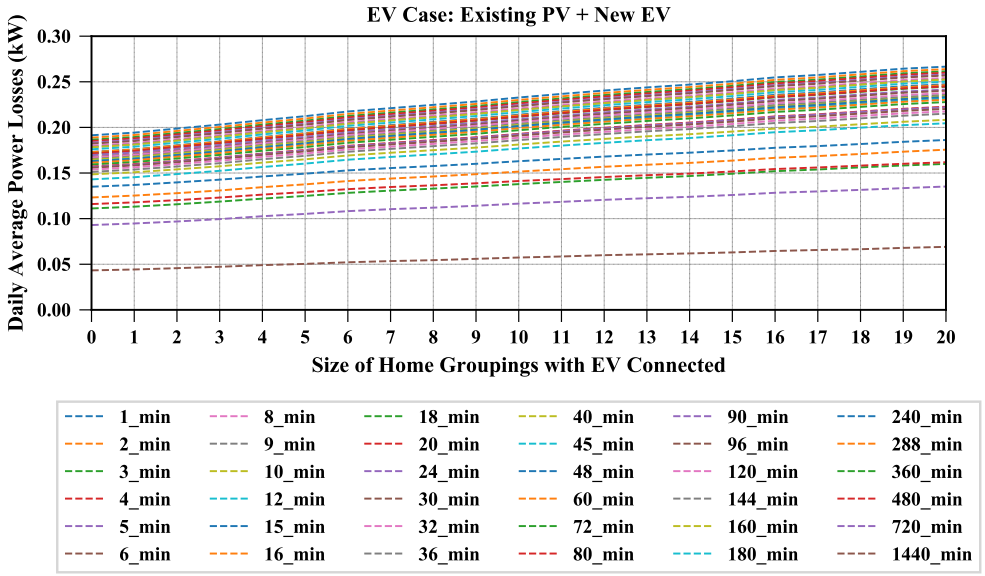

Figure 5.25: The network average losses versus aggregation levels across different time granularities when incrementally adding new EVs to households with existing solar PV installation

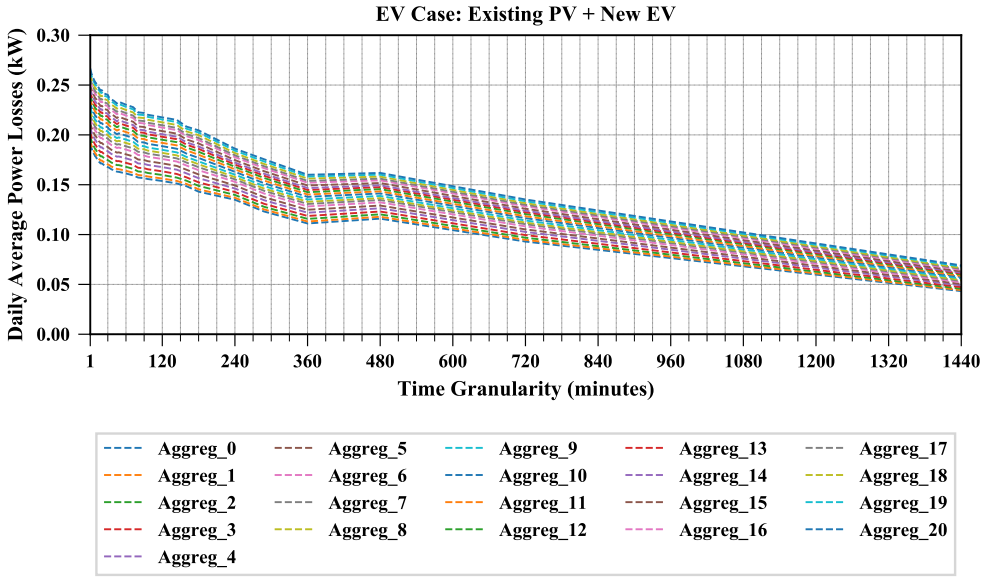

Figure 5.26: The network average losses versus time granularities across different aggregation levels when incrementally adding new EVs to households with existing solar PV installation

(c) *Load-dependency loss factor*

The characterisation of the load-dependency loss factor for the scenario of adding EVs to homes with existing solar PV generation is summarised

in Figures 5.27 and 5.28 for the aggregation and time granularity effects, respectively.

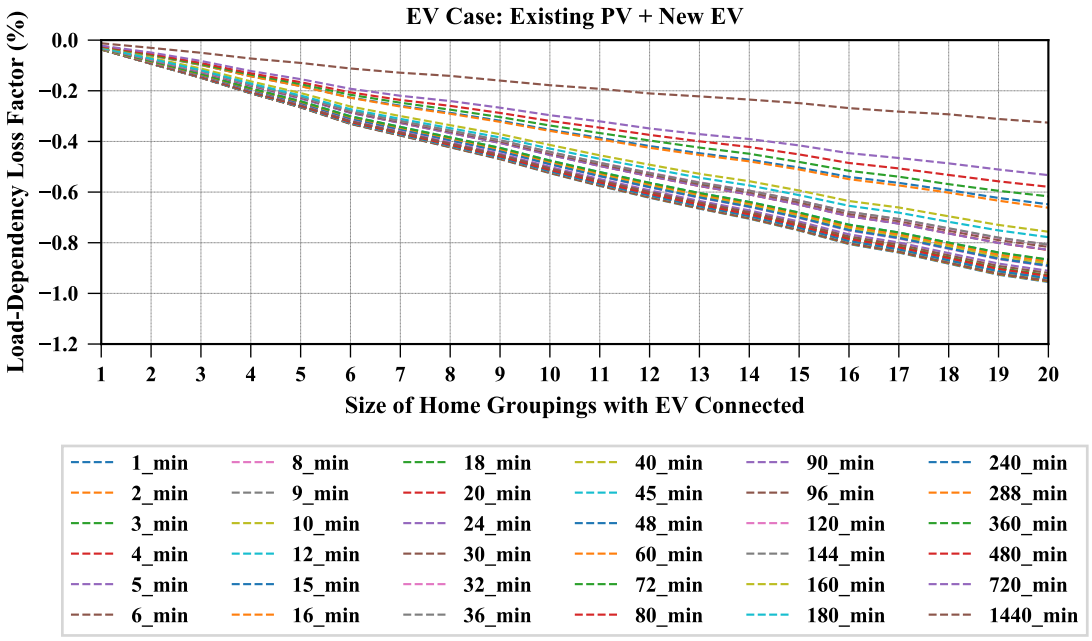

Figure 5.27: The network load-dependency loss factor versus aggregation levels across different time granularities when incrementally adding new EVs to households with existing solar PV installation

The variations in the load-dependency loss factor for this scenario are the same as described in Section 5.4.2.1-(c). Although the trends in the characterisation of the load-dependency loss factor are the same as for the EV scenario with no existing solar PV generation, we can observe from Figures 5.27 and 5.28 that the differential changes in losses due to the change in network demand are higher for the EV scenario with existing solar PV.

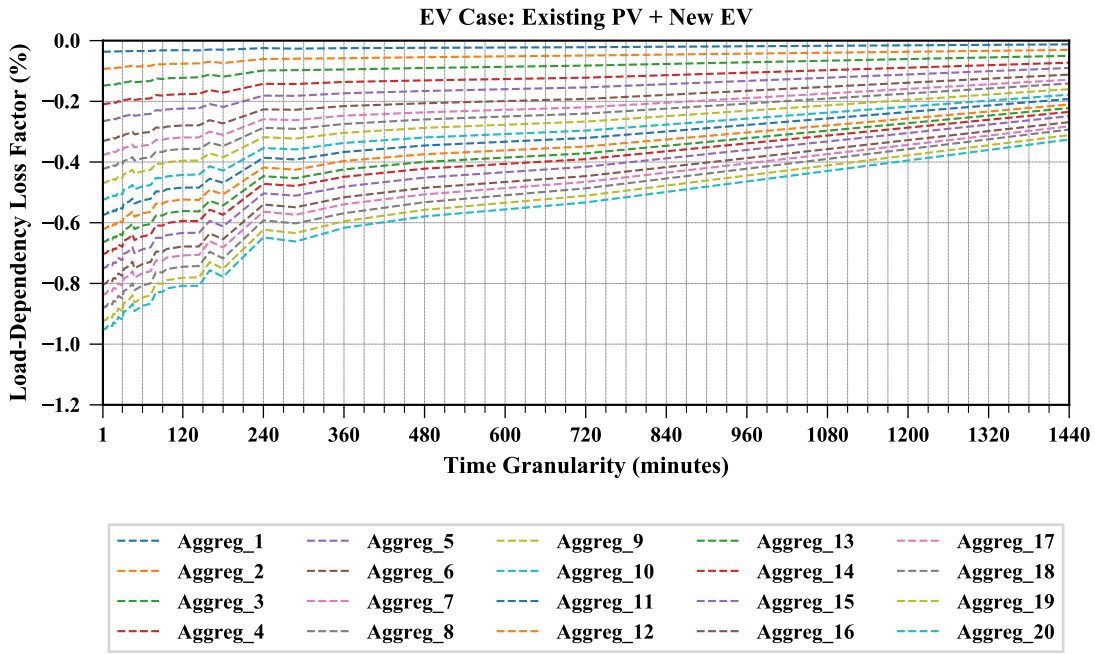

Figure 5.28: The network load-dependency loss factor versus time granularities across different aggregation levels when incrementally adding new EVs to households with existing solar PV installation

5.5 Concluding Remarks

This chapter builds on the spatio-temporal characterisation of the network design and operational parameters described in Chapter 4, where we characterised the network after-diversity maximum demand (ADMD), load variance, average power losses, and the load-dependency loss factor, when different sizes of home groupings were disconnected from the network at a time, using load profiles with different time granularities. The characterisation presented in Chapter 4 considered the base case scenario, where all homes connected on the network had no renewable energy resources or new energy applications installed. In this chapter, we characterised the impact of integrating renewable energy resources and new energy applications onto the network, where we considered adding a solar PV generation and electric vehicle (EV) charging to each home.

The characterisation was performed on a network with 21 load points, considering specific scenarios under each of the two considered case studies, viz. the solar PV case study, and electric vehicles (EVs) case study.
For the solar PV case study, two scenarios were considered, namely:

- *existing solar PV:* disconnecting households with existing solar PV installation; and
- *new solar PV:* adding new solar PV installation.

For the electric vehicles case study, two scenarios were also considered, namely:

- *new EVs without solar PV:* adding new EVs to households without solar PV installation; and
- *new EVs plus existing solar PV:* adding new EVs to households with existing solar PV installation.

Under each of these scenarios, we characterised the network diversified peak demand (i.e., the ADMD), average power losses, and the load-dependency loss factor. Unlike in Chapter 4, the load variance was not considered in this chapter as this parameter

was deemed implicit in the observations noted for all the other parameters, whereby the variability in the load (and also in all the other parameters – i.e., the network ADMD, average power losses, and the load-dependency loss factor) decreases with increasing sizes of home groupings and longer averaging temporal scales. We therefore only concentrated on the network ADMD, average power losses, and the load-dependency loss factor in this chapter.

Sections 5.5: (a), (b), and (c) give a summary of key observations drawn from the spatio-temporal characterisation of the network under the specified scenarios for the network ADMD, average power losses, and the load-dependency loss factor, respectively.

(a) ***After-diversity maximum demand***

The detailed observations in the spatio-temporal characterisation of the network ADMD are given in Sections 5.4.1.1-(a), 5.4.1.2-(a), 5.4.2.1-(a), and 5.4.2.2-(a), under the above-stated scenarios.

In summary, under all the considered scenarios, the network per-customer capacity requirement (ADMD) was found to decrease with the increasing size of home groupings in the characterisations for the respective scenarios, and also decreasing with the increase in the time granularity of the time-series dataset used in the characterisation. This observation has been consistent both in the base case scenario reported in Chapter 4, as well as in the studies reported in Chapters 2 & 3.

Figure 5.29 shows a comparison of the network ADMD across the 1, 30, 60, 120, 240, 480, and 1440 minute time granularities for four different sizes of home groupings, where the ADMD characterisations for the four scenarios are plotted on one chart. As evident from Figure 5.29, we can observe that the ADMD decreases as the time granularities tend to larger magnitudes, and this is true for all the sizes of home groupings and for all the scenarios.

From the 20-home home grouping in Figure 5.29(d), we notice that the scenario where new EVs were added to the the network with no existing solar PV yields

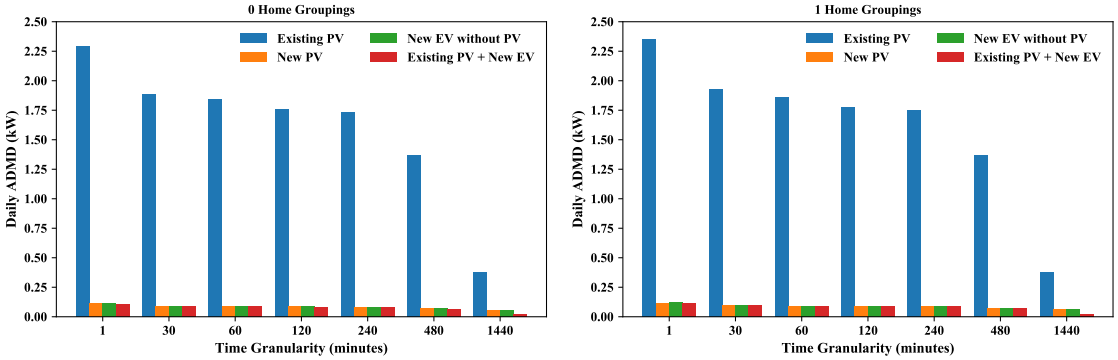

(a) *0-home groupings* **(b)** *1-home groupings*

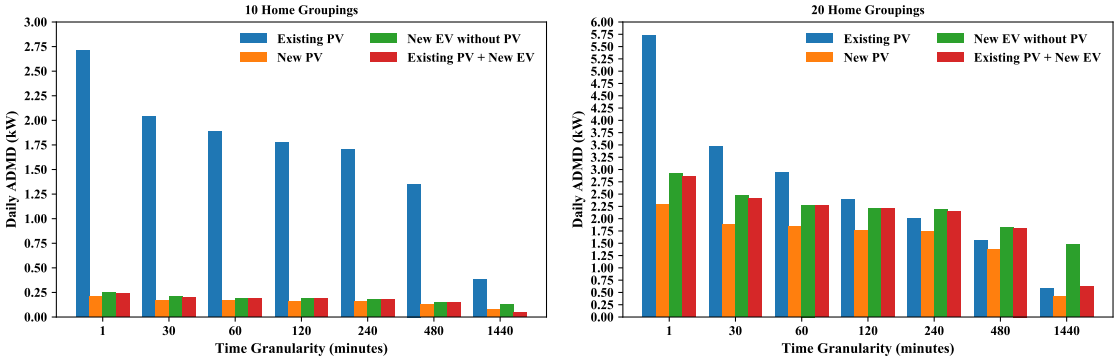

(c) *10-home groupings* **(d)** *20-home groupings*

Figure 5.29: This figure shows a comparison of the ADMD variations across a selected set of time granularities for different sizes of home groupings under different scenarios.

a higher level network ADMD across all time granularities when compared to the scenario where new EVs were added to the network with existing solar PV, and this is a plausible result.

(b) ***Average power losses***

The detailed observations in the spatio-temporal characterisation of the network average power losses are given in Sections 5.4.1.1-(b), 5.4.1.2-(b), 5.4.2.1-(b), and 5.4.2.2-(b), under the above-stated scenarios.

For the scenarios where homes with existing solar PV generation were disconnected from the network and where EVs were added to the network, we obtain higher average power losses when larger numbers of customers were connected on the network at once. In contrast, however, we obtain higher losses when fewer numbers of customers with solar PV generation are

connected on the network at once.

For temporal effects, we obtain lower levels of average power losses when load profiles with larger time granularities are used, and this is true for all the sizes of home groupings, under all the scenarios.

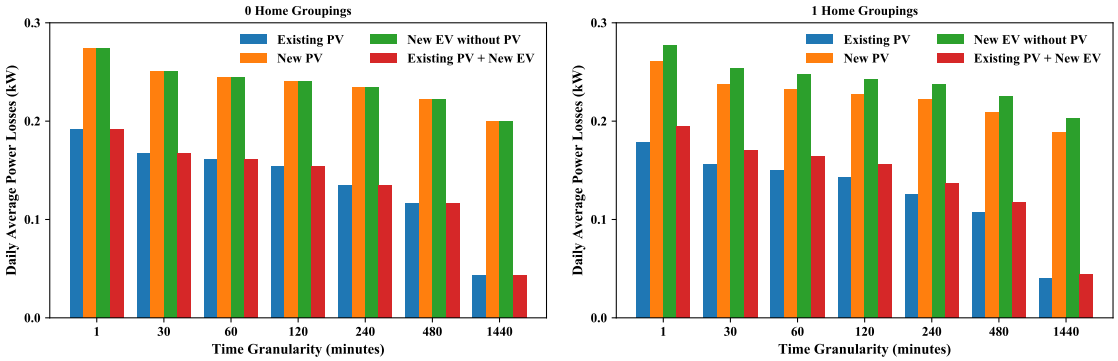

(a) *0-home groupings* **(b)** *1-home groupings*

(c) *10-home groupings* **(d)** *20-home groupings*

Figure 5.30: This figure shows a comparison of the variation in network average power losses across a selected set of time granularities for different sizes of home groupings under different scenarios.

Figure 5.30 shows a comparison of the network average power losses across the 1, 30, 60, 120, 240, 480, and 1440 minute time granularities for four different sizes of home groupings, where the network average power losses characterisations for the four scenarios are plotted on one chart.

For the zero-home grouping in Figure 5.30(a) where all homes are connected to the network, i.e., a case where no variation (not disconnecting any homes or adding any solar PV/EVs to any home) in the network conditions is made, we observe that the scenarios with existing solar PV generation (scenarios:

Existing PV & Existing PV + New EV) exhibit the same level of average power losses, and the scenarios with no existing solar PV generation (scenarios: *New PV & New EV without PV*) exhibit the same level of average power losses. This is true across all the time granularities.

For larger sizes of home groupings in Figures 5.30(b), 5.30(c), and 5.30(d), however, we notice that the scenario where homes with existing solar PV generation were disconnected from the network yields the lowest level of network average power losses across all time granularities; whereas, the scenario where EVs were added to homes with no existing solar PV generation yields the highest level of average power losses.

(c) ***Load-dependency loss factor***

For this parameter, we are interested in the change in losses in relation to losses at full load when varying the size of home groupings of customers and when considering different time granularities. The main objective is to quantify how much the differential change in network demand would contribute to the change in losses on the network.

The specific observations in the spatio-temporal characterisation of the load-dependency loss factor are given in Sections 5.4.1.1-(c), 5.4.1.2-(c), 5.4.2.1-(c), and 5.4.2.2-(c), under the above-stated scenarios.

Figure 5.31 shows a comparison of the load-dependency loss factor across the 1, 30, 60, 120, 240, 480, and 1440 minute time granularities for four different sizes of home groupings, where the load-dependency loss factor characterisations for the four scenarios are plotted on one chart.

Across all the sizes of home groupings, it is evident from Figures 5.31(a) - 5.31(d) that disconnecting homes with existing solar PV generation from the network yields the highest load-dependency loss factor; whereas, adding new EVs to homes with no existing solar PV generation yields the lowest load-dependency loss factor.

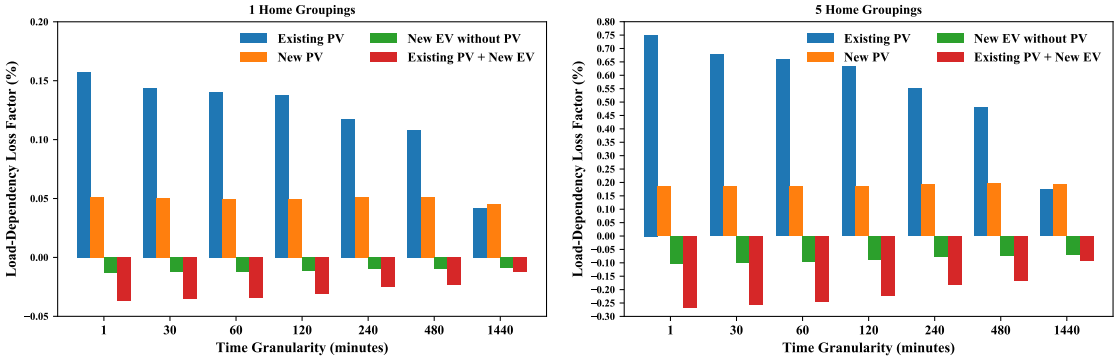

(a) *1-home groupings*

(b) *5-home groupings*

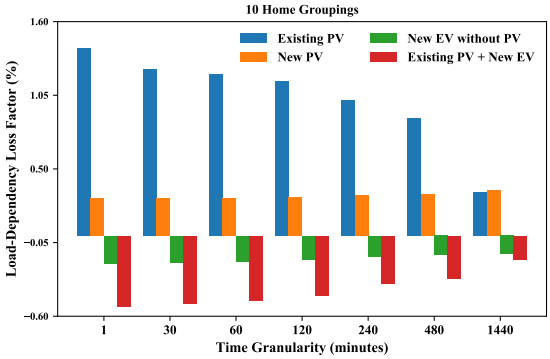

(c) *10-home groupings*

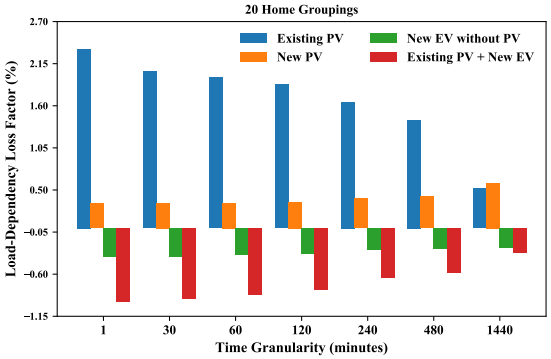

(d) *20-home groupings*

Figure 5.31: This figure shows a comparison of the variation in load-dependency loss factor across a selected set of time granularities for different sizes of home groupings under different scenarios.

It can also be seen from Figure 5.31 that the load-dependency loss factor characterisations for the solar PV case study scenarios are positive percentages; whereas, negative factors are obtained for the EVs case study scenarios. This is because, for the solar PV case study, we obtain lower power losses at larger aggregation levels as we disconnect more homes with existing solar generation or as we add more solar PV generation. In contrast, higher power losses are always obtained at larger aggregation levels when compared to the power losses at initial network conditions when no EVs are added to the network. Therefore, subtracting aggregation losses from losses obtained at initial network conditions will yield a positive value for the solar PV case study and a negative value for the EVs case study.

For the time granularity effects, lower load-dependency loss factors are

obtained at larger time granularities. This is in line with the observation that the estimated network power losses tend to be underestimated at larger time granularities – thereby yielding less variable results, and hence lower load-dependency loss factors.

Distribution network operators and planners must employ revised design and operational techniques to adapt to the inclusion of distributed energy resources, electric vehicles, and the use of other smart appliances.

— AI ELOMBO

Chapter 6
Conclusions and Further Work

Contents

6.1 Overview

This thesis explored the over-arching research question as stated below:

- **KEY RESEARCH QUESTION:** *Given the increasing adoption of distributed variable energy resources and smart appliances onto the electrical power system, what methods can be developed to help electrical power system planners and operators gain insight into the design and operational parameters of the electrical power system for purposes of enabling greater adoption of distributed variable energy resources and smart appliances in an efficient and sustainable way?*

Since the over-arching objective of this thesis was to develop a characterisation framework for design and operational parameters of the distribution network, especially in view of the increasing presence of distributed variable energy resources and smart appliances on the electrical power system, it was important that the over-arching research question covers a number of important elements that are essential to enabling the adoption of efficient and sustainable design and operational techniques to be applied on the modern electrical power system. It was therefore important to break down this question into further sub-questions in order to arrive at logical answers in respect of the over-arching research question explored in this thesis.

The important elements encompassed by the key research question are two-fold, namely: the one aspect pertains to the *planning and design of a modern electrical power system*, and another aspect relates to the *operation of a modern electrical power system*. For both of these elements, the emphasis is on the modern electrical power systems with a significant presence of distributed variable energy resources and smart appliances. For both aspects, i.e., planning & design and operation, *a characterisation of specific parameters was considered at different customer aggregation levels, using time-series customer load data with different time granularities*. Based on this approach, the following sub-questions were explored:

- **SUB-QUESTION 1:** *In view of increasing presence of distributed variable energy resources and smart appliances on the electrical power system, how do the planning and design parameters of a modern electrical power system vary when such parameters are characterised at different customer aggregation levels?*

- **SUB-QUESTION 2:** *With the objective to accurately estimate the planning and design parameters of a modern electrical power system, what effect does the use of time-series customer load data with different time granularities have on the estimated parameters?*

- **SUB-QUESTION 3:** *When considering a real electrical power system with a high presence of distributed variable energy resources and smart appliances,*

how do the design and operational parameters of a modern electrical power system vary when such parameters are characterised at different customer aggregation levels when using time-series customer load data with different time granularities?

Sub-questions 1 & 2 sought to provide a methodology to characterise planning and design parameters of time-series customer load profiles with different time granularities when aggregated at different sizes. These sub-questions are addressed in Chapters 2 and 3, where a characterisation technique (spatio-temporal characterisation framework) is developed using synthetic and real customer load profiles datasets, respectively.

Sub-question 3 is addressed in Chapters 4 & 5, where the design and operational parameters of a low-voltage distribution network with a high presence of distributed variable energy resources and smart appliances are characterised at different customer aggregation levels when using time-series customer load data with different time granularities.

On the whole, two major characterisation categories were conducted in this thesis, namely: *1) a characterisation of diversity and variability of electrical load profiles*, and *2) a characterisation of peak power and losses of a low-voltage distribution network*. Therefore, in line with the scope of this thesis as outline in Section 1.3 (see Chapter 1, Page 11) and in linkage to the key research contributions stated in Section 1.5 (see Chapter 1, Page 18), this chapter presents the key findings of this thesis in Section 6.2. The key results are presented under the two major characterisation categories, 1) & 2). Specific results of various studies explored in this thesis are included in the conclusion segments of the respective thesis chapters. Specific areas for further work that emanate from this thesis are presented in Section 6.3.

6.2 Conclusions

The key thesis findings are now presented in Sub-sections 6.2.1 and 6.2.2.

6.2.1 Characterisation of diversity and variability of electrical load profiles

Sub-questions 1 and 2 sought to provide a methodology to characterise planning and design parameters of time-series customer load profiles with different time granularities when aggregated at different sizes. These sub-questions were first addressed in Chapter 2, where a new characterisation technique (spatio-temporal characterisation framework) is developed using a synthetic customer load profiles dataset (generated using an Excel Workbook model developed by the Centre for Renewable Energy Systems Technology (CREST) of Loughborough University). This characterisation technique formed the basis for further characterisation studies presented in Chapters 3 - 5.

Chapter 2 considered planning and design parameters such as the after-diversity maximum demand (ADMD) and load variance. Both these parameters were characterised in relation to changing aggregation levels and time-scales of the considered load profiles dataset. The ADMD parameter was used as a measure for the diversity of peak demand of the individual customers, whereas the load variance parameter was used as a measure for the variability of load demand. The study considered in Chapter 2 led to the contribution of the ***methodology to characterise how the diversity and variability of electrical load profiles vary with different levels of customers aggregation and different sampling interval durations***.

Real customer load profiles datasets from four different jurisdiction areas (i.e., the United Kingdom (UK, Northern Grid), United States of America (USA, Texas), Belgium (Mons), and Australia (Ausgrid)) were considered in Chapter 3 in order to demonstrate the application of the spatio-temporal characterisation framework on realistic customer load profiles. A further characterisation metric was considered in Chapter 3. This additional characterisation metric is the load factor, which is useful for calculating the expected network power losses, and this was introduced to create a link to the consideration of the aspect of network power losses covered in Chapters 4 & 5. The work presented in Chapter 3 led to obtaining ***a new***

insight on the application of the proposed new methodology developed in Chapter 2 by using realistic customer load profiles datasets from four (4) different jurisdiction areas.

For both Chapters 2 and 3, the original time granularities of residential customer load profiles were converted to various time granularities, ranging from the original averaging time interval of one (1) minute to 1440 minutes. These time granularities were selected so that they were integer multiples of the original data time granularities, which would divide evenly into the total minutes of a full day (i.e., 1440 minutes). This was necessary for assessing the impact of temporal averaging time scales on the ADMD, load variance, and the load factor. Once this conversion was in place, up to 100 Monte Carlo simulations were then performed on the load profiles, choosing different sizes of load aggregation from one (1) customer up to 100 customers grouping size. For each time granularity, the spatio-temporal characterisation was performed to assess the considered characterisation parameters when customer grouping sizes were varied from one (1) customer up to a grouping size of one hundred (100) customers.

The characterisation of the ADMD, load variance, and load factor allows for a methodology for characterising the expected capacity and operational requirements, when customers or individual networks are interconnected at multi spatial scales. The use of load profiles sampled at different time granularities enables us to gain valuable insight into the required type of data to be used in estimating network design and operational parameters for planning purposes. This methodology could serve as a valuable tool to network planners and operators in conducting planning and operational studies. The ADMD serves as a guidance for sizing the network infrastructure, the load variance gives insight into the selection of active network management schemes, and the load factor is useful for deriving parameters necessary for estimating the expected network losses.

Both the ADMD (i.e. per customer capacity requirement) and load variance were found to asymptotically decrease toward a settling value, when both the size of customer groupings and averaging time intervals approached large numbers.

Conversely, the load factor asymptotically increases toward a settling value, when both the size of home groupings and averaging intervals increase.

Dependent upon the application, it is important that the time scales employed are optimally chosen in accordance with different spatial scales of the network. For settlement of energy sharing contracts, for instance, smaller customer groupings would require longer time periods, since the variability of the aggregate load will be higher; whereas larger customer groupings may require shorter time periods as the variability of the aggregate load will be lower. Another example would be for active network management, such as voltage regulation, where shorter time scales would be required for a network with smaller customer groupings due to the resulting high variability of the aggregate load. While the load factor bears proxy to the expected network losses, it also reveals information about the flatness/spikiness of the load profiles. In this case, we observe that the load factor shows a close correlation to the shape of the resulting aggregate load profile. A high load factor implies that the load profile is significantly flat when compared to a low load factor, which suggests that the load has a peak which is widely varied from the base load.

6.2.2 Characterisation of peak power and losses of a low-voltage distribution network

Sub-question 3 has been addressed in Chapters 4 & 5, where the design and operational parameters of a typical UK low-voltage distribution network with a high presence of distributed variable energy resources and smart appliances are characterised at different customer aggregation levels when using time-series customer load data with different time granularities.

Chapter 4 presented a base case scenario characterisation of the network ADMD, load variance, power losses, and the load-dependency loss factor, when different sizes of home groupings were disconnected from the network at a time, using time-series customer load profiles with different time granularities.

Chapter 5 considered two case studies, i.e., the case study that focused on the integration of solar PV based renewable energy, and another case study that

focused on the inclusion of plug-in electric vehicles (PEVs). Two scenarios (as explained in Section 1.3, Page 11) were considered under each of the case studies explored in Chapter 5. For each of these scenarios, the network ADMD, power losses, and the load-dependency loss factor were characterised using the spatio-temporal characterisation framework. On the whole, five scenarios were considered as below:

- Base Case Study:
  - *scenario 1 - base case scenario:* where all homes connected on the network had no renewable energy resources or any new energy applications installed.
- Solar PV Case Study:
  - *scenario 2 - existing solar PV:* where households with existing solar PV installations were incrementally disconnected from the network; and
  - *scenario 3 - new solar PV:* where solar PV installations were incrementally added to households connected on the network.
- PEV Case Study:
  - *scenario 4 - new PEVs without solar PV:* where new electric vehicles were added to households with no solar PV installation; and
  - *scenario 5 - new PEVs with existing solar PV:* where new electric vehicles were added to households with existing solar PV installation.

Scenario 1 has been covered in Chapter 4, which is representative of a scenario of a conventional distribution network. As we move to de-carbonise society, there will be new classes of high energy loads coming onto the electrical power system, including electric vehicles, heat pumps, and distributed generation. In particular, roof-top solar PV based renewable energy and plug-in electric vehicles were considered under scenarios 2 - 5. The characterisation studies considered under these scenarios (i.e., scenarios 2 - 5) are presented in Chapter 5 and these studies help shed new light on

the impact of the energy transition on the distribution network peak power and losses over different aggregation levels of customers and time-scales.

The main contribution of Chapters 4 and 5 is the ***methodology to characterise the peak power and power losses on a distribution network when the penetration level of distributed variable energy resources and smart appliances is varied across different customer aggregation levels when using time-series customer load data with different time granularities***. An additional contribution of these chapters is the ***new theoretical parameter, termed: load-dependency loss factor, which was introduced as a metric for characterising the impact of solar PV and plug-in electric vehicles on the power losses of a distribution network***.

Unlike in Chapter 4, the load variance was not considered in Chapter 5 as this parameter was deemed implicit in the observations noted for all the other parameters, whereby the variability in the load (and also in all the other parameters – i.e., the network ADMD, average power losses, and the load-dependency loss factor) decreases with increasing sizes of home groupings and longer averaging temporal effects.

Under all the considered scenarios, the network per-customer capacity requirement (ADMD) was found to decrease with the increasing size of home groupings in the characterisations for the respective scenarios, and also decreasing with the increase in the time granularity of the time-series dataset used in the characterisations. This observation has been consistent both in the base case scenario reported in Chapter 4, as well as in the characterisation studies reported in Chapters 2 & 3. A comparative discussion of the ADMD results for all the scenarios is given in Section 5.5-(a) (refer to Page 131).

For the scenarios where homes with existing solar PV generation were disconnected from the network and where EVs were added to the network, we obtain higher average power losses when larger numbers of customers were connected on the network at once. In contrast, however, we obtain higher losses when fewer numbers of customers with solar PV generation are connected on the network at once. For temporal effects, we obtain lower levels of average power losses

when load profiles with larger time granularities are used, and this is true for all the sizes of home groupings, under all the scenarios. Please refer to Section 5.5-(b) on Page 132 for a comparative discussion of the average power losses results obtained under all the scenarios.

Across all the sizes of home groupings, it has been evidently observed that disconnecting homes with existing solar PV generation from the network yields the highest load-dependency loss factor; whereas, adding new EVs to homes with no existing solar PV generation yields the lowest load-dependency loss factor. Additionally, the load-dependency loss factor characterisations for the solar PV case study scenarios yielded positive values; whereas, negative values were obtained for the EVs case study scenarios. This is because, for the solar PV case study, we obtain lower power losses at larger aggregation levels as we disconnect more homes with existing solar generation or as we add more solar PV generation. In contrast, higher power losses are always obtained at larger aggregation levels when compared to the power losses at initial network conditions when no EVs are added to the network. Therefore, in relation to the formula for calculating the load-dependency loss factor in Equation 4.6, 5.1, 5.2 and 5.3, subtracting aggregation losses from losses obtained at initial network conditions will yield a positive value for the solar PV case study and a negative value for the EVs case study. For the time granularity effects, lower load-dependency loss factors are obtained at larger time granularities. This is in line with the observation that the estimated network power losses tend to be underestimated at larger time granularities – thereby yielding less variable results, and hence lower load-dependency loss factors. A comparative discussion of the load-dependency loss factor results for all scenarios is given Section 5.5-(c) (refer to Page 134).

In summary, the spatio-temporal characterisation framework developed in this thesis provides a useful tool for distribution network planners and operators to derive planning parameters of a distribution network with a particular load size on the basis of the per-customer capacity requirement, and devise network-specific active management schemes with carefully tailored control time scales on the basis of load variability. The characterisation of network power losses allows the DNOs to

assess the network performance and implement appropriate network interventions for optimal network operation.

6.3 Further Work

As explained in Section 1.3 (refer to Page 11), the scope of the research work covered in this thesis pertains to the characterisation of design and operational parameters of the electrical power system, with a particular focus on distribution networks with significant penetration of distributed solar PV based renewable energy and plug-in electric vehicles.

Although a variety of design and operational parameters of the electrical power system were considered in this thesis as characterisation metrics, it was not within the scope of this work to provide extensive discussions on the application of these parameters to both the design and operation of the electrical power system. The scope of this thesis was to provide a framework that could be used by distribution network planners and operators to understand how the design and operational parameters of the power system vary from the perspective of different sizes of customer load aggregation when using load profiles with different time granularities. These characterisation results provide new insight into future network design and operation rules for distribution networks, especially with cognisance of the variable nature of future network energy resources and applications.

Through the use of both synthetic and real customer load data and through usage of a real distribution network, the spatio-temporal characterisation framework developed in this thesis has been proven to be an effective methodology and it will be a useful tool for distribution network planning and analysis. This characterisation methodology can be used to study any given characteristic of the electrical power system. For customer load profiles, the diversity (ADMD), variability (variance), and load factor were considered; whereas, for a real distribution network, the diversified peak demand (ADMD), load variability (variance), average power losses, and the new theoretical parameter, termed: load-dependency loss factor, were considered.

In order to expand on this work, the following aspects have been identified as possible areas for further work:

(a) Additional to the characterisation parameters considered in this thesis, viz. the ADMD, load variability, load factor, power losses, and load-dependency loss factor, it would add more insight into the design and operational requirements of a distribution network if a study is conducted on the characterisation of the reliability and stability parameters of a distribution network. This should be performed both under the base case scenario and also under the scenarios that include solar PV and plug-in electric vehicles.

(b) As extension of the case studies considered in Chapters 4 and 5, including the work proposed above in 6.3-(a), it would be useful to apply the spatio-temporal characterisation framework on a distribution network that includes energy storage applications. This is particularly important to assess the variations that would occur in the diversified peak demand and power losses, as well as the reliability and stability parameters of the network.

(c) The ultimate purpose for developing the spatio-temporal characterisation framework was to provide a novel framework that enables distribution network planners and operators to accurately design and operate distribution networks given the large scale presence of distributed variable energy resources (i.e., solar PV, wind power, etc.) and energy prosumers with vast energy applications (i.e., plug-in electric vehicles (PEVs), energy storage systems, etc.). Using the understanding gained from the characterisation of the distribution network diversified peak demand, load variability and the variation of network power losses in relation to spatio-temporal load aggregation, a further study should be conducted to determine a scalable optimisation model to estimate the optimal composition of solar PV based renewable power and other energy applications (i.e., plug-in electric vehicles (PEVs), energy storage systems, etc.), as well the optimal siting/placement of these resources. These optimisation studies must be conducted with the view to reduce network power losses and improve

the reliability and stability of distribution systems, as well as to maximise the penetration of distributed energy resources.

(d) Another important area is to explore the derivation of optimal customer load data time granularities that could be used for estimating capacity and operational requirements of a distribution network in relation to load aggregation, especially in the presence of solar PV, PEVs, and energy storage systems.

References

[1] Igor Sartori et al. “Estimation of load and generation peaks in residential neighbourhoods with BIPV: bottom-up simulations vs. Velander”. In: *World Sustainable Building 2014 Conference*. 2014, pp. 17–24.

[2] J. Dickert and P. Schegner. “Residential load models for network planning purposes”. In: *Proceedings - International Symposium: Modern Electric Power Systems, MEPS'10*. 2010, pp. 1–6.

[3] Ning Zhang, Luis F Ochoa, and Daniel S Kirschen. “Investigating the impact of demand side management on residential customers”. In: *2011 2nd IEEE PES International Conference and Exhibition on Innovative Smart Grid Technologies*. IEEE, Dec. 2011, pp. 1–6.

[4] Jeremy Pitt, Ada Diaconescu, and Aikaterini Bourazeri. “Democratisation of the SmartGrid and the active participation of prosumers”. In: *IEEE International Symposium on Industrial Electronics* (2017), pp. 1707–1714.

[5] G. R. Aghajani, H. A. Shayanfar, and H. Shayeghi. “Demand side management in a smart micro-grid in the presence of renewable generation and demand response”. In: *Energy* 126 (2017), pp. 622–637.

[6] Chathurika Mediwaththe et al. “Competitive Energy Trading Framework for Demand-side Management in Neighborhood Area Networks”. In: *IEEE Transactions on Smart Grid* (2017). arXiv: 1512.03440.

[7] Intisar A Sajjad, Gianfranco Chicco, and Roberto Napoli. “A probabilistic approach to study the load variations in aggregated residential load patterns”. In: *2014 Power Systems Computation Conference*. IEEE, Aug. 2014, pp. 1–7.

[8] UK Power Networks. *Development of new network design and operation practices*. Tech. rep. 2014.

[9] T Strasser et al. “A review of architectures and concepts for intelligence in future electric energy systems”. In: *Industrial Electronics ...* 62.4 (2015), pp. 2424–2438.

[10] Rory V. Jones and Kevin J. Lomas. “Determinants of high electrical energy demand in UK homes: Socio-economic and dwelling characteristics”. In: *Energy and Buildings* 101 (2015), pp. 24–34.

[11] David G. Infield et al. “Potential for domestic dynamic demand-side management in the UK”. In: *2007 IEEE Power Engineering Society General Meeting, PES*. July 2007. 2007.

[12] UK Power Networks. *Use of smart meter information for network planning and operation*. Tech. rep. 2014, p. 48.

[13] Eoghan McKenna, Ian Richardson, and Murray Thomson. "Smart meter data: Balancing consumer privacy concerns with legitimate applications". In: *Energy Policy* 41 (2012), pp. 807–814.

[14] Km Svehla. "A Specification for Measuring Domestic Energy Demand Profiles". Master of Science in Renewable Energy Systems and the Environment. University of Strathclyde, 2011.

[15] Charles Trevor Gaunt et al. "Data collection, load modelling and probabilistic analysis for LV domestic electrification". In: *15th International Conference on Electricity Distribution*. 1999, pp. 1–6.

[16] Ian Richardson et al. "Domestic electricity use: A high-resolution energy demand model". In: *Energy and Buildings* 42.10 (2010), pp. 1878–1887.

[17] Raffi Sevlian and Ram Rajagopal. "Short Term Electricity Load Forecasting on Varying Levels of Aggregation". In: *Transactions on Power Systems* (Mar. 2014), pp. 1–8. arXiv: 1404.0058.

[18] Raffi Sevlian and Ram Rajagopal. "A Scaling Law of Short Term Electricity Load Forecasting". In: *Transactions on Power Systems* (Mar. 2014), pp. 1–8. arXiv: 1404.0058.

[19] Christian Barteczko-Hibbert. *After Diversity Maximum Demand (ADMD) Report*. Tech. rep. Durham: Customer-Led Network Revolution Project: Durham University, 2015, pp. 1–23.

[20] P. Boait, V. Advani, and R. Gammon. "Estimation of demand diversity and daily demand profile for off-grid electrification in developing countries". In: *Energy for Sustainable Development* 29 (Dec. 2015), pp. 135–141.

[21] E. Ortjohann et al. "Cluster fractal model - A flexible network model for future power systems". In: *4th International Conference on Clean Electrical Power: Renewable Energy Resources Impact, ICCEP 2013*. 2013, pp. 293–297.

[22] Intisar A. Sajjad, Gianfranco Chicco, and Roberto Napoli. "A statistical analysis of sampling time and load variations for residential load aggregations". In: *2014 IEEE 11th International Multi-Conference on Systems, Signals and Devices, SSD 2014*. IEEE, Feb. 2014, pp. 1–6.

[23] Intisar A. Sajjad, Gianfranco Chicco, and Roberto Napoli. "Effect of aggregation level and sampling time on load variation profile - A statistical analysis". In: *Proceedings of the Mediterranean Electrotechnical Conference - MELECON*. 2014, pp. 208–212.

[24] Alejandro Navarro, Luis F. Ochoa, and Pierluigi Mancarella. "Learning from residential load data: Impacts on LV network planning and operation". In: *Proceedings of the 2012 6th IEEE/PES Transmission and Distribution: Latin America Conference and Exposition, T and D-LA 2012*. 2012.

[25] Andrew J. Urquhart and Murray Thomson. "Impacts of Demand Data Time Resolution on Estimates of Distribution System Energy Losses". In: *IEEE Transactions on Power Systems* 30.3 (2015), pp. 1483–1491.

[26] Goudarz Poursharif et al. "Using smart meters to estimate low-voltage losses". In: *IET Generation, Transmission & Distribution* 12.5 (2018), pp. 1206–1212.

[27] Zhaoyu Wang et al. “Stochastic DG Placement for Conservation Voltage Reduction Based on Multiple Replications Procedure”. In: *IEEE Transactions on Power Delivery* 30.3 (June 2015), pp. 1039–1047.

[28] Daniel E. Olivares et al. “Stochastic-Predictive Energy Management System for Isolated Microgrids”. In: *IEEE Transactions on Smart Grid* 6.6 (Nov. 2015), pp. 2681–2693.

[29] CCB Oliveira et al. “A new method for the computation of technical losses in electrical power distribution systems”. In: *16th International Conference and Exhibition on Electricity Distribution, 2001. Part 1: Contributions. CIRED. (IEE Conf. Publ No. 482)*. Amsterdam: IEE, 2001.

[30] Antonio Gomez Exposito et al. “Fair allocation of transmission power losses”. In: *IEEE Transactions on Power Systems* 15.1 (2000), pp. 184–188.

[31] K.R. Devabalaji et al. “Power Loss Minimization in Radial Distribution System”. In: *Energy Procedia* 79 (Nov. 2015), pp. 917–923.

[32] Eric Sortomme et al. “Coordinated Charging of Plug-In Hybrid Electric Vehicles to Minimize Distribution System Losses”. In: 2.1 (2011), pp. 198–205.

[33] Andreas I. Elombo et al. “Residential load variability and diversity at different sampling time and aggregation scales”. In: *2017 IEEE AFRICON: Science, Technology and Innovation for Africa, AFRICON 2017* (2017), pp. 1331–1336.

[34] José Luis Ramírez-Mendiola, Philipp Grünewald, and Nick Eyre. “The diversity of residential electricity demand – A comparative analysis of metered and simulated data”. In: *Energy and Buildings* 151 (2017), pp. 121–131.

[35] Morris R Driels and Young S. Shin. *Determining the number of iterations for Monte Carlos Simulations of weapon effectiveness*. Tech. rep. April. Monterey, California: Naval Postgraduate School, 2004, p. 30.

[36] Samik Raychaudhuri. “Introduction to Monte Carlo simulation”. In: *2008 Winter Simulation Conference*. 2008, pp. 91–100.

[37] Chris Thompson et al. *CLNR Customer Trials: A guide to the load and generation profile datasets*. Tech. rep. August. 2014, pp. 1–40.

[38] Pecan Street Inc. *Electricity eGauge 1-minute Database: Pecan Street Inc. Dataport*. 2018.

[39] Elizabeth L. Ratnam et al. “Residential load and rooftop PV generation: an Australian distribution network dataset”. In: *International Journal of Sustainable Energy* 36.8 (2017), pp. 787–806.

[40] E Bukaçi et al. “Number of iterations needed in Monte Carlo Simulation using reliability analysis for tunnel supports”. In: *International Journal of Engineering Research and Applications* 6.6 (2016), pp. 60–64.

[41] J Dickert, M Hable, and P Schegner. “Energy loss estimation in distribution networks for planning purposes”. In: *2009 IEEE Bucharest PowerTech* (2009), pp. 1–6.

[42] Keith Malmedal and P. K. Sen. “A better understanding of load and loss factors”. In: *Conference Record - IAS Annual Meeting (IEEE Industry Applications Society)* (2008), pp. 1–6.

[43] Carlos A. Dortolina and Ramón Nadira. "The loss that is unknown is no loss at all: A top-down/bottom-up approach for estimating distribution losses". In: *IEEE Transactions on Power Systems* 20.2 (2005), pp. 1119–1125.

[44] Ali Khoshkholgh Dashtaki, Mahmoud Reza Haghifam, and Senior Member. "A New Loss Estimation Method in Limited Data Electric Distribution Networks". In: *IEEE Transactions on Power Delivery* 28.4 (2013), pp. 2194–2200.

[45] PauloMoisés M. Costa and Manuel A. Matos. "Loss Allocation in Distribution Networks With Embedded Generation". In: *IEEE Transactions on Power Systems* 19.1 (2004), pp. 384–389.

[46] Enrico Carpaneto, Gianfranco Chicco, and Jean Sumaili Akilimali. "Branch current decomposition method for loss allocation in radial distribution systems with distributed generation". In: *IEEE Transactions on Power Systems* 21.3 (2006), pp. 1170–1179.

[47] Kushal Manoharrao Jagtap and Dheeraj Kumar Khatod. "Loss allocation in distribution network with distributed generations". In: *IET Generation, Transmission & Distribution* 9.13 (2015), pp. 1628–1641.

[48] Kushal Manoharrao Jagtap and Dheeraj Kumar Khatod. "Loss allocation in radial distribution networks with different load models and distributed generations". In: *IET Generation, Transmission & Distribution* 9.12 (2015), pp. 1275–1291.

[49] M. Thomson and D.G. Infield. "Impact of widespread photovoltaics generation on distribution systems". In: *IET Renewable Power Generation* 1.1 (2007), p. 33.

[50] D. F. Frame, G. W. Ault, and S. Huang. "The uncertainties of probabilistic LV network analysis". In: *IEEE Power and Energy Society General Meeting* (2012), pp. 1–8.

[51] Rita Shaw and Dan Randles. *Dissemination Document " Low Voltage Networks Models and Low Carbon Technology Profiles "*. Tech. rep. June. Manchester: University of Manchester, 2015, pp. 1–27.

[52] Roger C. Dugan. *Reference Guide: The Open Distribution System Simulator (OpenDSS)*. 2013.

[53] J A Alberts. "Impact of energy efficiency and renewable energy on electricity master planning and design parameters". PhD thesis. North-West University, 2017.

[54] J A Alberts and J A de Kock. *The impact of small scale embedded generation on existing networks*. Tech. rep. 2014, pp. 56–60.